ID: AGE 002

1st International Conference on Advances in Civil Engineering 2012 (ICACE 2012)
12 –14 December 2012
CUET, Chittagong, Bangladesh

BEHAVIOUR OF BURIED FLEXIBLE PIPE UNDER SURFACE LIVE LOAD

M. J. ABADIN[1] , Z. A. BHUYAN[2], M. H. ROSHID[3], S. S. AHMED[4] & M. S. ISLAM[5]

[1] *Post Graduate Student, Department of Civil Engineering, BUET, Dhaka, 1000, Bangladesh*
[2,3]*Post Graduate Student, Department of Civil Engineering, BUET, Dhaka, 1000, Bangladesh*
4Lecturer, Department of Civil Engineering, CUET, Chittagong-4349, Bangladesh
[5]*Professor, Department of Civil Engineering, BUET, Dhaka, 1000, Bangladesh*

ABSTRACT
The effect of the surface live load on buried flexible pipe has been investigated based on soil-pipe interaction analysis. Two-dimensional finite element analysis was performed through the idealization of the concentrated surface load as an equivalent live load. A general purpose finite element program ABAQUS was used for modeling of the pipe soil interaction under surface live load. HDPE pipe in soft soil with lower material modulus of soil are used for the study. A compressive study on different parameters of large diameter flexible pipe like sectional area, moment of inertia, pipe and soil material modulus, burial depth and position of load etc. Soil stresses, deflection and internal force are the investigation parameters. The study revealed that the deflection of pipe significantly affected by all parameters. The vertical stress in soil is largely influenced by Material modulus of pipe. The horizontal stress depends on soil and pipe material property, sectional area and moment of inertia of pipe wall. The thrust of pipe is totally independent from pipe sectional properties. The effects of the pipe properties, modulus of elasticity of pipe and soil are very significant on bending moment of pipe. The movement of loading point from the crown also changes the stress distribution and affects thrust and moment. Increase of burial depth decreases the significance of all the parameters accept the effects from loading position. The arching effect of pipe always encounters the soil stress matching with Boussinesq's solution. AASHTO and ASCE code yielded conservative values of the average soil stress for pipes with deeper pipe.

Keywords: ABAQUS, HDPE, Material Modulus, Soil Stress, Deflection, Internal Forces

INTRODUCTION
A buried pipe can be defined as a pipe which is located beneath the surface of the earth. Buried pipes have been used to improve the standard of living for city dwellers through transporting portable and waste water since being the modern civilization. Moreover, gas and oil are transported from source to the distribution zone is also done by buried pipe line. Recently telecommunication wires, internet cables, satellite cables are also laid under the ground surface inside a pipe. Buried pipes can be made of different types of material and work is still continued to improve the performances and minimize the cost of buried pipe. Buried pipes are mainly two types, flexible and rigid buried pipe. Flexible and rigid pipes are generally differentiated by deflection consideration, for rigid pipe deflection is negligible whereas 30% deflection can be allowed for flexible pipe. Flexible pipes with different materials such as steel, High Density Polythene (HDPE), Polyvinyl Chloride (PVC), copper, aluminum etc. were developed with a variety of wall profile geometry. Rigid pipes are usually made by vitrified clay and concrete.

Use of flexible pipe for underground application started in the early twentieth century, when pipes were installed without engineering design. Design of the flexible pipe was started in the mid-1900 when spangler developed the deflection equation for corrugated steel pipe (spangler, 1941). The main applications of flexible polymer pipes (HDPE and PVC) are in agriculture, construction industry and highway and roads. It is also used for runway drainage and telephone and internet line transmission. In Bangladesh, flexible pipes are mainly used for irrigation system, sometimes are used as buried culverts

for drainage of water across roads and embankments. However, use of flexible pipes is increasing for sewer systems and underground gas, water, telephone and electric distribution system.

The pipes are laid under the ground; the load from the soil column above the pipe is huge. Moreover there is certain possibility of overburden pressure from traffic and superstructures above the ground surface resulting in a great overburden pressure in addition to the pressure from soil mass. The analysis of buried pipe, in our study we considered only the surface live loads. Because, the effects of live load are more complex, where dead load or overburden pressure of soil is predictable in nature. The effects of surface load on the buried pipe varied with depth of the flexible buried pipe and horizontal distance from the crown of the buried flexible pipe. Vertical and horizontal stress of soil, deflection, internal force (axial force or thrust and bending moment) are considered as investigation parameters for the analysis. The analysis of soil-pipe interaction under live loads is performed with ABAQUS 6.7. The effects of vehicle loads are generally accounted as an additional uniform pressure over the pipe crown (ASCE, AASHTO) which is added to the overburden pressure.

The main attempt is to study the behavior of buried flexible pipe under surface live load to understand the behavioral change of pipe by 2D finite element method. Development of a model for numerical analysis of buried flexible pipe under live loads. Verification of developed model with previous studies, performing a parametric study to identify the parameters affecting the soil pipe interaction behavior and evaluation of the current design method for live load analysis for flexible pipe are the specific objectives.

MATERIALS AND METHODS

The early designs of flexible pipe were based on extensions of rigid pipe theory. Although flexible pipes can be deflected 30% without reverse curvature, generally either 5 or 7.5% deflection is allowed in design. A semi empirical deflection equation developed at the Iowa University has generally been used to calculate pipe deflections. Spangler (1941) developed the equation known as “Iowa Formula”, using assumptions based on his observations during field-loading experiments on corrugated metal pipe culverts. Spangler (1941) expressed horizontal deflection as a function of the vertical load and the bending resistance provide by the pipe and the surrounding soil. Watkins and Spangler (1958) provided Modified Iowa Formula. The Modified Iowa Formula has been the principal tool for estimating deflection for flexible pipe for the past 50 years. However, it has been recognized that the modified Iowa formula, which only consider the flexural deflection, is not applicable for very flexible pipes like pipes make thermoplastic materials. Dhar et al. (2002) presented a simplified equation for the deflection of flexible pipe that account for the shortening due to hoop forces in addition to the flexural/bending deflection. The simplified equation has been adopted in AASTHO for flexible pipe design. There are some software has been developed for finite element modeling and analyze the pipe. Among them ABAQUS, Staad Pro, SIGMA-W, PLAXIS etc are well known.

Richard W. Bonds, P.E (DIPRA Research/Technical Director) calculated the effect of wheel load of buried flexible pipe. Depth of cover less than 2 feet is generally not recommended under roads and highways due to the possibility of high dynamic loading. Such loadings could result in damage to the pavements and/or the pipes. The procedure for calculating truck loads on buried Ductile Iron pipe is provided in ANSI/AWWA Standard C150/A21.50.1 This procedure is based on the teachings of Merlin Spangler and others and utilizes the same procedures used in the venerable design standard ANSI A21.12 for Cast Iron pipe. The design method is based on two assumptions as a single concentrated wheel load at the surface and uniform load distribution over an effective pipe length of 3 feet.
Regarding the point load assumption, Boussinesq’s equation gives the vertical stress at any point in an elastic medium when a point load is exerted at the surface is,

$$\sigma_t = \left(\frac{3P}{2\pi}\right)\left(\frac{H^3}{R_t^5}\right)$$

Where,

σ_t = Vertical stress in pounds per square inch
P = Point load at surface in pounds
H = Depth in inches
R = Distance from the point load to the point at which the stress is to be determined in inches

Quite obviously, the actual distributed load of a truck tire "footprint" will produce less concentrated effects on a pipe than will the assumed "point" load. The typical dual truck tire imprint may have a contact area of approximately 200 square inches. Also, the length of pipe "effective" in carrying the load may be much greater than that assumed, particularly for large-diameter pipe. Further, in shallow cover situations under highways, the road bed stability will necessitate well-compacted fill around the pipe, which will increase its load bearing capacity.

Pipes performance under vehicular loading depends on the depth of backfill cover, properties of both the backfill and the native soil , the geometry of the trench installation and relative and bending stiffness of the buried pipe . Boussinesq calculated the distribution of stresses for point load applied on the surface in a sem infinite elastic medium without any consideration of pipe. An elastic, homogeneous, isotropic medium was assumed in the process of calculation for distribution of soil stress. The vertical stress in the soil mass due to a concentrated surface load was expressed as:

$$\Delta\sigma_z = \frac{P}{Z^2}\left\{\frac{3}{2\pi}\frac{1}{\left[\left(\frac{r}{2}\right)^2+1\right]^{2.5}}\right\}$$

Where,

$\Delta\sigma_z$= Pressure transmitted to the soil
P = Concentrated load at surface
H = Depth below the ground surface
r = Offset distance of ground point from line of application of surface load

The AASHTO design loads commonly used in the past were the HS 20 with a 32,000 pound axle load in the Normal Truck Configuration, and a 24,000 pound axle load in the Alternate Load Configuration. The AASHTO LRFD designates an HL 93 Live Load. This load consists of the greater of a HS 20 with 32,000 pound axle load in the Normal Truck Configuration, or a 25,000 pound axle load in the Alternate Load Configuration.

The total live load in pounds per linear foot, W_L is calculated by dividing the Total Live Load, W_t, by the Effective Supporting Length, L_e of the pipe:

$$W_L = \frac{W_t}{L_e}$$

Where,
$L_e = L + 1.75(3/4R_0)$
R_0 = outside vertical Rise of pipe, feet

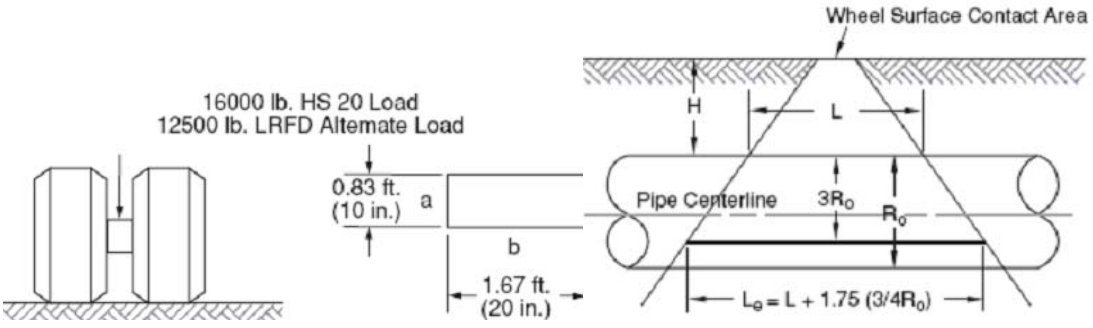

Fig. 1: Standard wheel loading and load distribution on pipe.

Fernando and Carte (1998) performed numerical study with a wide parametric variation to develop a non-dimensionalized graph for incorporating the effects of surface loads. Parametric study was performed to assess the effects of the various geometric and material parameters on the behavior of buried pipe under vehicular live loads approximate as a patch of vertical stresses over square centrally

placed area. Predictions of the maximum circumferential bending moments induced in the buried pipe were presented in a non-dimensionalized design charts. This was developed using ratio between height of cover to pipe diameter as 0.1, 0.25, and 0.5 and ratio of pipe modulus to soil modulus as 100,000, 10,000, and 1,000. A semi-analytical finite element scheme was used based on fourier transform for three dimensional modeling of patch load. Thus, the analysis was limited to the solid wall pipes with uniform wall thickness of pipe was varied from 0.05 to 10% of the pipe diameter.

Dhar et al. (2004) investigated small diameter pipes under surface live load with a wide variation in burial depth and sectional and geometric properties of pipe. Different burial depth of 600 mm , 900 mm and 1200 mm was used for polyvinyl chloride pipes diameter 203 to 790 mm under quasi-live load along with clayey backfill in context of Bangladesh. Areas per unit length were used as 13 to 34mm^2/mm with a moment of inertia of 266 to 7,925 mm^4/mm. Full scale load test was performed with a load of 73.3 kN. Pipes were placed in a trench of 2.4 m X 2.4 m X 2.4 m in such a way that it was equidistance from walls horizontally. Soil bedding below the pipe varied from 350 mm to 1000 mm for 1200 mm burial depth. For 600 mm burial depth 960 to 1620 mm soil bedding was used. Load was applied with the help of a steel plate of width 300 mm and length as same as the trench to simulate plain-strain condition. A load increment rate of 5 kN/m was provided in a faster way to represent live load. Seven different profiled polyvinyl chloride pipes were used for this purpose. To measure the load-deformation data, electronic deformation transducer was used and stored in computer through an ADU-700 data logger. It was revealed from the study that calculations using a load –spreading rate of 1.15 times the depth performed better in calculating the live load deflections. Deflections were underestimated by 30% to 48% for pipes at 600 mm depth and by 25% to 60% for the pipes at 1200 mm depth load spreading rate of 1.75 times the depth was used.

The pipe-soil interaction under surface load is a three dimensional problem and vehicular or traffic load also three dimensional. The wheel load idealized as a concentrated load in various code (i.e. AASHTO 1996), while idealization as a distributed load over the area of tire foot-print is also used (AASHTO, 1998). The concentrated or patch load induce a three dimensional stress pattern around the pipe. The three dimensional finite element analyses is extremely time consuming and requires a lot of computer memory, particularly when a large soil mass with nonlinear stress field is discretized (Dutta S. 2008). In this research we conducted two dimensional finite element analyses to the problems and simplification. Some researchers have analyzed the buried pipes and culverts using two dimensional idealizations of three dimensional loads (Moore and Brachman, 1994; Fernando and Carter, 1998; Jayawickrama et al., 2002). In other analyses, the Boussinesq solution for a vertical load at the surface of an elastic half space were used to convert the three dimensional loading to an equivalent two examined using conventional two Taleb,1999; Jayawickrama et al., 2002).
Concentrated load can be converted to equivalent line load by using (Jayawickrama et al., 2002)

$$(P/b) = r(P/BL)wheel\ load$$

Where,
(P/b) = Load per unit length;
(P/BL) = Load per contact area used in the full scale testing;
r = Reduction factor
Jayawickrama et al. (2002) used the reduction factor as 0.5335 for wheel load based on Boussinesq's solution.

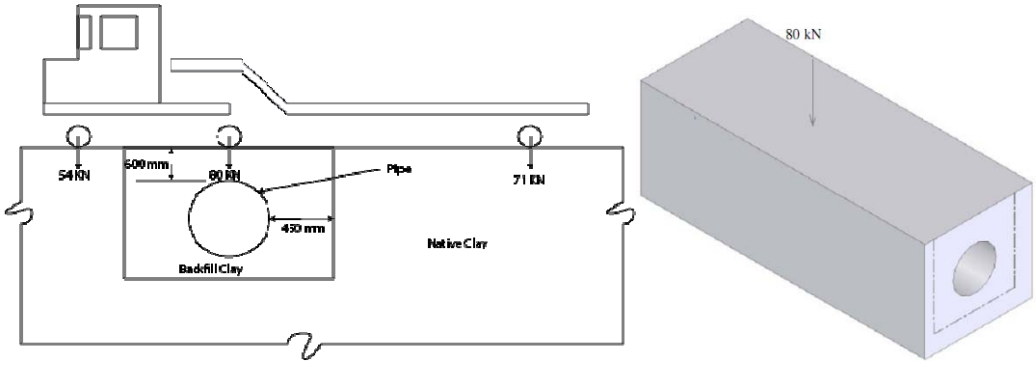

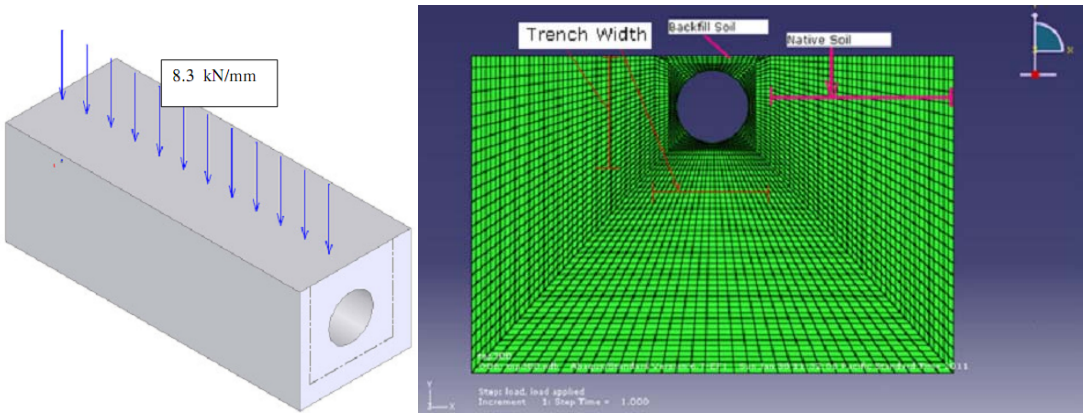

Fig. 2: Idealization of wheel load and ABAQUS model formation

Finite element modeling the structure of interest is subdivided into number of element. Finer mesh and more elements would be required in non-linear stress field. In our work, the soil was modeled using the two-dimensional 4-noded plane strain element (CPE4 in ABAQUS) and the buried pipe wall modeled as plane stress or beam-column element (B21 in ABAQUS). The plane strain soil elements are axisymmetric elements which are capable of simulating plasticity, creep, swelling, stress stiffening, large deflection and large strain. The beam-column elements are uniaxial element with tension, compression, and bending capabilities. The pipe circumference divided into 72 elements (Dutta S. 2008). Soil and pipe interacted in ABAQUS with tie constraint, pipe surface allocated as master surface and soil surface as slave surface and their connection provided as surface to surface discretization method. The soil mass divided into two different zone backfill and native soil where backfill is limited to a smaller area. As if, the soil parameters are same for our analysis to reduce the complexity, but generally backfill and native soil parameters are slightly different for differential compaction condition and soil type. We modeled our soil-pipe interaction geometry by using the SIDD recommended type I installation procedure, where the bedding thickness (the depth below the invert of soil cut) at least $1/24^{th}$ of the outer diameter of the pipe. Our modeled bedding thickness is 450mm which prefers the recommended value. Trench width minimum is 125% of pipe outer diameter or pipe outer diameter plus 200 mm. The modeled trench width is 2400mm which is 160% of pipe outer diameter. The greater bedding thickness and trench width chosen for better bedding support and easy handling consideration (in practical case) correspondently.

An extensive analysis has been performed with different side width and bottom height from the invert to obtain the dimensions so that the boundary effects on the results of FE analysis can be minimized. From the graph, it is revealed that pipe crown or crest and invert moment reduces and moment of springline increases as the distance of boundary from pipe center increases. However, the moment of crown, invert and springline stabilized beyond the distance of 5000mm from the center of pipe. Thus, reducing or neglecting the boundary effects the side boundary placed at a distance of 5000mm from the center of pipe for the finite element analysis of the buried pipe under live load. The vertical or bottom boundary placed at distance of 5500mm from the invert to improve the surface load pattern on pipe. At the time of horizontal movement of surface load, it was revealed that if the boundary placed at distance of 4600mm from the load application point effect can be minimized. Smooth rigid boundary was chosen along the side boundary line on left and right of the soil mass (YSYMM in ABAQUS) and hinge was used at the bottom of the soil mass (PINNED in ABAQUS).

As boundary effect investigation, to determine the optimum mesh size or density in finite element meshing similar investigation was performed. The optimum mesh size may be defined as the size of the mesh after reducing the size, the stress values are not change significantly. Every FE program method has automatic mesh size (default) which is not always used for FE model. It was revealed that smaller size of mesh than the size of 100 mm the moment of the crown, spring line and invert settled. Higher number of mesh or smaller size of mesh required larger size of computer memory. So, 100 mm mesh size chosen as the optimum mesh size. Near of the pipe sweep meshing provided and native soil meshed as structure meshing and both are tetrahedral shaped elements.

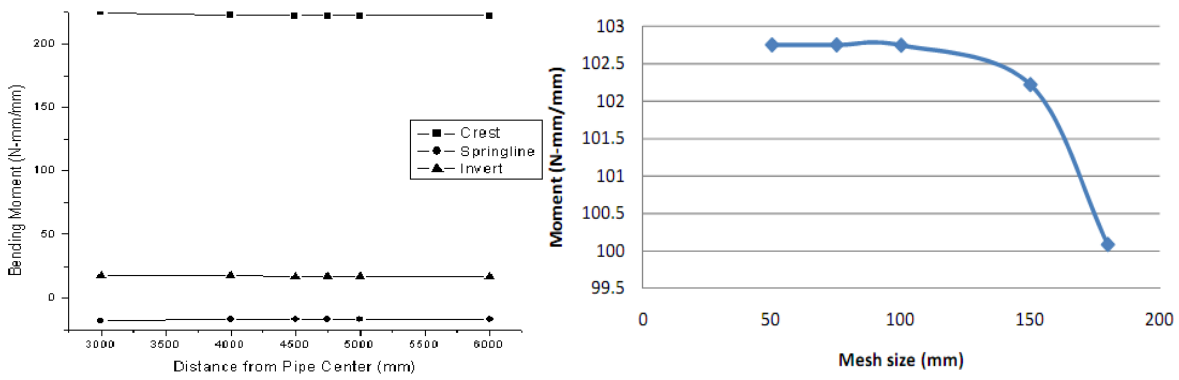

Fig. 3: Effect of boundary position and mesh size.

Table 1: The Values of Parameters used in FEM using ABAQUS

Parameter	Value
Pipe Diameter	150mm, 900mm, 2400mm
Buried Depth	300mm, 750mm
Pipe Material Modulus	$E_p = 200$MPa, 760 MPa, 1000 MPa, 10000 MPa, 210000 MPa
Soil Poisson's Ratio	$\nu_s = 0.25$
Soil Material Modulus	$E_s = 10$MPa, 50 MPa, 100MPa, 180MPa
Moment of Inertia of Wall	$I_p = 300\ mm^4/mm, 7000\ mm^4/mm, 15700\ mm^4/mm$
Area of Pipe Wall	$A_p = 20\ mm^2/mm, 30\ mm^2/mm, 60\, mm^2/mm$

RESULTS & DISCUSSIONS

Vertical Deflection

a) Vertical deflection decrease with increase of sectional area and burial depth.
b) For shallow pipe vertical deflection more than deeper one and deflection is near about independent from sectional inertia.
c) For higher Ep, deflection almost zero.
d) After E_s=50 MPa, effect of soil modulus of elasticity is negligible.

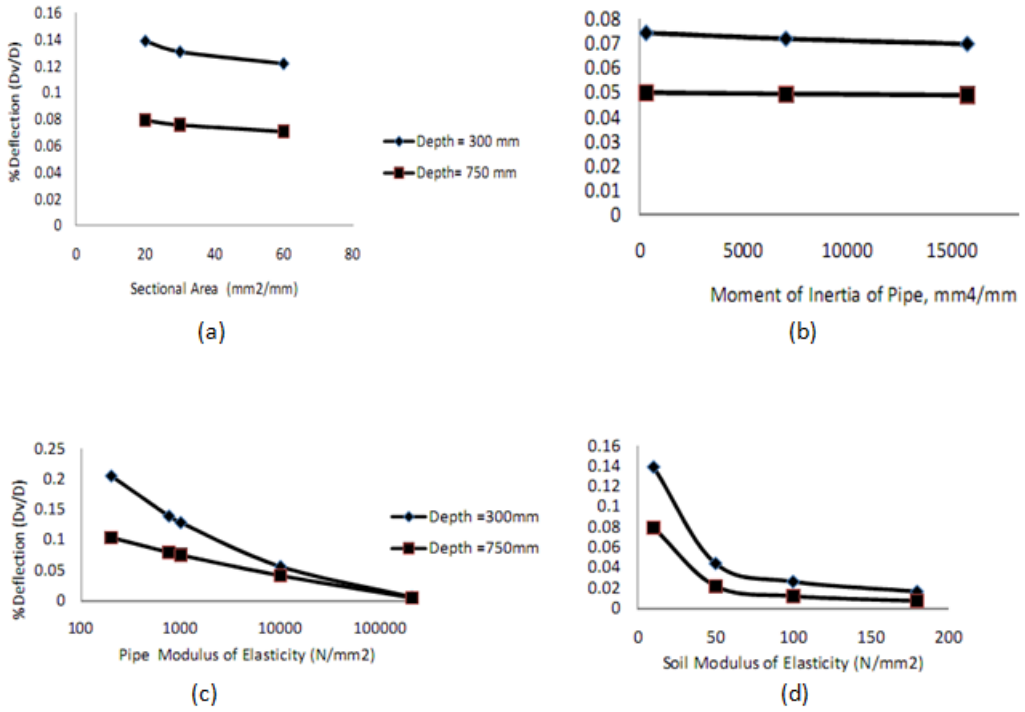

Fig. 4 : Vertical deflection for different depth and (a) Sectional area (b) Moment of inertia (c) Pipe modulus of elasticity (d) Soil modulus of elasticity.

Horizontal Stress

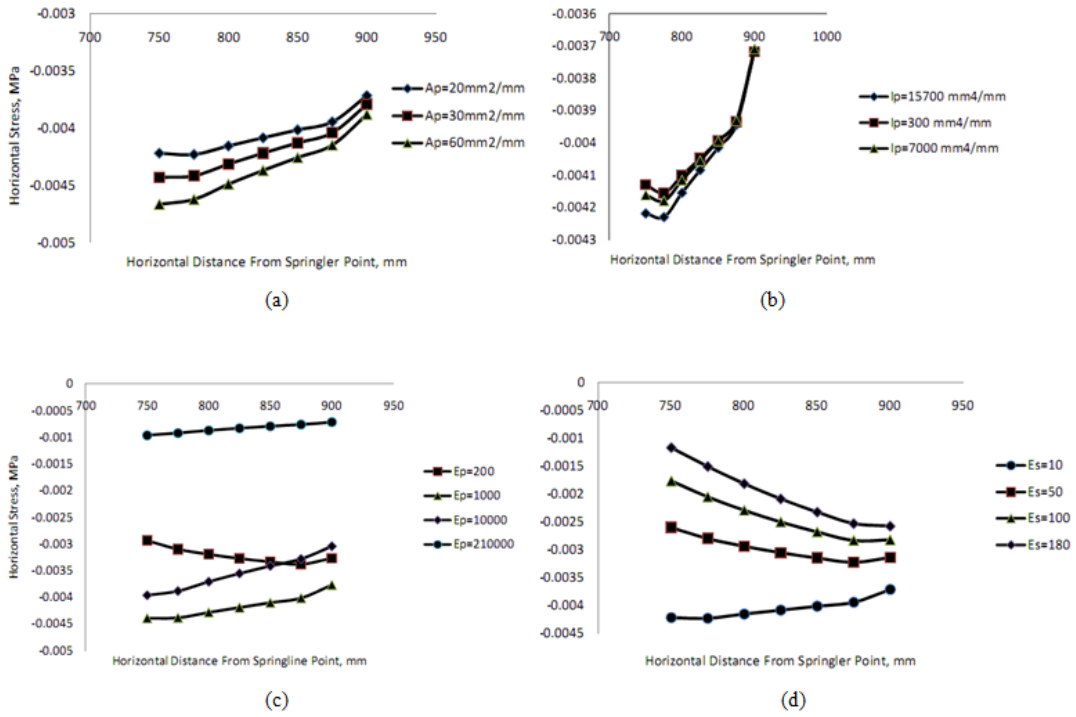

Fig. 5 : Horizontal stress for different (a) Sectional area (b) Moment of inertia (c) Pipe modulus of elasticity (d) Soil modulus of elasticity.

a) Slightly increase of lateral compressive stress with cross sectional area.
b) Horizontal compressive stress increases with increase of moment of inertia but decreases with increase of distance from Springline.
c) Very significant Influence of Ep and Stress decreased 4.5 times for higher pipe modulus (steel pipe).
d) Horizontal compressive stress decrease with increase of soil modulus.

Vertical Stress

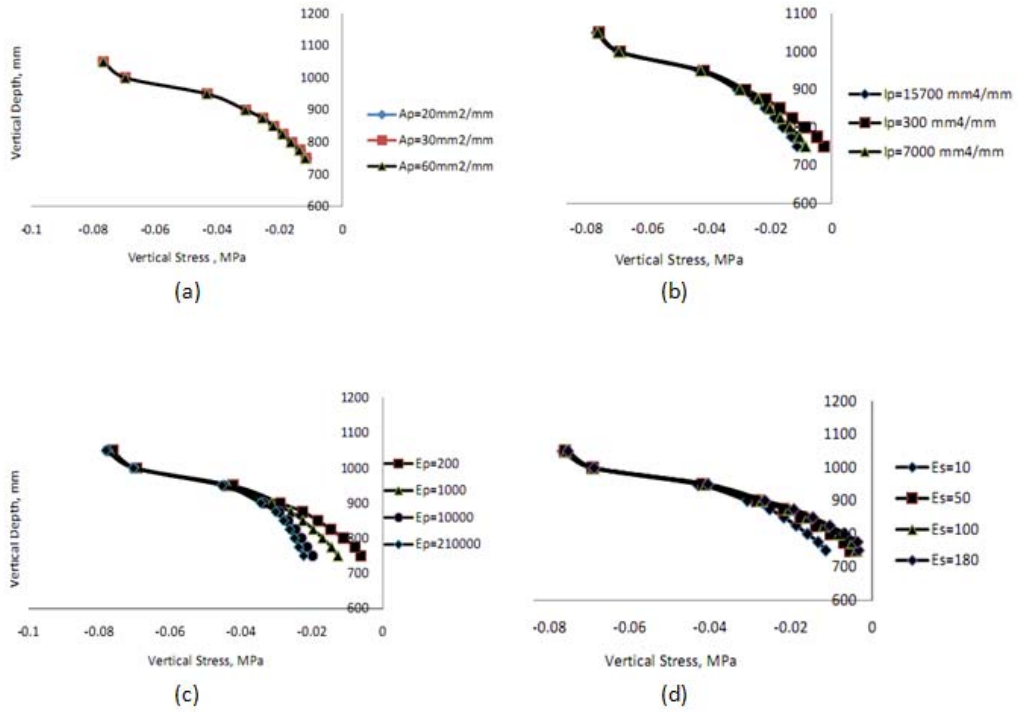

Fig. 6 : Vertical stress for different (a) Sectional area (b) Moment of inertia (c) Pipe modulus of elasticity (d) Soil modulus of elasticity.

a) No change of vertical stress at different sectional area.
b) Small increment of vertical stress at crest level with increase of moment of inertia.
c) Vertical stress increase with increase of pipe modulus of elasticity Ep and at crown level change more significant.
d) Vertical stress decreases with increase of soil modulus at crown level.

Axial Thrust and Bending Moment

a) Maximum thrust occurs at shoulder and moment occurs at crown.
b) Thrust and moment independent from X-sectional area.
c) No change of axial force increase of moment of inertia.
d) Bending moment increased 2465% of minimum moment with increase of moment of inertia 5467%.
e) Compressive thrust increased 57% & Moment increased 1133% and 1255% for crest and invert for increase of E_p 1049%.
f) Maximum thrust and moment both are decreased with increase of E_s, 17%. Thrust decreased 61% and moment decreased 87%.

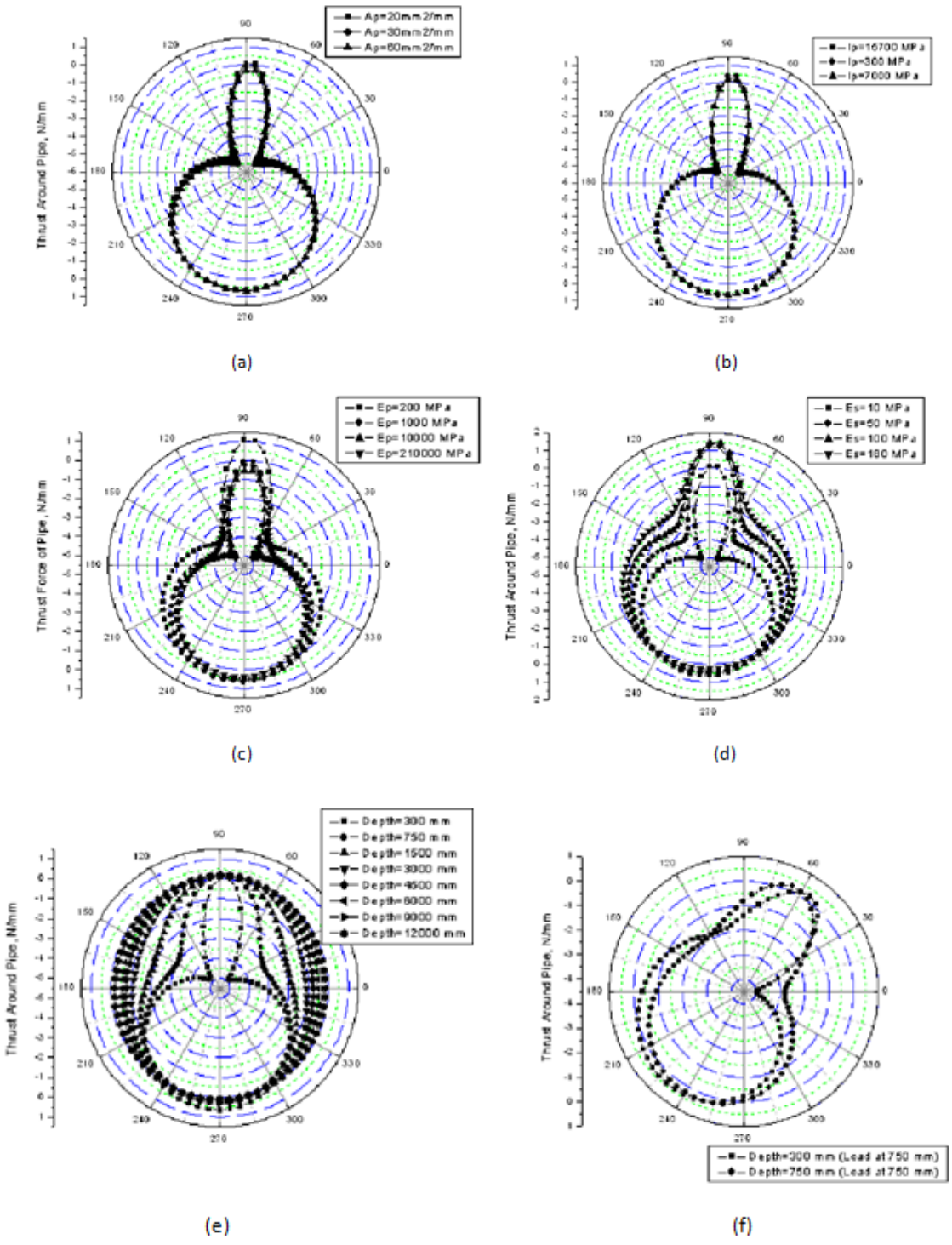

Fig. 7: Axial thrust for different (a) Sectional area (b) Moment of inertia (c) Pipe modulus of elasticity (d) Soil modulus of elasticity (e) Burial depth and (f) Wheel Position.

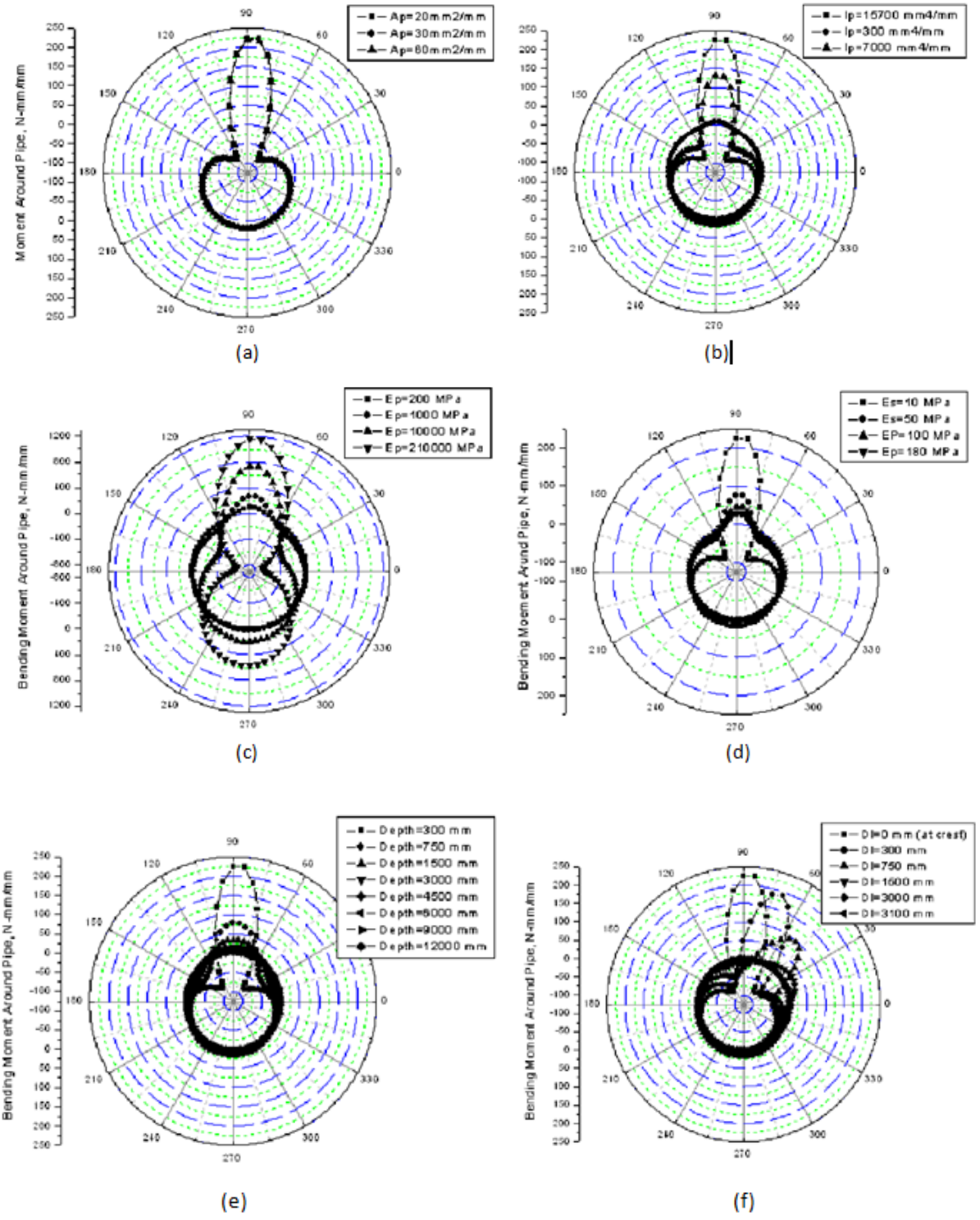

Fig. 8: Bending moment for different (a) Sectional area (b) Moment of inertia (c) Pipe modulus of elasticity (d) Soil modulus of elasticity (e) Burial depth and (f) Wheel Position.

CONCLUSION

Material modulus (pipe & soil) influences all the behaviour like stress, deflection, thrust and moment. Sectional properties influence stress, deflection and moment.Increase of the distance of the loading point from pipe crown maximum moment, thrust and deflection goes towards springline from the crown and deflection and moment are deceased.The pattern of vertical and lateral stress distribution quite similar for pipes buried at depth greater than 2 times of the pipe diameter. For a particular pipe, bending moment and thrust around pipe becomes insignificant (10% of the maximum) for 2 times and 3 times of pipe

diameter, respectively.Boussinesq's solution always over predicts the maximum stress at crown level for shallow depth. Arching effect of pipe reduces the soil stress in soil pipe interaction where Boussinesq's Equation refers the stress in homogenous soil mass. ASCE and AASHTO both yield good result for deeper pipe but AASHTO is more conservative. Elastic-plastic modeling of soil and pipe under multiple wheels loading with considering non-linear soil behavior like consolidation, creep, swelling etc. may can be marched with practical situation.

LIST OF REFERENCES

ABAQUS 6.7 Simula user's manual

Burns J.Q. and Richard , R.M (1964) "Attenuation of Stresses for Buried Cylinder"
Proceedings of Symposium on soil-structure interaction , University of Arizona, pp:379-392

Dhar, A.S., Moor, I.D. and McGrath, T. J. (2004) " Thermoplastic Culvert Deformation and Strain Evaluation Using Two-dimensional Analysis" Journal of Geotechnical and Geo-environmental Engineering, AACE, Vol-130, no. 2, PP-199208.

Dutta, S.(2008) "Behavior of Large Diameter Buried Flexible Pipes under Surface Live loads."Unpublished Master's Thesis, Department of Civil Engineering, Bangladesh University of Engineering and Technology, Dhaka, Bangladesh.

Hoeg, K. (1968) "Stress against Underground Cylinder" Journal of Soil Mechanics and Foundation Engineering, ASCE, vol-94, SM4, 833-858.

Moser, A.P. (2001) "Buried Pipe Design" McGraw-Hill.

Rajkumar, R., &Ilamparuthi, K. " Experimental Study on the Behaviour of Buried Flexible Plastic Pipe". *EJGE, 13*.

Richard W. Bonds, P.E. "Truck Loads Pipe Buried At Shallow Depths" DIPRA Research.

ID: AGE 005

1st International Conference on Advances in Civil Engineering 2012 (ICACE 2012)
12 –14 December 2012
CUET, Chittagong, Bangladesh

APPLICATION OF NOVEL DOE PRINCIPLE IN LATERAL RESISTANCE DETERMINATION FOR PARTIALLY EMBEDDED OFFSHORE PIPELINES

S. DUTTA[1*] & S. S. AHMED[2]

[1] *Faculty of Engineering and Applied Science, Memorial University of Newfoundland, NL, CANADA, E-mail:sd3451@mun.ca*
[2] *Department of Civil Engineering, Chittagong University of Engineering and Technology, Bangladesh, E-mail: sharifce05@gmail.com*
**Corresponding Author*

ABSTRACT

Offshore pipelines play vital role in transporting hydrocarbon from offshore to onshore. For shallow water, typical practice is buried pipelines whereas as-laid pipelines are for deep water. Previous studies show that pipelines can penetrate a fraction of its diameter due to pipe self weight and also for laying procedures. After installation, as-laid pipelines can experience large lateral displacement (up to 20 pipe diameter) due to high temperature and pressure from oil and gas. Pipeline lateral buckling can generate huge bending moment and pipeline can fail. Controlled lateral buckling is the best mitigation option for large lateral displacement. However, controlled lateral buckling mainly depends on accurate estimation of pipeline lateral resistance. Uncertainties regarding lateral pipeline resistance make this issue more challenging. Preliminary studies show that pipe lateral resistance depends primarily on soil modulus, undrained shear strength of soil, poisson's ratio, soil unit weight and pipe embedment depth. Statistical design of experiments (DOE) methodology (using a face centered CCD) is adopted with finite element analysis to select the governing parameters for pipeline lateral resistance. It is observed that pipe embedment depth and undrained shear strength of soil are the governing factors and novel DOE methodology can be used in partially embedded offshore pipeline analysis.

Keywords: Pipe, Undrained shear strength of soil, Lateral resistance, Design of Experiment.

INTRODUCTION

Offshore pipelines are widely used to transport hydrocarbon from offshore. Both buried and partially embedded pipelines are used. Partially embedded offshore pipelines are generally used in deep sea where trenching is very difficult and not economic. During installation, depending upon sea state, lay vessel conditions, pipeline stiffness and seabed soil state, pipeline can embed a fraction of its diameter (Westgate et al., 2010). After installation, pipeline can be laterally unstable due to wave current during severe storm, lay tension (from catenary shape of installation) and high temperature and pressure phenomenon. In deep sea, wave induced lateral instability is not significant as shallow water (White and Cheuk, 2008). Lay tension is remained in the pipeline but high temperature and pressure from oil and gas is the most susceptible one. It is observed that pipeline can move laterally 10 to 20 pipe diameters (Bruton et al., 2008) due to high temperature and pressure. This might also happen for

offshore geotechnical hazards like submarine landslides and pipe can slide several times of its diameter (Swanson and Jones 1982).

Pipe lateral displacement creates huge bending moment at pipe crown and pipe can fail. Literature shows that best mitigation procedure against pipe lateral buckle is controlled lateral buckling. However, for controlled lateral buckling, allowance in pipe length calculation to buckle (known as pipe feed) is the most important one. Pipe feed calculation mainly depends on pipe lateral resistance which come mainly from soil/pipe interaction and different researchers proposed different empirical equation which varies widely with each other (Verley and Lund, 1995; Bruton et al.,2006; Cardoso and silveira, 2010; White and Dingle, 2011). Thus, initiative has been taken to understand the soil/pipe interaction through statistical approach with finite element analysis using ABAQUS 6.10EF-1. For statistical approach, design of experiments (DOE) principles is used to identify the influential parameters for soil/pipe interaction.

MODEL DEVELOPMENT

Numerical model

Finite element model was developed using ABAQUS 6.10EF-1. A model size of 8m×3m was considered. Plain strain condition was used for simulation. Uniform undrained shear strength of soil was used and a soil constitutive model of von Mises was adopted. Pipe was pre-embedded at soil for different embedment depth and displaced horizontally for different soil parameters. This modelling is performed in Lagrangian framework and therefore, pipe was displaced always 0.1m for pipe reaction calculation. Higher pipe displacement cause mesh tangling and convergence issues occur. For boundary conditions, fixed support was used at bottom whereas rollar support was used at left and right sides.

Statistical model

Using the statistical approach, initiative had taken to select (a) sensitive parameters (b) Maximum pipe reaction and (c) uses of DOE in geotechnical engineering. Different statistical approaches are available in the literature to use. However, among the available methods (OFAT) are very poor in a sense from experimental results (Lye, 2002; Montgomery, 2005). In fact, DOE becomes popular after factorial theory of Ronald A. fisher. (Hawkins et al. 2006). Design of experiments applies the systematic behaviour of statistics on any experiments. Depending upon problem criteria, choice of methodology (either full factorial or fractional factorial or CCD or BBD etc.) may vary because some problems require only relative answers like one policy is better than other of not. Therefore, model for DOE is developed depending upon such criteria. A two level face centered CCD (center composite design) has been chosen here with 1 replication to determine the influential factors of maximum pipe reaction using five factors (soil modulus, un-drained shear strength, poison's ratio, unit weight and embedment depth).

Design of experiment (DOE) and statistical techniques are widely used to optimize process parameters and to develop a mathematical relationship between the input parameters and the output variables. It involves the study of any given system by a set of independent variables (factors) over a specific region of interest (levels) and provides a straightforward technique with linear graphs to determine the relationship (interactions) between the considered factors, which can be used for practical experimentation. By using DOE, it is possible to investigate the experimental process, to screen the important variables (or factors), to build a mathematical model with prediction and even to optimize the responses where necessary. Among the different techniques in design of experiment method, Fractional factorial design is one of the common DOE techniques for experimentation which is used in this study.

DISCUSSION OF FACTORS, LEVELS WITH RANGES AND RESPONSE

Five factors had considered for the experiment and they are: (i) Soil elastic modulus (factor A) (ii) Undrained shear strength of soil (factor B) (iii) Poison's ratio (factor C) (iv) Soil unit weight (factor D) and (v) Pipe embedment depth (factor E). For each factor three levels have been considered. Pipe reaction was considered as the response. Ranges of the adopted factors are listed in Table 1.

EXPERIMENTAL DESIGN

Face centered CCD with five factors had used here to determine the pipe reaction. As response surface methodology (face center CCD) was chosen, three levels were required. Thus, total 43(2^5+5*2+1) finite element models are required. However, 43 finite element models had simulated using ABAQUS 6.10-EF1 (a finite element software package) to find out the pipe reaction. Calculated pipe reactions with finite element method had used as an input parameter in Design-Expert software (version 7.1.3) for further analysis. All combinations of factors have been created to find out the pipe reaction through finite element model. Thus, pipe reactions with various combinations of factors are given as input parameters in Design-Expert software for further analysis.

Table 1: Input Parameters Summary for Experiment

Factor	Name	Unit	High level	Intermediate level	Low level
A	Soil Modulus	kPa	5000	4000	3000
B	Undrained Shear Strength	kPa	15	12.5	10
C	Poisson's ratio		0.498	0.495	0.49
D	Unit weight	kN/m^3	8.5	7.5	6.5
E	Embedment Depth	m	0.5	0.375	0.25

RESULT ANALYSIS

ANOVA Table Analysis

ANOVA table (Table 2) shows that the model is significant as p-value is less than 0.05. Also A, B, D, E, AB, BE, DE, E^2 are very significant since p-value is less than 0.05 for these terms. ANOVA table also shows that factor C (poisons ratio) do not have significant contribution on pipe reaction. Again, F-value for factor B (Undrained shear strength) and factor E (Embedment Depth) are much higher than the other term which shows that these two terms may significantly affect the model. F-value for interaction between factor B and factor E is high and they are significant. It was observed that value for R-squared is 1.00. Therefore,there are not signifcant experimental error which make sense since it is a numerical experiment. Again, value for adj R-squared and pred R-squared (Table 3) are also same which reveals that model is good enough for prediction.

Regression model equation

DOE also proposed equation to calculate pipe response using a regression analysis. Proposed equation is stated below. Coefficient of factor B and factor E are larger than the other terms which show the same as in ANOVA table. Hence, these two factors (B & E) can be recognized as sensitive factors. Final equation to calculate the pipe reaction in terms of factors is:

Reaction on pipe = 3.834 - 7.555E-005*soil modulus + 0.7518*un-drained shear strength + 0.0008796*unit weight-21.42*Embedment depth + 7.906E-006*soil modulus*Un-drained shear strength + 1.646*un-drained shear strength*embedment depth + 0.1277* unit weight * Embedment depth + 29.22* Embedment $depth^2$

ANOVA assumptions analysis

ANOVA assumption analysis is the effective way to check the errors in the model. It was observed from normality plot of internally studentized residuals that most of the points are very close to the straight line. However, it shows that data points are normally distributed as assumed for analysis. Residuals vs predicted plot shows scattered data points and they do not follow any particular trend. Since the pattern of data points are not look like outward going funnel shape, it can be said that constant variance assumption is satisfied. Therefore, no transformations are performed. Also, Box-Cox plot do not recommend for any transformation. Predicted vs Actual graph shows that model gives accurate values. However, the sequence of run was random.

Table 2: ANOVA table

ANOVA for Response Surface Reduced Quadratic Model

Analysis of variance table [Partial sum of squares - Type III]

Source	Sum of Squares	df	Mean Square	F Value	p-value Prob > F	
Model	684.5	8	85.57	9.976E+004	< 0.0001	significant
A-Soil Modulus	*0.01842*	*1*	*0.01842*	*21.48*	*< 0.0001*	
B-Undrained Shear Streng	*416.9*	*1*	*416.9*	*4.860E+005*	*< 0.0001*	
D-Unit Weight	*0.08089*	*1*	*0.08089*	*94.31*	*< 0.0001*	
E-Embedment Depth	*257.6*	*1*	*257.6*	*3.003E+005*	*< 0.0001*	
AB	*0.01250*	*1*	*0.01250*	*14.58*	*0.0005442*	
BE	*8.464*	*1*	*8.464*	*9868.*	*< 0.0001*	
DE	*0.008157*	*1*	*0.008157*	*9.510*	*0.004041*	
E^2	*1.483*	*1*	*1.483*	*1729.*	*< 0.0001*	
Residual	0.02916	34	0.0008577			
Cor Total	684.6	42				

Table 3: Summary table

Std. Dev.	0.02929	R-Squared	1.000
Mean	17.84	Adj R-Squared	0.9999
C.V. %	0.1641	Pred R-Squared	0.9999
PRESS	0.04580	Adeq Precision	944.3

OPTIMIZATION

Optimization chart (Table 4) is set to determine the maximum pipe reaction whereas all other factors are set to as goal of in range. It shows that two probabilities for maximum pipe reaction (24.81 KN) (Fig.1) with maximum desirability (99.98%). Again, it is clear that two other combinations are available for maximum pipe reaction but with lower desirability than the previous one. For higher desirability any one of two options will be good one because ANOVA table reveals that poisons ratio do not effect pipe reactions significantly and therefore it is totally absent in the predicted model. Maximum pipe reaction (from prediction model) falls between the lower and higher confidence interval which means that developed model is quite good. Also, two experiments are performed in addition and experiments give same pipe reactions as in the optimization chart.

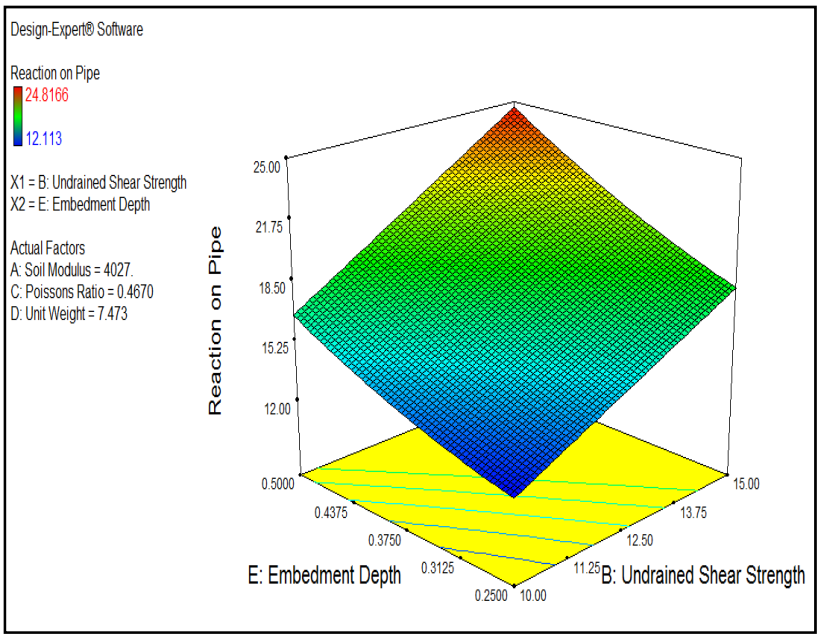

Figure 1: 3D Surface plot

Table 4: Point prediction table

Solutions

Number	Soil Modulus	Undrained Shear Stre	Poissons Ratio*	Unit Weight	Embedment Depth	Reaction on Pipe	Desirability	
1	5000.	15.00	0.4850	8.500	0.5000	24.81	0.9998	Selected
2	5000.	15.00	0.4535	8.500	0.5000	24.81	0.9998	
3	4889.	15.00	0.4845	8.500	0.5000	24.81	0.9994	
4	5000.	15.00	0.4850	8.463	0.5000	24.81	0.9993	
5	4677.	15.00	0.4779	8.500	0.4999	24.80	0.9985	
6	5000.	15.00	0.4638	8.226	0.5000	24.80	0.9984	

CONCLUSIONS

This article shows how design of experiment can be used successfully for offshore geotechnical analysis to detect the sensitive parameters. It shows easier and simpler way to understand the parameters that affect the pipe response. Although poisson`s ratio is an important soil parameter but statistical model shows that it does not have significant effect on pipe reaction. The study reveals that most important parameters are embedment depth and undrained shear strength that affect the response (pipe lateral reaction). Other parameters like soil modulus and unit weight are seems to be less important. However, for more sophisticated analysis, 5-level CCD can be performed to understand the pipe lateral movement more elaborately. Since this analysis deals with partially embedded pipeline in offshore, more factors can be accumulated here. Pipe is used to transport oil or gas and factors like self weight of oil or gas, temperature of pipe (both inside and outside), internal pressure at pipe (both inside and outside) and flow velocity inside pipe can also be considered as factors.

ACKNOWLEDGEMENTS

Authors would like to express his sincerest thanks to Dr. Leonard Lye, Memorial University of Newfoundland for his valuable suggestion and guidance to prepare this paper. The work presented in this article has been funded by MITACS and C-CORE.

REFERENCE

ABAQUS, 6.10EF-1. 2010. Dassault Systèmes, Waltham, MA, United States.

Bruton, DAS; Boreas, A; White, DJ; Carr, M; and Cheuk, JCY. 2008. Pipe-soil interaction during lateral buckling and pipeline walking-the SAFEBUCK JIP. *In Proceedings of the Offshore Technology Conference*, Houston, Texas, USA. OTC 19589.

Bruton, DAS; White, DJ; Cheuk, CY; Bolton, MD and Carr, MC. 2006. Pipe-soil interaction behaviour during lateral buckling, including large amplitude cyclic displacement tests by the safebuck JIP. *In Proceedings of the Offshore Technology Conference*, Houston, USA. OTC 17944.

Cardoso, OC and Silveira, MSR. 2010. Pipe-soil interaction behaviour for pipelines under large displacements on clay soils-A model for lateral residual friction factor. *In Proceedings of the Offshore Technology Conference*, Houston, Texas, USA. OTC 20767.

Verley, R and Lund, KM. 1995. Soil resistance model for pipelines placed on clay soils. *In Proceedings of the 14th International Conference on Offshore Mechanics and Arctic Engineering (OMAE)*, Copenhagen, Denmark, June 18, 1995–June 22, Vol. 5, pp. 225-232.

Hawkins, D; and Lye, LM. 2006. Use of DOE methodology for investigating conditions that influence the tension in marine risers for FPSO ships.*1st International structural Speciality Conference*, CSCE, Calgary, Alberta, Canada.

Lye, LM. 2002. Design of Experiments in Civil Engineering: *Are We Still in the 1920s*. *Proceedings of the 30th Annual conference of the Canadian Society for Civil Engineering*, Montreal, Quebec.

Montgomery, DC. 1997. *Design and Analysis of Experiments*, 5th Edition, John Wiley and Sons, Inc., USA.

Swanson, RC and Jones, WT. 1982.Mudslide Effects on Offshore Pipelines, *Transportation Engineering Journal*, 108(6):585-600.

Westgate, ZJ; Randolph, MF; White, DJ; and Li, S. 2010. The influence of sea state on as-laid pipeline embedment: A case study, *Applied Ocean Research*, 32(3): 321-331.

White, DJ and Cheuk, CY. 2008. Modelling the soil resistance on seabed pipelines during large cycles of lateral movement, *Marine Structures*, 21(1): 59-79.

White, DJ and Dingle, HRC. 2011. The mechanism of steady friction between seabed pipelines and clay soils, Géotechnique, 61(12): 1035-1041.

ID: AGE 008

1st International Conference on Advances in Civil Engineering 2012 (ICACE 2012)
12 –14 December 2012
CUET, Chittagong, Bangladesh

STRENGTH AND COMPRESSIBILITY CHARACTERISTICS OF RECONSTITUTED ORGANIC SOIL AT KHULNA REGION OF BANGLADESH

T. RABBEE[1*], M. R. ISLAM[2], MD. ASSADUZZAMAN[3] & MUHAMMAD ALAMGIR[4]

[1, 3] Department of Civil Engineering, America Bangladesh University (ABU), Dhaka-1216, Bangladesh,* <*purnarabbee@yahoo.com*>
[2,4] Department of Civil Engineering, Khulna University of Engineering & Technology (KUET), Khulna-9203, Bangladesh, <imrafizul@yahoo.com, alamgir63dr@yahoo.com>

ABSTRACT

This study depicts the experimental investigations into the effect of organic content (OC) on the shear strength and compressibility parameters of reconstituted soil (RCS). To these attempts, disturbed soil samples were collected from two selected locations of Khulna region. The RCS having OC of 5-35 % were prepared in the laboratory to mix at various proportions of inorganic and organic soil at the water content equal to 1.25 times of liquid limits of collected soil samples. The usual procedure of preparation of soil slurry, deposition in a mold and application of surcharge were used to reconstitute sample. The mold diameter was 152 mm and height 222 mm and applied ultimate surcharge was about 60kN/m^2. In the laboratory, ASTM (2004) methods were followed for the determination of strength properties and compressibility parameters of RCS at varying OC. Here, it can be depicted that OC significantly influence the shear strength and compressibility parameters of RCS. Moreover, some important correlations were developed based on strength and compressibility parameters and OC which can be expressed by equations that may be proposed to estimate the various properties of soil of Khulna region using its OC.

Keywords: Organic content, Pre-consolidation Pressure, Strength and Compressibility Properties, Correlations, Comparison.

INTRODUCTION

Khulna region is situated at the south-western part of Bangladesh near the world largest mangrove forest, Sundarbans. The sub-soil of this region consists of fine-grained soils with a considerable part of decomposed and semi-decomposed organic matter (Alamgir et al. 2006). Due to presence of thick organic soil layers, the civil engineering constructions in such sites need special attention to against possible shear failure as well as total and differential settlement. To quantify the effects of such organic deposits on the adopted foundation systems, it is required to establish the behaviour of OC with the soil parameters. In Khulna region, the organic soil layer exists in most of the places within a depth of 10 to 25 ft below the existing ground surface (Rafizul et al. 2009). Moreover, the nature of OC, strength and compressibility properties of this soil are found to vary from place to place. The soil is also erratic in nature both in the vertical and horizontal directions. The bearing capacity of this soil is very low and always leads to adopt a costly foundation for the construction of infra-structures. Sometimes the valuable structures are collapsed due to excessive total and differential settlement while constructed in Khulna region without proper foundation. So, it is obligatory to perform a comprehensive study on the RCS, prepared in the laboratory based on the procedure followed by Burland (1990) to obtain the wide range of OC under a pre-consolidation pressure. Moreover, develop

some correlations among the strength and compressibility properties in relation to the variation of OC of RCS. However, to depict the validity of the developed model then compared with the results available in the literature.

LABORATORY INVESTIGATION

In this study, disturbed soil samples were collected from two selected locations of Khulna region, one from Beel Dakatia, 2 Km away from KUET campus, Khulna at a depth of about 10 feet and another from KUET campus at a depth of about 5 feet from the existing ground surface. The detailed methodology followed for this laboratory investigation presented in Figure 1. In the laboratory through ASTM (2004) methods the physical properties of soil samples were determined provided in Table 1.

Table 1 Physical properties of soil used to prepare RCSs

Location	OC (%)	w (%)	w_L (%)	w_P (%)	G_s	Percentages of constituted soil particles in samples			USCS Symbol
						4.75-0.076mm	0.076-0.002mm	<0.002 mm	
KUET campus	6	21	27	18	2.75	6.0	53.8	40.2	ML
Beel Dakatia	38	192	86	76	2.0	38.0	49.5	15.5	OH

Note: OC=organic content, w=moisture content, w_L=liquid limit, w_P=plastic limit, G_s=specific gravity and USCS=Unified Soil Classification System.

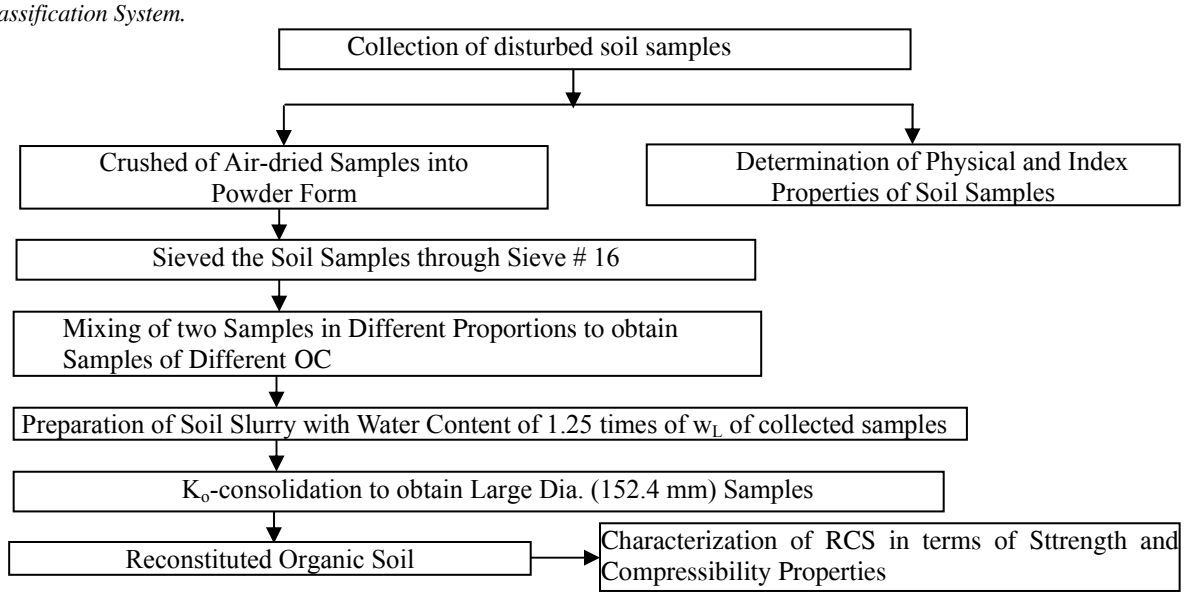

Figure 1: Flow chart of laboratory investigation

Preparation of soil slurry

In this study, the samples were first air-dried and then powdered. The powered samples were then sieved through No 16 sieve and the samples were then mixed with a water content equal to 1.25 times of liquid limits of collected soil samples, which was found as sufficient to yield uniform and homogeneous slurry.

Consolidation of slurry

The slurry was consolidated to form a uniform RCS cake in a cylindrical consolidation mold of 152 mm diameter and 222 mm height. Such types of slurry are consolidated under the pressure of 60kN/m^2. This pressure was maintained until the end of primary consolidation. Initially the slurry was allowed to consolidate by the self-weight and the weight of the porous metal discs for about 24 hours. Then a small pressure of 3kN/m^2 was applied for the next 24 hours. Similarly, the pressure was increased gradually by about 3, 5, 8, 12, 15, 20, 25, 30, 40, 50 and ultimately 60kN/m^2.

Selection of overburden pressure

Earlier the minimum pre-consolidation pressure of 276kN/m^2 that make the clay soil just stiff enough & latter as the skill in testing it was found of 150kN/m^2. (kirkpatrick and khan 1984). Singh (1992) suggested that soil containing high organic matter shows large volume changes on loading & expulsion of water, low shear strength & low dry density. So, in this study, the RCSs were prepared in k_o-consolidation cell by a consolidation pressures, σ_c of 60kN/m^2.

RESULTS AND DISCUSSIONS

This article deals with the presentation and discussions on the observed shear strength and compressibility properties at applied pre-consolidation pressure (σ_c) and varying OC.

Strength properties of RCS

The stress-strain behavior and undrained shear strength (s_u) of RCS at varying OC has been established by conducting unconfined compression test and the findings are discussed in followings.

Stress-strain behavior

The Figure 2 reveals that stress was increased with the increase of axial strain and the strength decreases with the increase of OC and showing almost similar behavior for RCSs at any OC.

Analysis of undrained shear strength

The s_u varies with the increase of OC shown in Figure 3. Results showed that s_u has decreased significantly from 41.0-18.34 kPa for the increase of OC from 5-35 %. Here, it is important to note that a correlation between S_u and OC can be expressed by the following Equation 1.

$$s_u = -0.819*OC+36.35 \quad \text{for OC = 5 to 35\%} \quad \text{.....(1)}$$

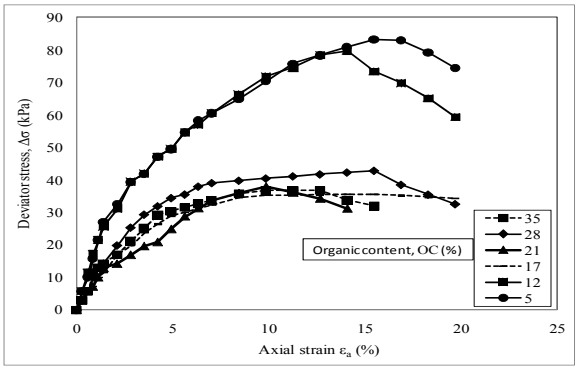

Figure 2 Deviator stress and axial strain of RCSs at varying OC

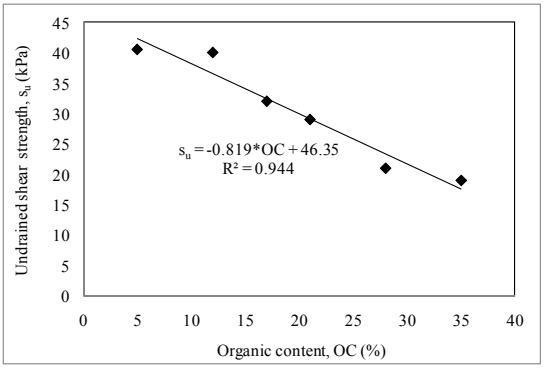

Figure 3 Variation of undrained shear strength with OC of RCS.

Compressibility properties of RCS

Conducting a series of K_o-consolidation tests in the laboratory, compressibility parameters in terms of initial void ratio (e_0), compression index (C_c) and coefficient of consolidation (C_v), as well as primary consolidation period were evaluated and discussed in followings.

Variation of initial void ratio

The Figure 4 shows that e_o has increased significantly from 1.26-1.47 and 1.47-1.94 with the increase of OC from 5-17% and 17-35 %, respectively. The finding is in good agreement with the general behavior of e_o versus OC. In organic soil the void space is more and filled up by air or/and water Oades (1989). Moreover, the correlation between e_0 and OC can be expressed by the Equations 2(a) and 2(b).

$$e_o = 0.017*OC+ 1.165 \quad \text{for } 5\% \leq OC \leq 17\% \text{.....} \quad \text{(2 a)}$$

$$e_o = 0.025*OC+ 1.054 \quad \text{for } 17\% \leq OC \leq 35\% \text{.....} \quad \text{(2 b)}$$

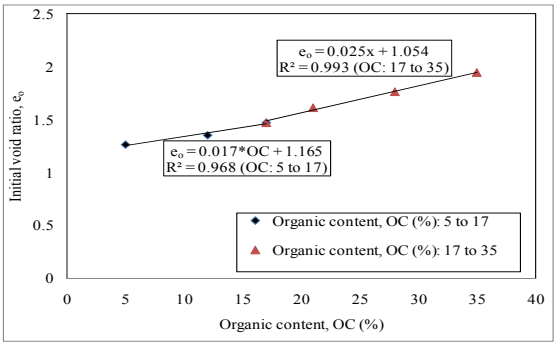

Figure 4 Variation of initial void ratio with OC of RCS.

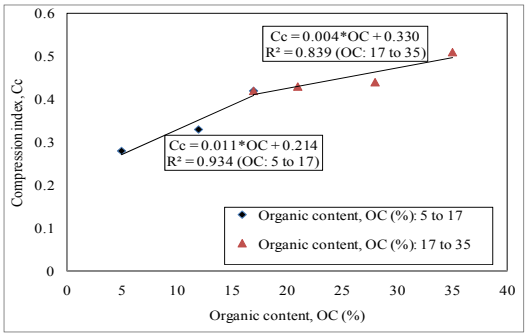

Figure 5 Variation of compression index with OC of RCS.

Analysis of compression index

From the Figure 5, it can be perceived that the values of C_c has increased significantly from 0.28-0.42 in comparatively flatter rate and from 0.42-0.51 in comparatively higher rate with the increase of OC respectively from 5-17% and 17-35 %. Edil (1997) suggested that if the value of OC lies in between 6-20%, it behaves of organic silts and clays and if 21-74%, it behaves of clayey organic soil. The findings of the present study agree well with the postulation given by Edil (1997). It can be seen from here that, a correlation between c_c and OC is expressed by the Equations 3(a) and 3(b).

$$Cc = 0.011*OC + 0.214 \quad \text{for } 5\% \leq OC \leq 17\% \text{..... (3 a)}$$

$$Cc = 0.004*OC + 0.330 \quad \text{for } 17\% \leq OC \leq 35\% \text{..... (3 b)}$$

Analysis of coefficient of consolidation with OC

The variation of coefficient of consolidation (C_v) with different OC as presented in Figure 6. The figure depicts that at a particular applied pressure, say 100 kPa, the value of C_v has changed from 0.0037-0.0308 cm^2/sec for the increase of OC from 5-35%.

Analysis of coefficient of consolidation with applied pressure

The Figure 7 reveals that for OC 35%, C_v increases from 0.0135-0.120cm^2/sec for the increase of applied pressure from 25-800kPa. Similar degree of increment was also observed for the other OC.

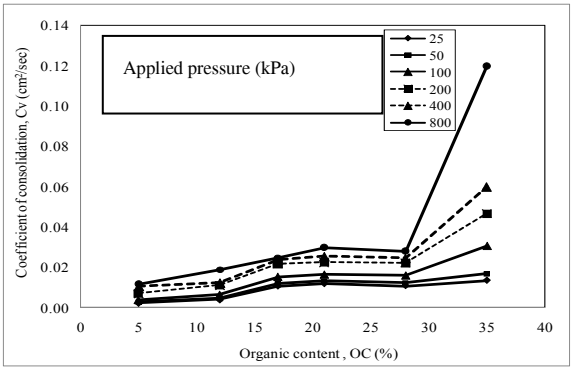

Figure 6 Variation of C_v with OC at varying pre-consolidation pressure.

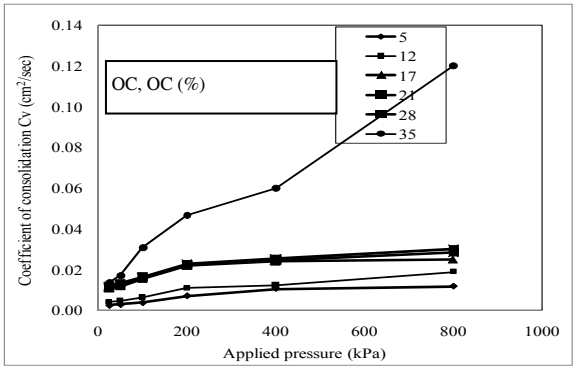

Figure 7 Variation of C_v with applied pressure at varying OC.

Analysis of primary consolidation period with OC

The Figure 8 shows that for the applied pressure 100kPa, t decreases from 6.20-0.74mins. for the increase of OC of 5-35 %. The figure also depicts that the values of t, was found insignificant at high pressure and then it was significant for low pressure.

Analysis of primary consolidation period with applied pressure

The Figure 9 depicts that, for the OC of 35%, the value of t, decreases from 1.69-0.19 mins. with the increase of applied pressure from 25-800kPa. From the figure it can be concluded that the values of t, was found significant at low OC and then insignificant for the high OC.

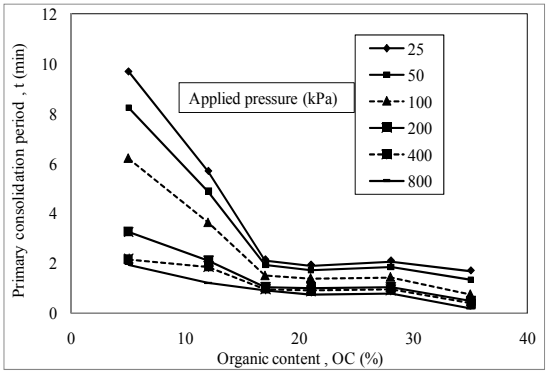

Figure 8 Variation of primary consolidation period with the increase of OC.

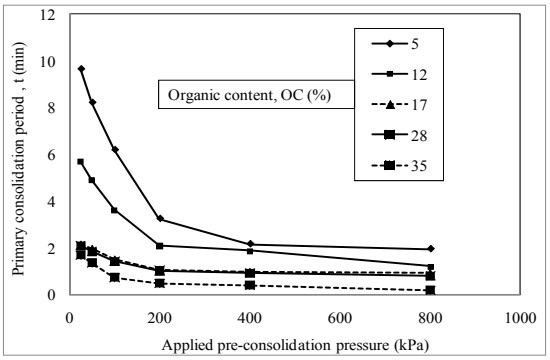

Figure 9 Variation of primary consolidation period at varying applied pressure.

VERIFICATION AND COMPARISON

Any developed correlation is subjected to verification with the existing literature proposed by the other researchers. To these attempts, the relevant statistical model was considered, proposed by the other researchers and hence discussed in the following sections.

Undrained shear strength

The results reported by Franklin et al. (1973) in case of reconstituted organic soil, was compared with the evaluated results in the present study in Figure 10 and it was revealed that the s_u also decreases with the increase of OC. The factors on which the magnitude of s_u depends on are:. Due to these important factors such as soil types, composition, fabrics and structures, depositional environment, stress history and physical and mechanical properties the results obtained from present study and that of reported by Franklin et al. (1973) differs from each other significantly. From the figure, it can be seen that the value of s_u for the RCSs, decreases significantly from 41.0-35.5, 158.5-132.50 and 41.5-31.5 kPa, respectively, with the increase of OC from 5-15%.

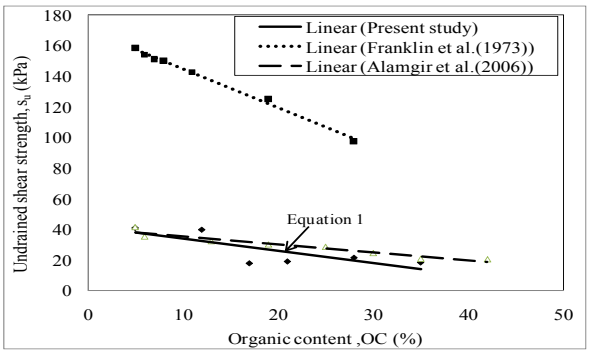

Figure 10 Comparison of s_u obtained from the present study with other sources.

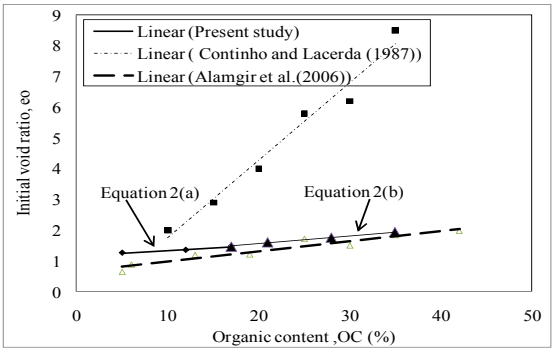

Figure 11 Comparison of e_0 obtained from the present study with other sources

Initial void ratio

Figure 11 represents the comparison of predicted present study results of e_o with those reported by Coutinho and Lacerda (1987). The values of e_o as reported by Coutinho and Lacerda (1987) increases with the increase of OC, and it was also observed for the proposed empirical equation. It can be seen that e_o for the reconstituted organic soils, Coutinho and Lacerda (1987) and published results by Alamgir et al. (2006) increases significantly from 1.26-1.41, 1.0-2.90 and 0.646-1.195, respectively, with the increase of OC from 5-15%.

4.4 Compression index

Figure 12 illustrate that in all cases, the C_c increases with the increase of OC and the results were found in good

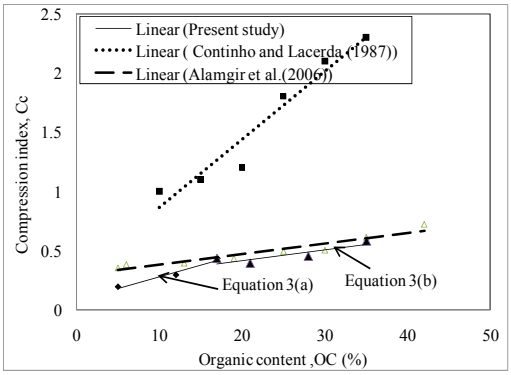

Figure 12 Comparison of proposed equation with other sources.

agreement. The results reported by Coutinho and Lacerda (1987) were found as higher than that of predicted by the present study and Alamgir et al. (2006). From the figure it was also observed that the increasing rate of C_c is 0.143 for the present study with the increase of OC from 5-15 %, while the increasing rate of C_c was found 0.357 and 0.485, respectively, for the published results by Coutinho and Lacerda (1987) and Alamgir et al. (2006).

CONCLUSIONS

Based on this study, the following conclusions can be made:

(i) The shear strength has decreased with the increase of OC and the stress-strain diagram showing the almost similar behaviour for all the RCSs.

(ii) Compression index has increased with the increase of OC in RCSs. Moreover, the coefficient of consolidation has increased for all applied loading conditions and increase of OC of RCS. From consolidation test, it was concluded that the primary consolidation period has decreased for all applied loading conditions and with the increase of OC.

(iii) Here, it can be concluded that the strength and compressibility properties of RCS at varying OC can be expressed by a series of empirical equations with reasonable degree of accuracy and judgment. Among the proposed empirical equations, the following equations (where the symbols bear their usual meanings) can be considered as very important, considering the evaluation of most important parameters of organic soils.

(iv) Finally, based on observed results, it can be depicted that the findings in case of present study was well agreed with the results populated by the other researchers.

$s_u = -0.819*OC+36.35$ for OC = 5 to 35%.....(1)

$e_o = 0.017*OC+ 1.165$ for 5%≤ OC≤ 17%..... (2 a)

$e_o = 0.025*OC+ 1.054$ for 17%≤ OC≤ 35%..... (2 b)

$Cc = 0.011*OC+ 0.214$ for 5%≤ OC≤ 17 %..... (3 a)

$Cc = 0.004*OC+ 0.330$ for 17%≤ OC≤ 35 %..... (3 b)

REFERENCES

ASTM (2004). Manual Book of ASTM Standards, *soil and rock (1)*, D420-D4914. V-04.08-.09, section 4)

Burland, J. B. 1990. The Thirtieth Rankine Lecture: On the compressibility and shear strength of natural soils. *Geotechnique 40, No.3,* pp. 329-378.

Kirkptrick, W. M. and Khan, A. J., 1984. The Reaction of Clays to Sampling Stress Relief. *Geotechnique*, Vol. 34, No.1.

Oades, J.M. (1989) *An Introduction to Organic Matter in Mineral Soils*, Chap. 3. In: J. B. Dixon and S. B.. Weed (EDS.), Minerals in Soil Environment, 2nd edition, SSSABS,1, Madison, WI.

Franklin, A.F., Orozco, L.F. and Semrau, R.(1973). Compaction of slightly organic Soils, *J. of SMFD, ASCE,* 99:SM7:541-557.

Bashar, M. A., 2002, *Stress-Deformation Characteristics of Selected Coastal Soils of Bangladesh and their Sampling Effects*, Ph. D. Thesis, Department of Civil Engineering, BUET, Dhaka, Bangladesh.

Alamgir, M. Rafizul, I. M. and Bashar, M. A.(2006). Physical Properties of Reconstituted Organic Soils at Khulna Region of Bangladesh. *59th Canadian Geotechnical Conf.* October 1-4, 2006.

Rafizul, I. M., Alamgir, M. and Bashar, M. A. (2009). Strength and Compaction Properties of Reconstituted Organic Soils of a Selected Site in Khulna Region. *PrOC. of the Bangladesh Geotechnical Conference, BGS 2009,* December 17, 2009.

Edil, T. B., 1997, Construction Over Peats and Organic Soils, *Proc. Conf. On Recent Advances in Soft Soil Engineering*, Kuching.

Coutinho, R. Q., and Lacerda, W. A., (1987). Characterization and Consolidation of Juturnaiba Organic Clays, *Proceeding of the International Symposium on Geotechnical Engineering of Soft Soils, Mexico, Vol. I.*

ID: AGE 009

1st International Conference on Advances in Civil Engineering 2012 (ICACE 2012)
12 –14 December 2012
CUET, Chittagong, Bangladesh

THE EFFECT OF ADDITIVES ON THE GEOTECHNICAL PROPERTIES OF STABILIZED SOFT SOIL IN KHULNA REGION OF BANGLADESH

MD. ASSADUZZAMAN[1*], M. R. ISLAM[2], T. RABBEE[3] & MOHAMMED ALAMGIR[4]

[1,3]*Department of Civil Engineering, America Bangladesh University (ABU), Dhaka-1216, Bangladesh*
asad_kuet06@yahoo.com, purnarabbee@yahoo.com
[2,4] *Department of Civil Engineering, Khulna University of Engineering &Technology, Khulna, Bangladesh*
imrafizul@yahoo.com & alamgir63@yahoo.com

ABSTRACT
This study has been conducted to investigate the geotechnical characteristics of stabilized Khulna soft soil through cement and lime as the additives. The sub soil in Khulna region consists of very soft soil up to a considerable depth and the bearing capacity is very low. To conduct the experiment of soil stabilization through additives, disturbed soil sample was collected at KUET campus, at a depth of 5 feet from the existing ground surface. After air drying the soil samples then mixed thoroughly with additives at varying content of 5-35 % of the dry mass of soil. The mixing was done properly to get a uniform mixture of soil cement and lime to prepare a uniform paste. The soil paste was then poured in to the cylindrical plastic mold, then after 24 hours, the wrapped specimens were placed under water in the room temperature until testing at the designated rest period of 1-28 days. In the laboratory, ASTM (2004) standard methods were followed for the determination of required parameters of soil. Experimental result reveals that moisture content and unit weight of stabilized soil decreases with the increasing of additives content and rest period. In contrary, compressive strength significantly increases with the increasing of additives content and rest period. Moreover, the stress-strain behavior of stabilized soil shows almost similar for small percentages of cement and lime content as well as rest period. Finally it can be concluded that higher strength was obtained from samples that have been cured for 28 days compared with 1, 3, 7, 14-days cured samples and also obtained that cement stabilized samples shows high strength than lime stabilized soil samples.

Keywords: Additives, stabilized soil, geotechnical parameter, soft soil, Khulna.

INTRODUCTION

In the south and South-east Asian region, due to the increasing trend urbanization and industrialization, marginal sites need to be utilized for the development of infrastructure facilities (Rafizul et al. 2006). Marginal site in this region generally consists of very weak soil deposits. The Civil Engineering construction in such sites needs special attention in terms of Geotechnical Engineering context (Rafizul et al. 2012). The inherent limitation of the conventional foundation lead to choose an alternative solution namely ground improvement technique for solving Geotechnical Engineering problem in the marginal site. Amongst the various ground improvement methods, Shallow soil stabilization and in situ deep mixing technique are widely used for soft ground improvement. Although lime/ cement mixing method has been used to improve the properties of soils near the ground surface since ancient time, deep stabilization of soft soils with lime or cement stabilized columns has been the subject of research. In recent years, construction industries and agencies of Bangladesh concentrated its attention towards invention of suitable substitute of bricks

and therefore have decided to discourage the mass use of bricks where possible to protect the environment. But modern construction technology has provided us with the scope of using soil as universal construction materials for use in building elements, road structure and similar construction by improving the properties of soil using different stabilizing/cementing agents as cement, lime, bitumen, polymer etc. Soil cement i.e. soil mixed with cement, is the most universal and cost effective kind of stabilized soil. The strength development in cement and lime stabilized soil were examined by unconfined compressive strength test at rest period 1, 3, 7, 14 and 28 days for the additives content of 5, 10, 15, 20, 25 and 35 % of the solid weight of soil. The soil stabilization involves combining soils in such 3 ways that when it is compacted under specified condition and to a specified extent, would undergo, material change is it properties and would remain in its stable compacted state without any change under the effect of exposure to weather or traffic. In short stabilization emphasis is given for maximum utilization of local materials so that cost of construction may be minimized to maximum extent.

Information on soil condition of the future Khulna city is important to developers, as it an important factor in construction decision. The sub soil in Khulna region consists of very soft soil up to a considerable depth and the bearing capacity is very low. Their sub soil investigation were carried out in their locations as certain selected geotechnical aspects relating to constructions sub soil condition in Khulna region consists of very soft soil to considerable depth from the ground surface and it often creates problems to geotechnical engineering in designing economical foundation for structure. Chemical admixture always involves treatment of the soil with some kind of chemical compound, which when added to the soil would result in chemical reaction. The chemical reaction modifies or enhances the physical and engineering properties of a soil, such as, volume stability and strength. Chemical stabilized like cement/ lime has two folds effect on the soil characteristics of fluctuation, the clay particles are electrically attracted and aggregated with each other. This results in an increase in the effective size of the clay size aggregation. Such aggregation converts clay into the mechanical equivalent of fine silt. Also, a strong chemical bonding force develops between the individual particles in such aggregation. The chemical bonding depends upon the type of stabilizer employed. The physical and mechanical properties of stabilized soils depend on several factors, mainly the properties of base material and the environmental aspects. The strength development of admixture stabilized soil depends on many factors such as type and properties of soil, quantity and type of admixture, soil moisture content, mixing and compaction method, condition and curing time, temperature, soil minerals and used admixture. The main objectives of this study are (i) to find out the stress strain behavior of cement and lime stabilized soil; (ii) to observe the change of water content in the stabilized soil cement and lime content and rest period and (iii) to observe the strength development in stabilized soil with lime and cement content**.**

MATERIALS AND METHODOLOGY

Soil sampling and laboratory investigations

To conduct the study of soil stabilization disturbed soil near the Khan Jahan Ali Hall in KUET was collected from a depth of about 5 ft below the ground surface. The soil sample was brought to the laboratory and tested for moisture content (%), organic content (%), unit weight, specific gravity, Atterberg limit and grain size distribution and mixed with cement and lime at pre specified percentage (5, 10, 15, 20, 25 and 35 %). The preparation stabilized soil through chemical admixture (cement/ lime) in the laboratory within a short elapsed time is very difficult, therefore, a mechanical study of cement/ lime stabilized soil was occasionally carried out in the laboratory to make out the mechanical properties of stabilized soils. The physical and index properties of the collected soil sample were investigated in the laboratory through the standards methods (ASTM D2487-90) and presented in the Table 1.

Table 1: Physical and index properties of disturbed soils used in this study

Properties	Unit	Value
Water content (w)	%	23.52
Liquid limit (LL**)**	%	30.26
Plastic limit(PL)	%	23.67
Plasticity index(PI)	%	6.59
Specific gravity (G_s)		2.65
Organic content (OC)	%	8

Preparation of stabilized soil

Portland cement mainly consists of four compounds namely tricalcium silicate (C_3S), dicalcium silicate (C2S), tricalcium aluminate (C_3A) and tetra calcium allumino ferrite (C_4AF) which are most strength producing compounds. When the soil encounters with the cement occurring and forms a cementaous compound and the hydrated of lime is deposited as separate crystalline solid phase. In addition, the hydration of cement leads to arise in the pH of the pore water which is caused by the hydrated lime. Moreover, the soil lime stabilization, reaction lime base exchange flocculation, cementing etc. take palace. Thickness of water film around soil particles also reduce. It is noticed that fine soil particles due to reaction with lime. This may be probably be due to flocculation of the lime, such as large size soil particles are susceptible to water , even under soaking condition. This change in size of the particle is more pronounced in case of clay soil rather than silty and sandy soils. Due to flocculation reaction grain size distribution of the soil gates changed. Lime also reduces plasticity of clayey soils. In this study, cement and lime were used for the stabilization of soil. The basic ingredients of cement and lime obtained from routine laboratory test are provided in Table 2.

Table 2: Basic ingredients of cement and lime used as a cementing material

Cement		Lime	
Type of cementing agent	Ordinary portland cement	Principle ingredients	Composition (%)
Normal consistency	25.30%	Calcium oxide	50
Initial setting time	1 hour 15 minutes	Magnesium oxide	25
Final setting time	4 hours 5 minutes	Aluminum oxide	3
Fineness	3.80	Silica	22

A sequence of test is performing in order to observe the effect of cement/lime on the physical and mechanical properties of stabilized soil. The collected undisturbed samples were first brought to the laboratory and spreader it over the floor to get air- dry soil samples. After drying, then soil chucks were broken and grinded by using wooden hammer as fine as possible without applying unnecessary pressure. The soil powder was passed through # 40 standard sieves to avoid the chuck. Air dry soil powder free from any chuck of foreign materials was used as the main ingredients to prepare stabilized soil-cement/lime specimen**.** The water content of air-dry soil sample was measured at a range of 3.75%- 5.5%. The soil paste was then poured in to the cylindrical plastic mould by the help of fingers so that no air voids entrapped into the soil sample. After six hours the specimen removed taken out from the cylindrical mould and it was tightly wrapped in polythene bags to prevent the loss of moisture from the stabilized soil due to evaporation. After 24 hours, the wrapped specimens were placed under water in the room temperature until testing at the designated rest period of 1, 3, 7, 14 and 28 days. Afterward the prepared sample was ready for unconfined compressive test.

RESULT AND DISCUSSION

The effect of additives on the geotechnical properties of stabilized soil in terms of admixture content and curing period of compressive strength, unit weight and moisture content as well as the laboratory on the stabilized soil prepared in the laboratory were analyzed and discussed in hence following.

Effect of additives on moisture content (%) at different rest period

The change of moisture content of cement/lime stabilized soil with the increases of cement/lime content was shown in Figure 1, a presentation of moisture content (%) versus cement content (%) diagram as measured for various rest period. The Figure 1 shows that here is a general trend of the decrease of moisture content with the increases of cement/lime content. As the value of cement/lime content increases, the differences of moisture content for the variation of rest period also increases. The trend of changing the moisture contents very much consistent with the properties of cement/lime stabilized soil. As the cement content /lime content increases, more water is required hydration and cementation to form the gel. From the Figure 1, it can be seen, for the increases of rest period from 1 to 28days, the value of moisture content reduces. The results reveals that as the rest period increases moisture content reduces at a comparatively steeper rate up to 28 days.

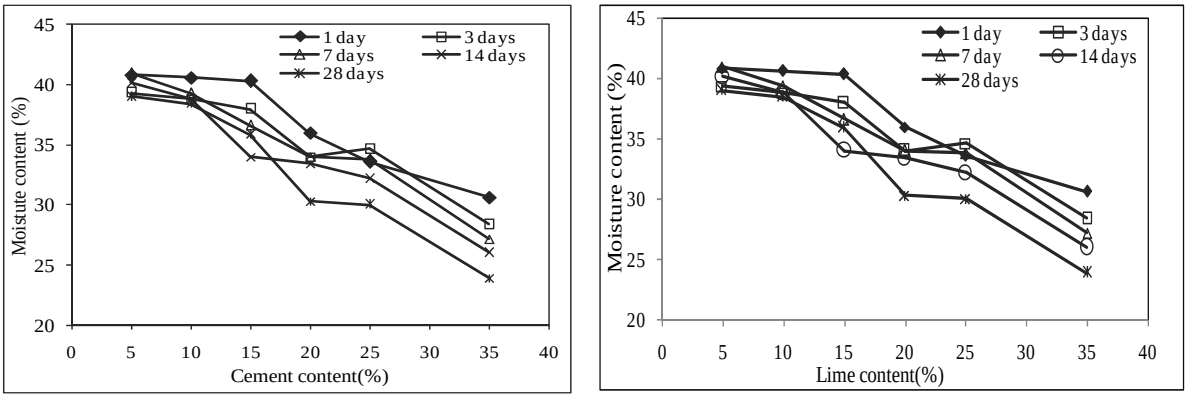

Fig. 1: Changes of moisture content of cement and lime stabilized soil for different rest period

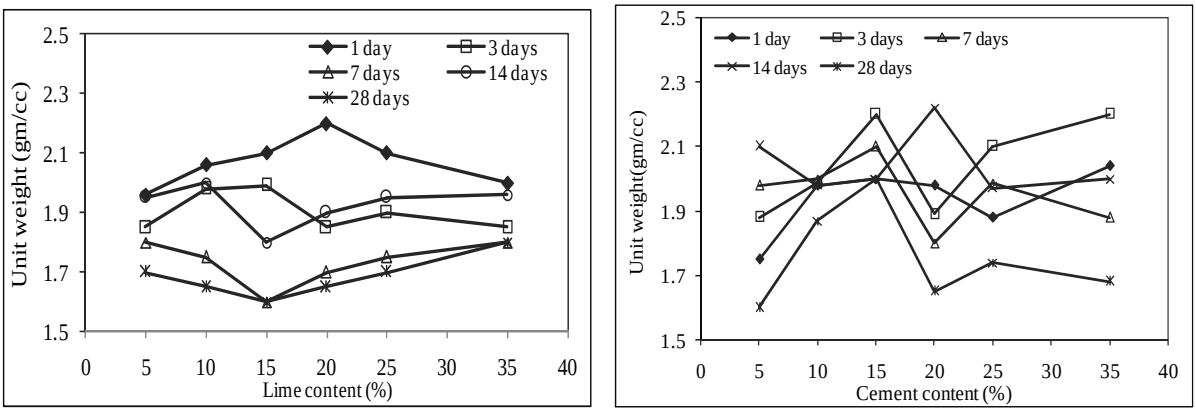

Fig. 2: Changes of unit weight of cement /lime stabilized soil with the increases of rest period for different cement/lime content.

Effect of additives on unit weight at different rest period

Unit weight of cement /lime stabilized soil changes with the increases of rest period for various cement/lime content as obtained from the series laboratory experiments as shown in Figure 2 in a presentation of unit weight versus rest period (days), diagram as obtained for different cement/lime content.

Effect of curing period on deviator stress of cement /lime stabilized soil

The variation of deviator stress with the change of axial strain at varying percentage of cement/lime as shown in Figures 3~6. As a general trend of stress of strain behavior of cement/lime stabilized soil, it can also be seen that as the cement/lime content increases, the stress strain curve stays above than the relatively lower cement/lime content. The compressive strength increases clearly for the increase of cement/lime content from 5-35 % of stabilized soil is provided in Figures 3~6. This phenomenon holds true for any rest period of 1-28 days considered in this study. The intensity of strength development varies with cement content. However, it was found that strength increases almost

linearly with the increase of cement/lime content for all the rest period. Moreover, comparison between Figures 3 and 4 and it was concluded that stabilized soil with more percentage cement content gives more compressive strength than stabilized soil with low percentage cement content. Result reveals that cement stabilized soil had the highest compressive strength than lime stabilized soil.

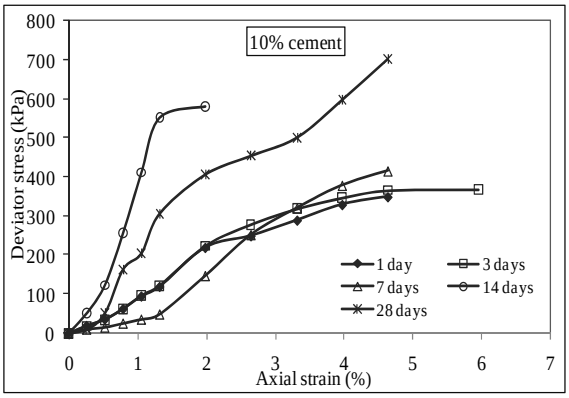

Fig. 3: Stress-strain behaviour of cement stabilized soil at 10% cement content

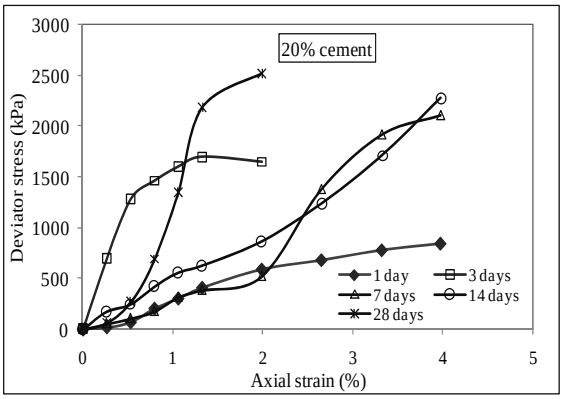

Fig. 4: Stress-strain behaviour of cement stabilized soil at 20% cement content

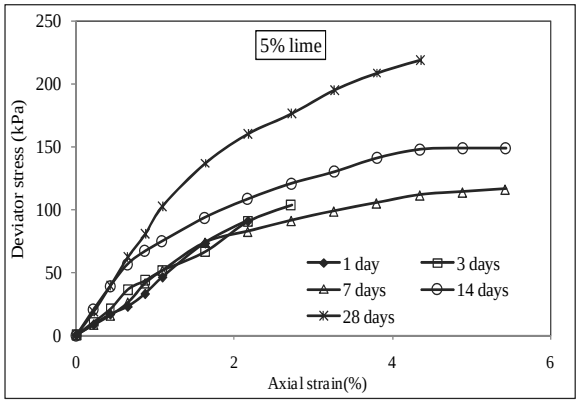

Fig. 5: Stress-strain behaviour of lime stabilized soil at 5% lime content

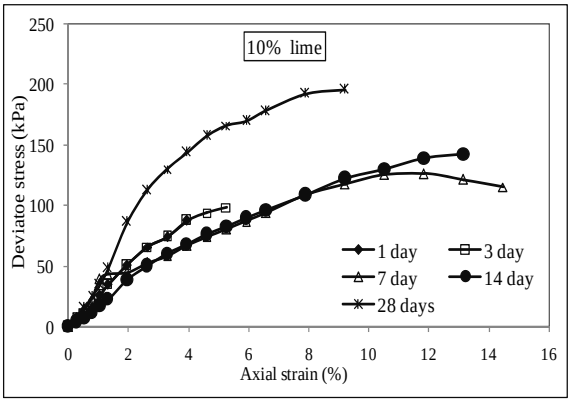

Fig. 6: Stress-strain behaviour of lime stabilized soil at 10% lime content

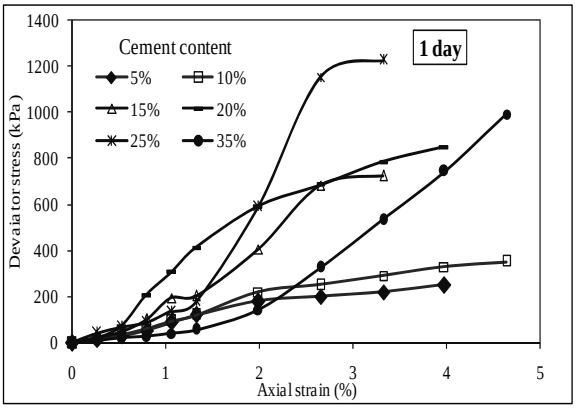

Fig. 7: Stress- strain diagram of cement stabilized soil at varying cement content at 1 day curing period.

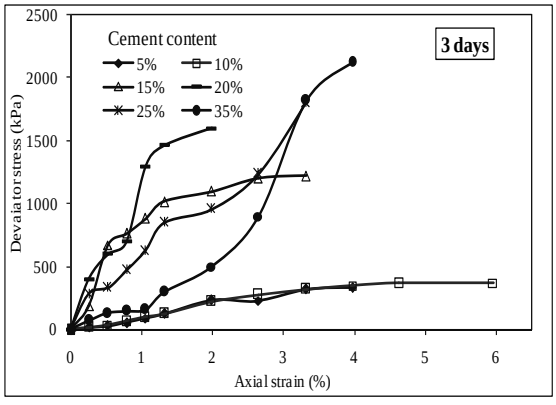

Fig. 8: Stress- strain diagram of cement stabilized soil at varying cement content at 3 days curing

Effect of admixture content on deviator stress of cement /lime stabilized soil

The strength behavior have been established by conducting unconfined compression test on stabilized soil samples prepared in the laboratory using cement/lime at varying content from 5-25 % for the rest period of 1, 3 and 14 days as shown in Figures 7~10. Moreover, studies are carried out to examine the effect of chemical admixtures in terms of admixture content and curing period on q_u of stabilized soil. The effect of cement content varying from 5 to 35%, on q_u of cement /lime stabilized soils at varying cement/lime content from 5 to 35% at rest period 1, 3 and 14 days after prepared as shown in Figure 7~10, respectively. Figures 7 and 8 reveals that the values of q_u increases in relation to the increasing of elapsed

period of cement stabilized soil for same the percentages of cement content. Here, it can be noted that the higher q_u was obtained at rest period 28 days for all the stabilized soil in compare to 1, 3, 7, and 14 days. The variation of q_u mainly depends on the amount of admixture content and curing period. Highest percentage admixture content and curing period shows highest compressive strength value.

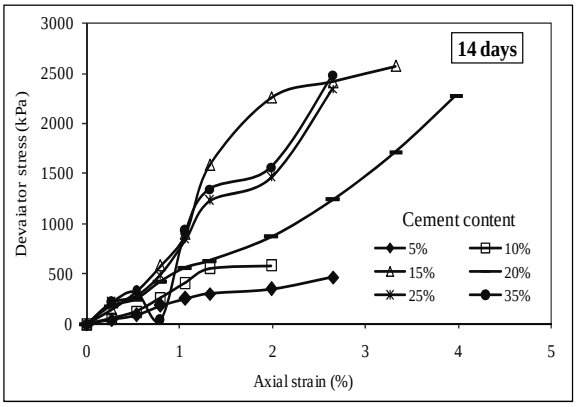

Fig. 9: Stress- strain diagram of cement stabilized soil at varying cement content at 14 days curing

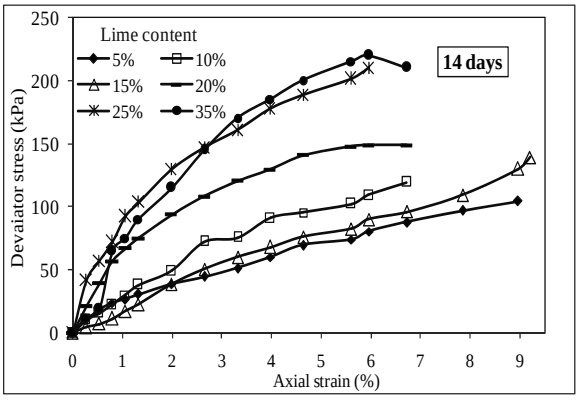

Fig. 10: Stress- strain diagram of lime stabilized soil at varying lime content at 14 days curing period.

CONCLUSIONS

From the results of this study it can be concluded that addition of the additives like cement and lime can improve the engineering properties of stabilized soils, especially after a long curing period. Result reveals that moisture content and unit weight of cement and lime stabilized soil decreases with the increasing of cement and lime content and rest period. In contrary, compressive strength significantly increases with the increasing of additives content and rest period of stabilized soils. Moreover, the stress-strain behavior of stabilized soil shows almost similar for small percentages of cement and lime content as well as rest period but it shows the behavior of hard material such as very hard clay for higher lime and cement content and rest period. Finally it can be concluded that higher strength was obtained from samples that have been cured for 28 days compared with 1, 3, 7, 14-days cured samples and also obtained that cement stabilized samples shows high strength than lime stabilized soil samples.

REFERENCES

Appolonia, D et al. 1971. *Initial settlement of structure on clay.* ASCE. Vol. 97. Pp-1359-1378

Alamgir, M. and Chowdhury, K. H.2004. Ground Improvement methods recently practiced to solve the Geotechnical Engineering problems in Bangladesh. *5th International Conference on case histories in Geotechnical Engineering*, New York, America

Alamgir et al. 2001. Performance of Some Ground Improvement Methods Recently Practiced in the Soft Ground of Bangladesh. *Proc. of the Indian Geotechnical Conf. (IGC2001),* Indore, India.

Broms and Boman. 1975. Lime stabilized column. *5th Asian regional conference on soil mechanics and foundation engineering*, Bangalore, India.

Rafizul et al. 2006. Compressibility Properties of Reconstituted Organic Soils at Khulna Region of Bangladesh. *4th International Conf. on Soft Soil Engg. (ICSSE),* Vancouver, Balkema, Canada.

Rafizul et al. 2012. Characterization and statistical analysis of geotechnical parameters of stabilized organic soil at south western region of Bangladesh. *International Conference on Civil Engineering for Sustainable Development (ICCESD2012),* KUET,Khulna, Bangladesh.

Razzaque, M.A and Alamgir, M. 1999. Long term settlement observation of a building in a peat deposits of Bangladesh. *International Conference on Civil & Environmental Engineering- New Frontiers and Challenges*. Bangkok.

Alamgir, M. 1996. *Analysis of soft ground reinforced by columnar inclusion.* Ph. D thesis, Department of Civil Engineering , Saga University, Saga, Japan

ID: AGE 011

1st International Conference on Advances in Civil Engineering 2012 (ICACE 2012)
12 –14 December 2012
CUET, Chittagong, Bangladesh

DEVELOPMENT OF A SIMPLE DESIGN PROCEDURE OF SAND COMPACTION PILE METHOD

S. S. AHMED[1*], A. MUQTADIR[2], M. J. ABADIN[3]

[*1]*Lecturer, Department of Civil Engineering, CUET, Chittagong-4349, Bangladesh, sharifce05@gmail.com*
[2]*Professor, Department of Civil Engineering, BUET, Dhaka-1000, Bangladesh*
[3]*Assistant Engineer, Bangladesh Water Development Board, Dhaka, Bangladesh*

ABSTRACT
Sand Compaction Pile (SCP) Method is gaining popularity as ground improvement technique in different countries of the world. The available design procedures of sand compaction pile method are based on empirical relations from field test results. The available design procedures are not so simple and convenient and the inadequate presence of design charts and graphs makes it a difficult task. This study focuses to develop a simple and straightforward design procedure of sand compaction pile method. In this study, empirical relationships developed by several authors are used to construct graphs relating the design parameters. The design charts and graphs are very useful in the reduction of calculations. The developed design method is compared with some case studies and the case study values compare well with the proposed method. The flow chart of proposed design procedure is also provided.

Keywords: Sand Compaction Pile, Ground Improvement Technique, Design Procedure

INTRODUCTION

Sand compaction pile method, shortly known as SCP method is a ground improvement technique which is applicable in both sandy soil and clayey soil. This method was developed in Japan in order to increase the density of loose sandy ground and to increase the uniformity of sandy ground, to improve its stability or compressibility to prevent liquefaction failure.

The available design procedures of sand compaction pile method are based on empirical relations from field test results. The design procedure for both sandy soil & clayey soil are different. A few methods are available for design approach of sand compaction pile. Design procedures available are proposed by-

1. Nurayama & Tanimoto (1957-1962);
2. Mizuno, Suematu & Okuyama (1987);
3. Aboshi, Mizuno & Kuwabara (1991).

All the available design approaches have both some advantages and some limitations.
In this study, a simple and clear design approach of sand compaction pile method is developed. In the present study the empirical relationships developed by Balaam & Booker (1981), Yoshida et. al. (1988), Tsukamoto et al. (2000) and Hatanaka et. al. (2008) are used. In developing a simple design approach, graphs are constructed using the empirical relations developed by the above stated authors. This method is developed focusing to reducing calculations.

The design of sand compaction pile in sandy soil is based on the normalized SPT N-value (N_1) of the soil, the angle of internal friction ($Ø_d$), the replacement ratio (a_s), the relative density of soil (D_r) and the bearing capacity (q_u) of the soil.

RELATION BETWEEN NORMALIZED SPT N-VALUE BEFORE AND AFTER SCP

According to Tsukamoto et al. (2000), the relation between normalized SPT N-value before and after SCP can be expressed as,

$$N_{1\_tr} = N_{1\_untr} + \frac{a_s N_{1\_untr}}{A + B a_s} \quad (1)$$

Where, N_{1_tr} is the modified SPT N_1 value of the treated soil; a_s is the replacement ratio expressed in percentage; and A and B are the parameters that depend on SPT N_1 value of untreated soil (N_{1_untr}) as,

$$A = 1.28e^{0.13N_{1\_untr}} \quad (2)$$

$$B = 0.03N_{1\_untr} \quad (3)$$

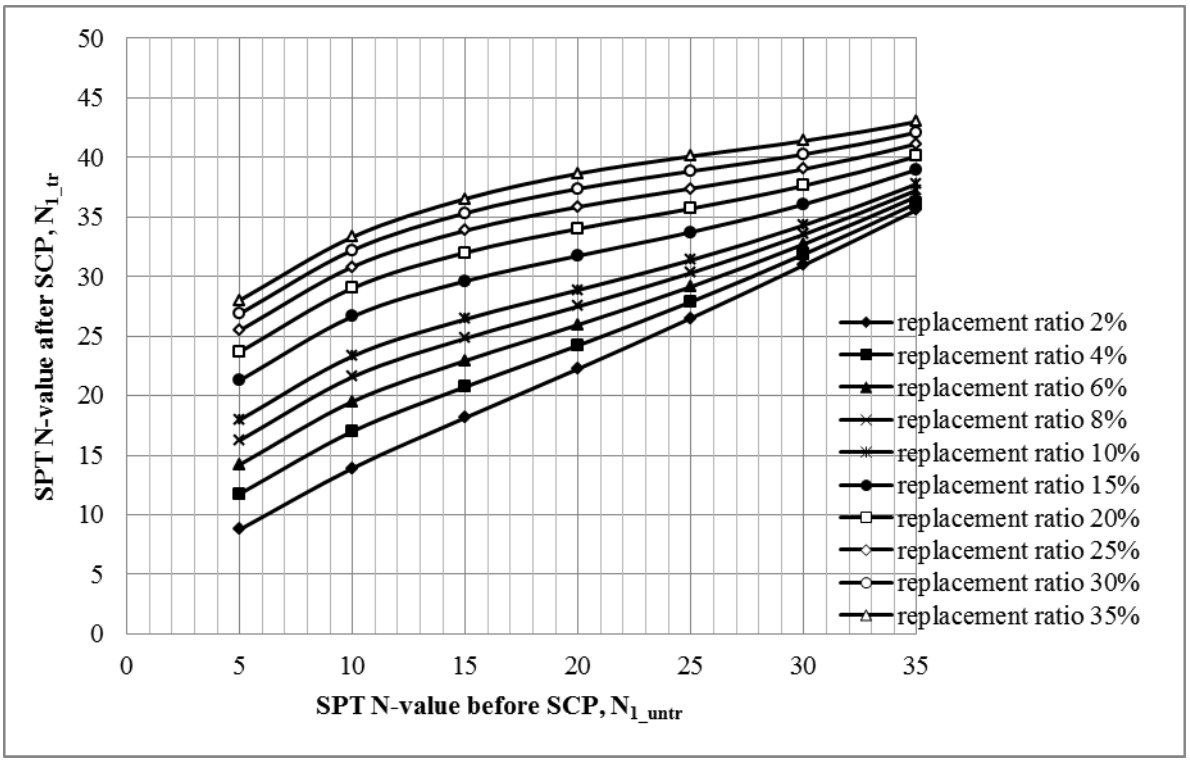

Fig. 1 Relation between SPT N-values before SCP & after SCP at different Replacement Ratio

RELATION AMONG REPLACEMENT RATIO, DIAMETER OF SCP AND CENTRE TO CENTRE SPACING OF SCP

The replacement ratio can be expressed as,

$$\mathbf{a_s = (d_c/d_e)^2 \times 100} \quad \mathbf{(4)}$$

Where, $\mathbf{d_c}$ is the diameter of the sand compaction pile and $\mathbf{d_e}$ is the diameter of the unit cell

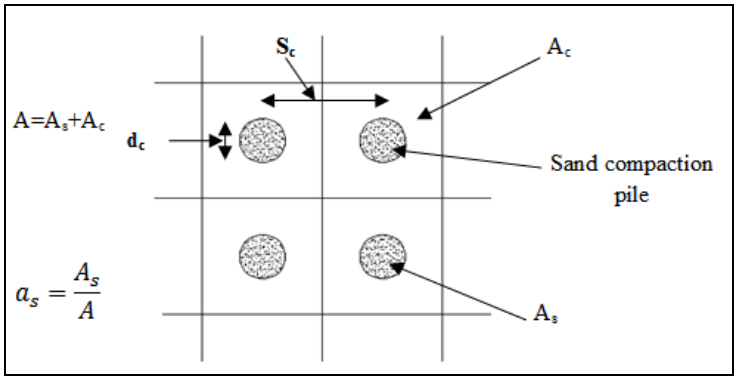

Fig. 2 Replacement Ratio

Balaam & Booker (1981) proposed the following relationship,

$$\mathbf{d_e = C_g.S_c} \qquad \mathbf{(5)}$$

Where, $\mathbf{S_c}$ = Center to Center Spacing of sand compaction pile
$\mathbf{C_g}$= Geometry dependent constant (1.05, 1.13 and 1.29 for triangular, square and hexagonal arrangements, respectively).

From the above two equations, relationship among Replacement Ratio (a_s), Diameter of SCP (d_c) and Centre to Centre Spacing of SCP (S_c) is shown here **(Fig. 3 and 4).**

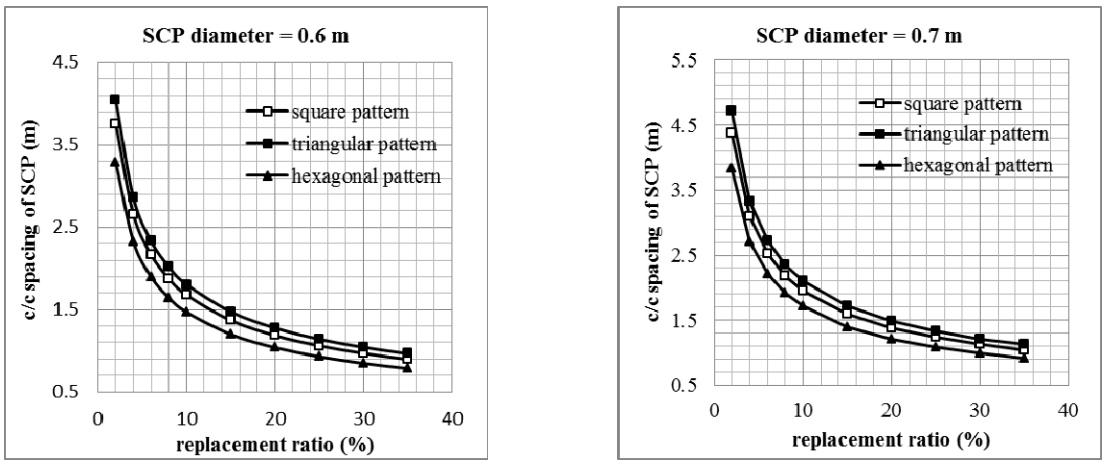

Fig. 3 Relation between c/c spacing & replacement ratio

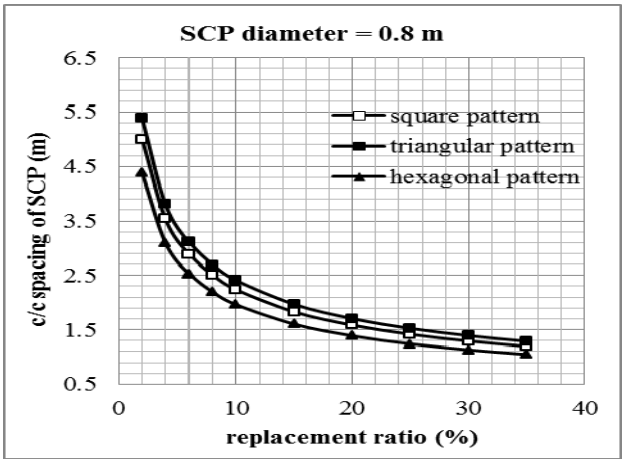

Fig. 4 Relation between c/c spacing & replacement ratio

RELATION BETWEEN SPT N-VALUE AND ANGLE OF INTERNAL FRICTION

The relation between SPT N-value and Angle of Internal Friction is presented here **(Fig. 5).**

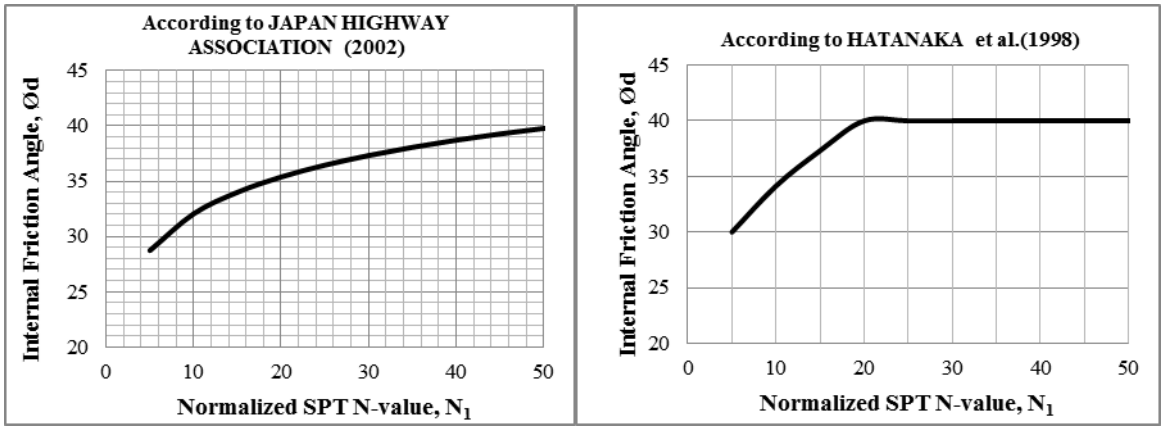

Fig. 5 Relation between Internal friction angle ($Ø_d$) & Normalized SPT N-value, N_1

RELATION BETWEEN RELATIVE DENSITY (D_R), REPLACEMENT RATIO (A_S) AND SPT-N VALUE

The SPT N value as well as the Relative density of treated soil by sand compaction pile method has been observed to increase significantly for increasing replacement ratio. The relation between normalized SPT N-value before and after SCP is already expressed in equation (**1**), (**2**) and (**3**). Again, **Yoshida et al. (1988)** suggested correlating relative density with SPT-N_1 value the following equation,

$$D_r = 25 P_0'^{(-0.12)} N_1^{(0.46)} \qquad (6)$$

Where, P_0' is the Existing overburden pressure

The equations have been used to prepare graphs (**Fig. 6)** to compare the increase of relative density with increase in replacement ratio for different SPT N_1 value before treating the ground by SCP. The existing overburden pressure of 100 KPa has been assumed.

It is seen that the relative density increases significantly for higher replacement ratio and lower SPT N-value obtained before SCP.

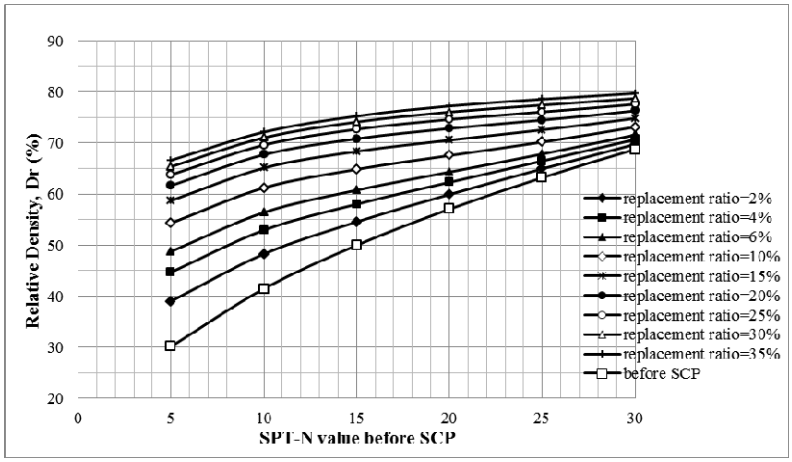

Fig. 6 Comparison of Relative Density at different Replacement Ratio

RELATION BETWEEN RELATIVE DENSITY AND ANGLE OF INTERNAL FRICTION

According to **Meyerhof (1959)**, the relation between relative density and angle of internal friction can be expressed as

$$\mathbf{Ø_d = 28 + 0.15\ D_r} \qquad \mathbf{(7)}$$

Where, $\mathbf{Ø_d}$ = Angle of internal friction, $\mathbf{D_r}$ = Relative density in percent

The above relationship is presented here in graphical form **(Fig. 7).**

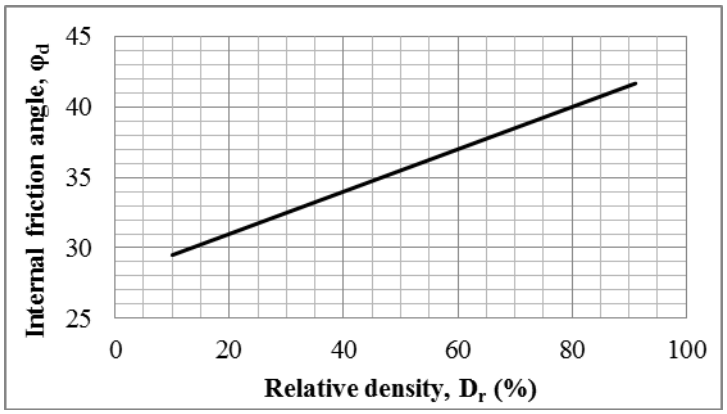

Fig. 7 Relation between Relative density & internal friction angle
(After Meyerhof, 1959)

Another relationship between relative density and angle of internal friction can be given by the following **(Gibbs & Holtz, 1957).**

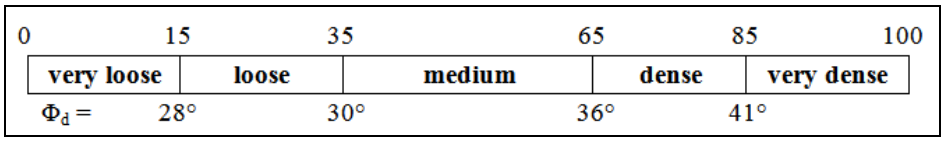

Fig. 8 Relation between Relative density & Internal friction angle of sand
(After Gibbs & Holtz, 1957)

DEPTH OF PENETRATION OF SCP IN HARD SOIL STRATUM

SCP improved ground is divided into two improvement types- fixed type and floating type. The fixed type improvement is a type where sand piles reach a stiff layer and the floating type improvement is a type where sand piles do not reach a stiff layer but end in a soft soil layer. Fixed type improvement is always preferable. But where the soft soil layer is quite deep, floating type improvement is recommended considering the influence of effective stress valve from structural loading.

PROPOSED SIMPLIFIED DESIGN PROCEDURE OF SCP FOR SANDY SOIL DISREGARDING FINE CONTENT

a) Find Normalized SPT N-value N_{1_untr} from SPT test of soil.
b) Compute the bearing capacity of soil using Terzaghi's bearing capacity equation $\mathbf{q_u = qN_q + \frac{1}{2}\gamma BN_\gamma}$ assuming a value of $Ø_d$.
c) Continue the above process by trial and error until required bearing capacity is not satisfied.
d) From the value of $Ø_d$, find the required normalized SPT N-value after SCP, N_{1_tr} **(Fig. 5)**

e) From the graphs of N_{1_tr} vs. N_{1_untr} for different replacement ratio a_s, select a suitable replacement ratio. (**Fig. 1**)
f) Select a diameter of SCP such as 700mm or 800 mm and choose a pattern such as square, triangular or Hexagonal.
g) From the available graph (**Fig. 3** to **Fig. 4)** choose the spacing of SCP.

ALTERNATIVE DESIGN PROCEDURE

a) Find Normalized SPT N-value N_{1_untr} from SPT test of soil.
b) Assume a replacement ratio and compute the Relative Density of soil after SCP corresponding to the N_{1_untr} from the available graphs **(Fig. 6)**
c) Find the angle of internal friction $Ø_d$ corresponding to the Relative Density **(Either from Fig. 7 or Fig. 8)**
d) From Terzaghi's bearing capacity equation, $\mathbf{q_u = qN_q + \frac{1}{2}\gamma BN_\gamma}$, compute the bearing capacity of improved ground.
e) Compare the computed bearing capacity with required.
f) Repeat the procedure until the required bearing capacity is not satisfied.
g) Then select a diameter of SCP such as 700mm or 800 mm and choose a pattern such as square, triangular or hexagonal.
h) From the available graph (**Fig. 3** to **Fig. 4)** choose the spacing of SCP.

A CASE STUDY: SURALAYA STEAM POWER PLANT IN INDONESIA

The Suralaya Steam Power Plant is located on the northwestern tip of the island of Java, Indonesia. Foundations for Units 1 and 2 of the first large steam power plant in Indonesia consist of concrete rafts supported on slender, end-bearing steel cased concrete piles. Soil investigation established the presence of layers and/or lenses of locally loose silty fine sands at various depths. It was necessary to density these materials to ensure that unacceptable differential settlement did not occur between separate shallow foundations and to reduce the potential for liquefaction of the looser zones in the event of seismic disturbance.

A program of testing was undertaken prior to the start of production work to establish the required pile spacing. Each test consisted of Standard Penetration Test (SPT) pre-testing, ground improvement of a 250- 1074 m² area with compaction piling in a set pattern, and then post-testing with the SPT. Spacing of 1.4 m, 1.6 m, and 1.8 m were used. Based on the test results, a triangular grid pattern with spacing 1.6 m between centers of 0.51 m diameter casings was used throughout the works.

The figure below (Fig. 9) indicates that after ground improvement by SCP, the SPT values increases significantly.

The average sand consumption was 0.51 m^3/m pile, corresponding to a sand column diameter of 0.76 m. The replacement ratio was nearly 17%. The average increase in SPT values was uniform and more than 10 where in this study the increase is well above 10. The required average spacing for diameters of 0.6m, 0.7m & 0.8m for triangular pattern is 1.6m in the present study. So, the case study values compare well with the proposed method. Again, for the replacement ratio of 17% and the SPT N-value before SCP of 10, the corresponding relative density from this study is found to be above 70% where the required relative density is 75%. So, the values by alternative method also compare well with the case study values.

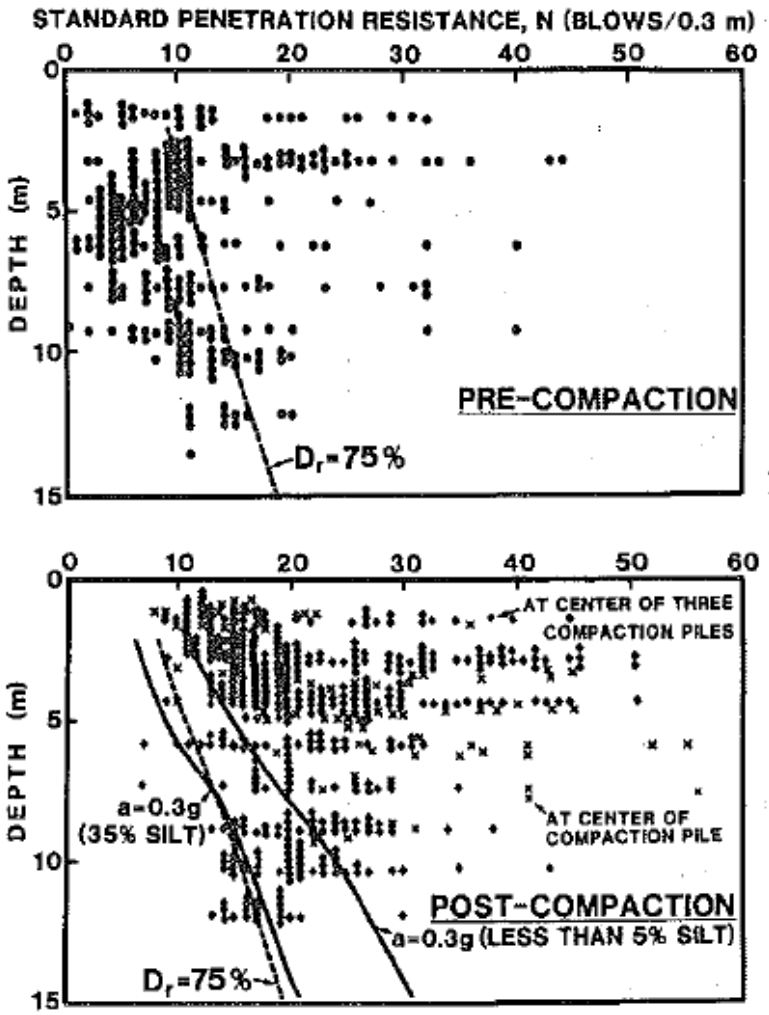

Fig. 9 Comparison of SPT values before and after SCP

CONCLUSIONS

From the above study the following remarks can be made.

a) A simple design procedure for ground improvement by sand compaction pile method is developed which is graphical in nature and straightforward.
b) Graphs have been constructed to reduce the calculation and to make the design method to be more effective.
c) The proposed design procedure is compared with a case study and is found to produce satisfactory results.
d) An alternative method is also presented which provides the opportunity of cross checking.
e) Flow charts of two design procedure are provided.
f) There are a few methods available for the design of sand compaction pile method and this method is believed to be used as the simplest and one of the efficient of them.

Flow chart of proposed design procedure

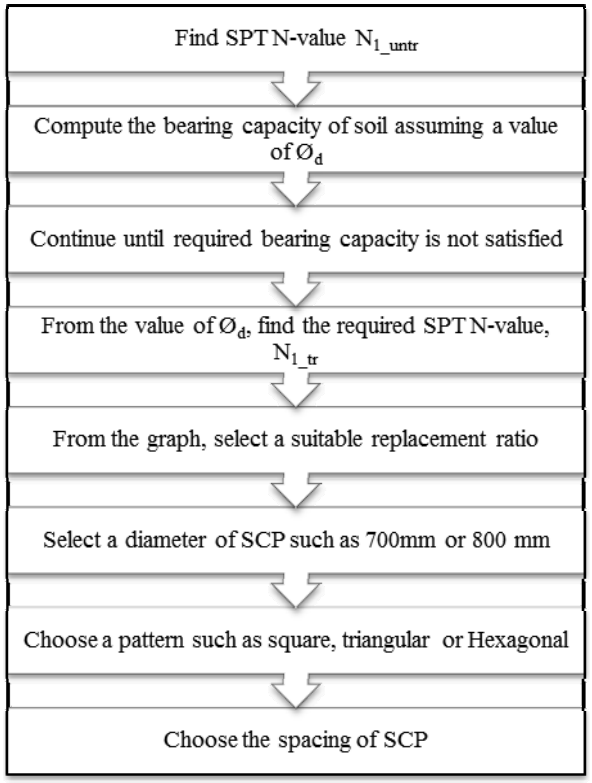

Flow chart of alternative design procedure

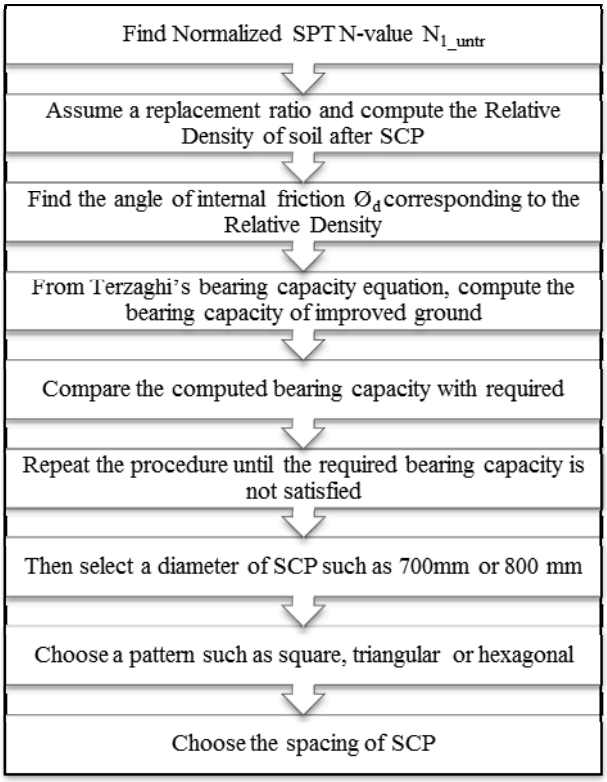

REFERENCES

Aboshi, H., Mizuno, Y. and Kuwabara, M. (1991), *"Present state of sand compaction pile in Japan."* Deep Foundation Improvements: Design, Construction and Testing, ASTM STP 1089, Melvin I. Esrig and Robert C. Bachus, Eds., American Society for Testing and Materials, Philadelphia, 1991.

Das., B.M., *"Principles of foundation engineering."* 5th edition.

Gibbs, H. J., and Holtz, W. G., "*Research on Determining the Density of Sands by Spoon Penetration Testing,"* Proceedings of the Fourth International Conference on Soil Mechanics and Foundation Engineering, Vol. 1, London, England, 1957, pp. 35-39.

Hasan, M.B., *"Chapter 4-1: Soil Improvement and Ground Modification."* Department of Civil and Environmental Engineering, Universiti Malaysia Pahang.

Hasan, M.B., *"Chapter 4-3: Soil Improvement and Ground Modification."* Department of Civil and Environmental Engineering, Universiti Malaysia Pahang.

Hatanaka, M., Feng, L., Matsumura, N. and Yasu, H. (2008), *"A study on the engineering properties of sand improved by the sand compaction pile method."* Soils and Foundations 48(1), pp. 73-85.

Krishna, A.M. and Madhab, M.R. (2009), *"Treatment of loose to medium dense sands by granular piles: Improved SPT 'N_1' values."* Technical note, Geotech. Geol. Engg. by Springer 27, pp. 455-459.

Moh, Z.C., Ou, C.D., Woo, S.M. and Yu, K. (1981), *"Compaction sand piles for soil improvement."* Proc. 10th Int. Conf. on soil Mech. and Found. Engg., pp. 749-752.

Solymar, Z.V., Samsudin, Osellame, J. and Purnomo, B.J. (1986), *"Ground improvement by compaction piling."* Journal of geotechnical engineering 112(12), pp. 1069-1083.

ID: AGE 012

1st International Conference on Advances in Civil Engineering 2012 (ICACE 2012)
12 –14 December 2012
CUET, Chittagong, Bangladesh

AN EXPERIMENTAL ANALYSIS OF PILE CAPACITY ON GRANULAR SOIL

R. SAHA[1*], A. AL JAHAN[2], A.K.M. M. MORSHED[2], MD. HASHINUZZAMAN[2]

[1]Institute of Water Modelling, Dhaka, 1000, Bangladesh
[2]Bangladesh University of Engineering & Technology, Dhaka, 1000, Bangladesh
**Corresponding Author*

ABSTRACT

The Direct Shear test has been performed following an experimental approach in order to obtain more simplified and less time consuming method of performing direct shear test to evaluate the shear strength parameter of cohesion less soil. Hence the pile capacity has been calculated using the strength parameter.

The test result of the conventional method and the test result of the experimental approach have been compared by means of which the acceptability of the experimental approach can be verified. During the conventional shearing process, the one portion of the soil is made to slide along another (soil/ foundation material) by the action of a steadily increasing horizontal shearing force while a constant load is applied normal to the plane of relative movement. In this method, the tests are performed for different normal load for different individual sample which requires large number of soil sample as well as long course of time. In order to avoid these disadvantages, the test can be performed by using different normal load but using the same sample which has been termed as experimental approach. The lateral stress of soil increases with the increase of normal load, the test has been performed with gradual increase of normal load in order to calculate the relative shear strength of the soil. Moreover, the change of normal load on the samples simulates the change of normal load on pile from the soil with the change of depth. Hence, the data obtained from the tests are can be used to predict the pile capacity in laboratory. Analyzing the data it has figured out that the skin friction of pile obtained from laboratory tests are quite higher than theoretical methods(Tomilinson, Terzaghi & Peck chart) of calculation, which ranged 10 to 30 percent higher than the theoretical value. So, it can be said that the conventional analysis of pile skin friction imparts higher factor of safety in context of granular soil of Bangladesh.

Keywords: Direct Shear test, Pile capacity, Granular soil, Theoretical methods, Conventional method, Experimental approach, Skin friction.

INTRODUCTION

Soil is a natural body consisting of layers (soil horizons) of mineral constituents of variable thicknesses, which differ from the parent materials in their morphological, physical, chemical, and mineralogical characteristics.

The strength of a soil depends of its resistance to shearing stresses. It is made up of basically the components:

1. *Frictional* – due to friction between individual particles.
2. *Cohesive* – due to adhesion between the soil particles.

In this study, direct shear test of soil in different conditions are considered from the point of view of comparing soil behavior, failure criteria and ultimate pile capacity in cohesionless soils.

Objectives

- To determine the pile capacity of cohesionless soil in variable void ratio and moisture content using rational approaches.
- To contrast the test result of different approaches.
- To find the shear stress of cohesionless soil with foundation materials (pile surface).
- To analyze the mechanical properties of soil sample.
- To plot shear stress vs. shear displacement, shear stress vs. normal stress graphs.

Scope of work

An experimental programmed was carried out through direct shear test involving foundation materials and cohesionless soil. The conventional method of direct shear test requires different individual sample for each individual normal load which is time consuming. Hence the direct shear test has been carried out in the same sample for different normal load. A comparison between different methods is presented to show the influence of the foundation materials on the angle of shearing resistance at failure, the shear characteristics, the failure criterion and the pile capacity.

Outline of paper

The test data obtained from laboratory test have been assembled and related graphs have been plotted. Analyzing the graphs various shear strength parameters and pile capacity have been calculated and congruency of the resulting values has been checked with standard values. Hence the soil samples have been categorized accordingly.

MATERIALS AND METHODS

The soil samples, for different geotechnical tests have done, were collected from Plot No-338/A, Bloc-E, Bashundhara R/A, Bashundhara, Dhaka. Samples were collected from two different bore holes. These were bore holes 12 and 26. **Bore hole 12** had SPT blows 50 per 8 inch penetration at depth of 114.5-116 ft. **Bore hole 26** had SPT blows 50 per 9 inch penetration at depth of 119.5-121 ft. Samples were gray in colour and silty fine sand in nature.

The #200 sieve wash test is used to separate silts and clays from sand and gravels. It is difficult to break up soil particles into individual soil grains so they can pass through the small openings of the #200 sieve. Washing the soil through the #200 sieve with water produces more accurate results as the water helps to break the soil down into its elemental particle size and wash the silts and clays off of individual sand and gravel particles.

Hydrometer analysis is based on the principle of sedimentation of soil grains in water. When a soil specimen is dispersed in water, the particles settle at different velocities, depending on their shape, size and weight and the viscosity of water.

There are several laboratory methods available to determine the shear strength parameters (c, φ, c', φ') of various soil specimen in the laboratory. Of them the direct test is simple to perform, but it has some inherent shortcomings. The reliability of the result may be questioned because the soil is not allowed to fail along the weakest plane but is forced to fail along the plane of split of shear box. Also the shear stress distribution over the shear surface of the specimen is not uniformed. Despite these shortcomings, the direct shear test is the simplest and most economical for a dry or saturated sandy soil.

Direct shear test is the straightforward procedure for measuring the immediate shear strength of soil in terms of total stress. The usual method of direct shear test needs individual sample for individual normal load and hence every change of normal load needs new sample to govern the test. Making new sample and arranging the shear box is quite time consuming as well as uncomfortable to maneuver. Hence considering this facts, an experiment has been made to figure out whether the test can be performed on the same soil sample for different normal load after unloading the previous load or not.

The soil sample placed in shear box has been subjected to normal load 12.5 kg then the shear test has performed, then the 12.5kg load has been withdrawn and the motorized shear force has unloaded. Then 25kg normal load has imposed and test data has been collected and then unloaded similarly the previous way. The test data has been collected for normal load of 50kg and 100kg also. Meanwhile, the usual direct shear test has also been performed on the soil sample by using different samples for different normal load applied in order to compare the results of both experiment. Analyzing the resulting graphs of the test data the shear strength parameter of the each soil sample has been calculated and compared with each other as well as with the international standards.

In many foundation design problems, one must determine the angle of friction between the soil and the material in which the foundation is constructed. The foundation material may be concrete, steel or wood. The shear strength along the surface of contact of the soil and the foundation can be given as

$$T_f = c_a' + \sigma' \tan \delta$$

Where, c_a' = adhesion

δ = effective angle of friction between the soil & the foundation material

The shear strength parameters between a soil and the foundation material can be conveniently determined from a direct shear test. This is a great advantage of direct shear tests. The foundation material can be placed in the bottom part of the direct shear test box and the soil can be placed above it.

The shear strength of dry sand depends upon several factors, such as the mineralogical composition of the grains, their size, shape, surface texture and grading, the soil structure i.e. packing of the grains, and the moisture content. For particular sand in the dry state the only variable is the state of packing, which has an important influence on shear strength.

The classic formula for calculating the skin resistance of piles in granular soil is expressed below:

$$\text{Skin friction (S.F.), psi} = 0.5 K_s \sigma_v' \tan\delta$$

Where σ_v' is the effective overburden pressure at pile base level, K_s is a coefficient of horizontal soil stress which depends on the relative density and state of consolidation of the soil, the volume displacement of the pile, the material of the pile and its shape, δ is the angle of friction between pile and soil.

RESULTS AND DISCUSSIONS

The test results that have been obtained from analyzing the data and graphs are given below from which the result can be analyzed and interpreted contrasting with standard values.

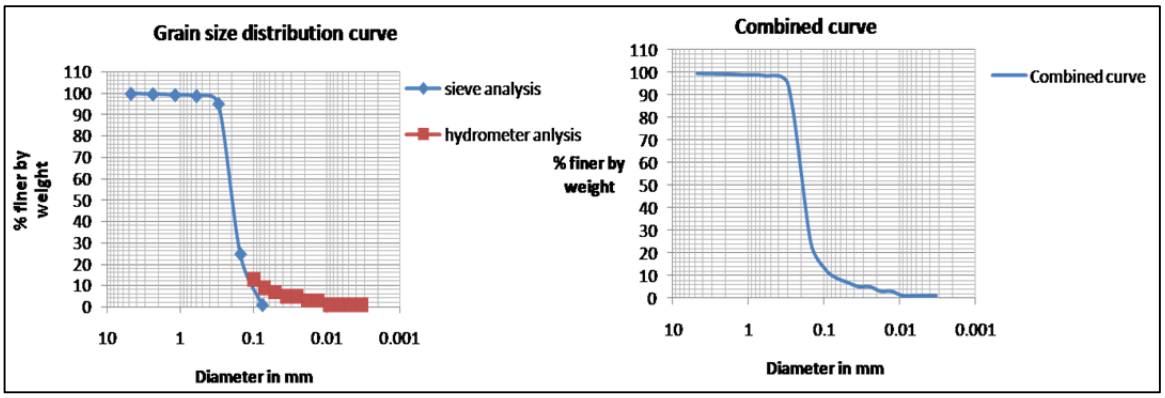

Fig1: Grain Size Distribution curve of Sample Bore Hole 12

Findings are given below:

Specification	Results	Specification	Result
10% finer materials, D_{10}	0.11mm	Uniformity coefficient, Cu	1.909
30% finer materials, D_{30}	0.16mm	Coefficient of Gradation, Cz	1.108
60% finer materials, D_{60}	0.21mm	Fineness Modulus, FM	0.84

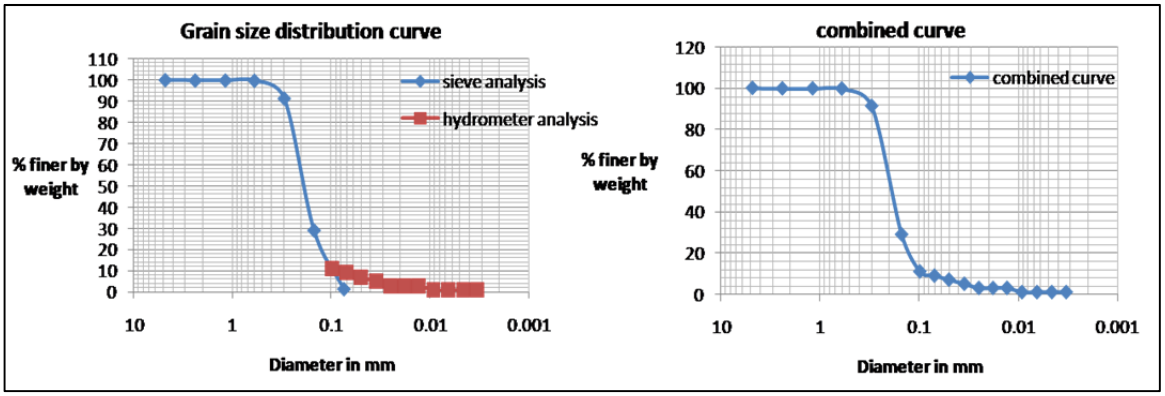

Fig2: Grain Size Distribution curve of Sample Bore Hole 26

Findings are given below:

Specification	Results	Specification	Result
10% finer materials, D_{10}	0.098mm	Uniformity coefficient, Cu	2.143
30% finer materials, D_{30}	0.115mm	Coefficient of Gradation, Cz	1.167
60% finer materials, D_{60}	0.21mm	Fineness Modulus, FM	0.805

Consultation on mechanical properties of soil sample

Values found of uniformity coefficient, gradation coefficient, fineness modulus vary with ASTM standard values indicating that the samples are poorly graded sand for both cases.

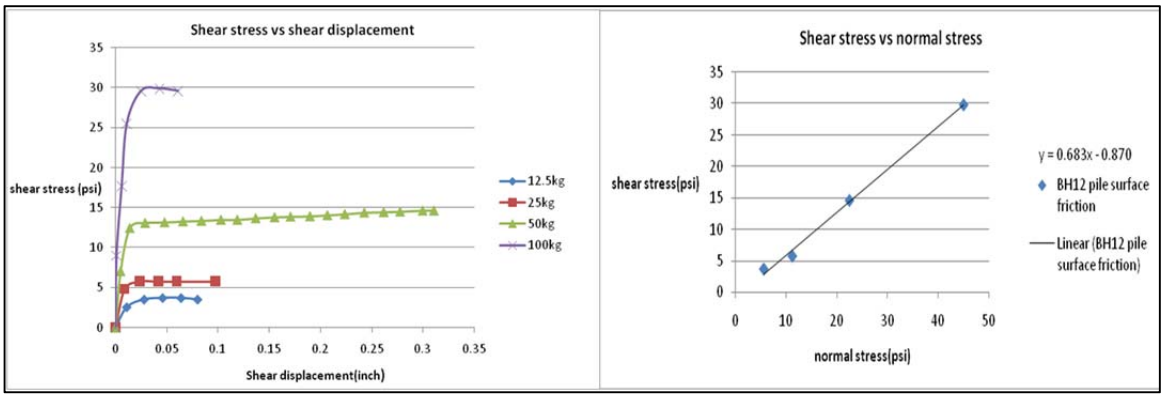

Fig3: Characteristics graph of Direct Shear Test of Sample Bore Hole 12

Findings are given below:

Normal load (kg)	**Maximum shear stress (psi)**
12.5	3.73
25	5.78
50	14.66
100	29.86
Method of Approach	**Angle of shearing resistance between pile surface & soil grain**
Experimental/Applied	34.33^0
Conventional	35.50^0

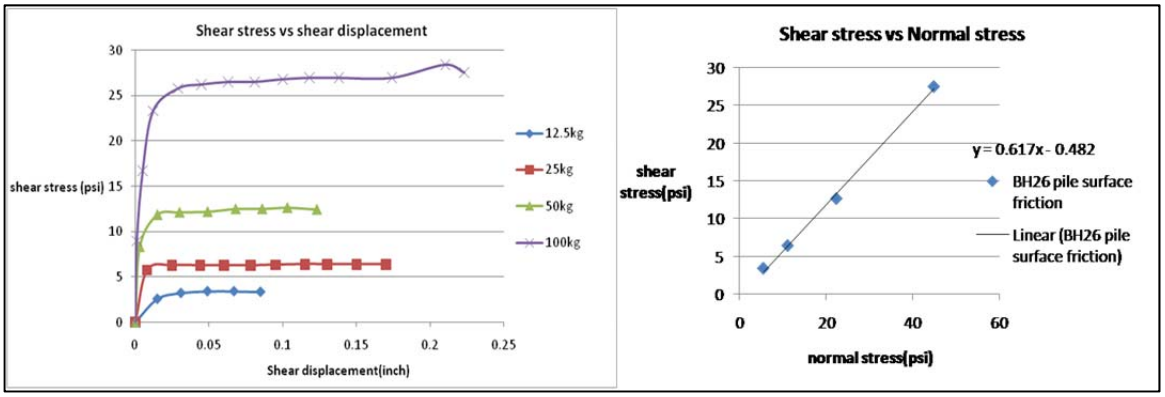

Fig4: Characteristics graph of Direct Shear Test of Sample Bore Hole 26

Findings are given below:

Normal load (kg)	**Maximum shear stress (psi)**
12.5	3.41
25	6.43
50	12.67
100	27.56
Method of Approach	**Angle of shearing resistance between pile surface & soil grain**
Experimental/Applied	31.67^0
Conventional	45^0

Discussion on direct shear test results between sample & foundation material

The maximum shear stresses obtained at various normal loads of 12.5kg, 25kg, 50kg, 100kg were 3.73, 5.78, 14.66, 29.86 psi and 3.41, 6.43, 12.669, 27.56 psi for bore hole 12 & 26 respectively.

The Shear stress vs. Shear displacement graph shows that for any specific normal load when the maximum shear stress is reached, then it remains almost constant with the increase of shear displacement. This indicates the sample as loose sand. The shear stress vs. normal stress graph is a straight line passing almost through the origin which indicates cohesionless sample. Direct shear test that performed between the pile surface and soil gives the angel of friction 34.33° & 31.67° for, Borehole 12 and Borehole 26 where for the given SPT value of the sample these should be 35.50° & 45° according to K. Terzaghi and R. B. Peck.

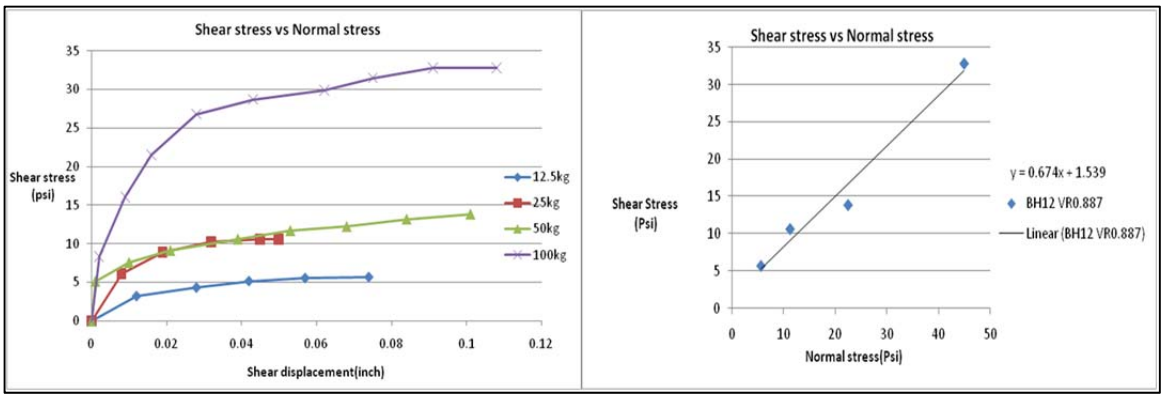

Fig4a: Characteristics graph of Direct Shear Test of Sample Bore Hole 12(Void Ratio 0.887)

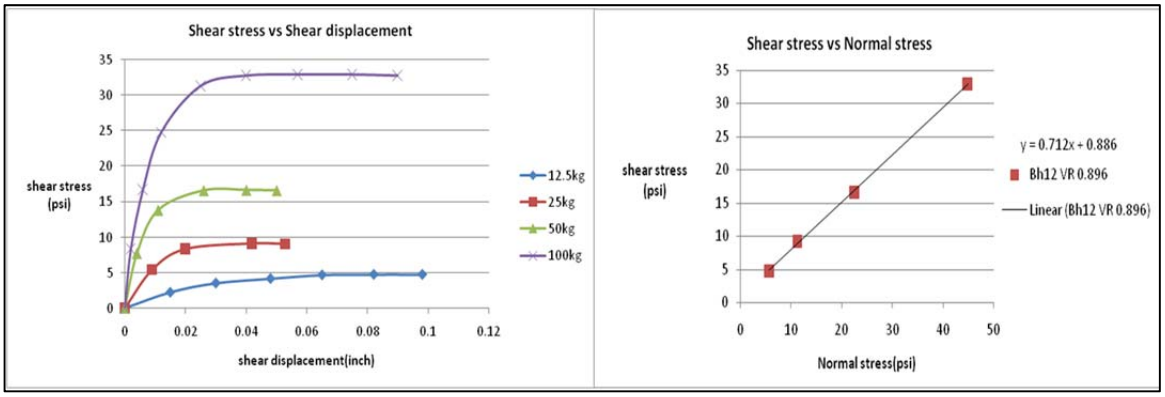

Fig4b: Characteristics graph of Direct Shear Test of Sample Bore Hole 12(Void Ratio 0.896)

Findings are given below:

Moisture Content	Maximum shear stress (psi)	Angle of shearing resistance
5%	32.82	33.98^0
6%	32.96	35.45^0

Discussion on direct shear test results of samples changing moisture content

For bore hole 12 from the shear stress vs. shear displacement graph changing moisture content, it is observed that for moisture content 5% & 6% obtained maximum shear stresses are 32.82psi & 32.96psi.

Angle of shearing resistance ◘ obtained from graphs for 5% & 6% water content were found 33.98^0 & 35.45^0. These values indicate that samples were loose and angular grains sand.

CONCLUSION & RECOMMENDATIONS

Direct shear test that has been performed between the pile surface and soil gives the angle of friction 34.33° & 31.67° for Borehole 12 and Borehole 26 where for the given SPT value of the sample these should be 35.50° & 45° according to K. Terzaghi and R. B. Peck. The above mentioned angle of friction is little bit of dissimilar with the standard value as it is known that there's nothing that can perfectly emulate the behavior of soil. But yet the test results of the different approach are quite nearly to the conventional method as well as homogenous with the specification of international standard. That will also increase the level of safety. Which means the different approach that has been stated and worked out in this paper can be carried out in order to get some quick shear strength parameter hence the property of the soil can be evaluated by means of less time and effort contrasting with the conventional method of direct shear test with soil vs. soil as well as with soil vs. pile surface. Analyzing the data it has been figured out that shear strength of granular soil has been increased with moisture content within a certain limit. After that it will be decreased.

In order to obtain more representative results for direct shear tests on cohesionless soils, the testing program should include a series of tests with a wide range of densities. While calculating pile capacity of given soil sample water table was not considered, length and diameter of pile was assumed that's why higher value of pile capacity was found. For better result water table should be considered.

Moisture content has a great impact on soil strength parameters. Further studies should be done regarding change of void ratio and its effect on shear strength parameters. The direct shear test was done on loose sand soil. For better analysis the test should be done on both dense and medium dense cohesionless soil.

ACKNOWLEDGMENTS

This research work is an imprint of many organization and individuals who have made significant contribution directly and indirectly by providing intellectual, technical and many other type and support to complete this work. At first we are immensely grateful to our supervisor Dr. Md. Hossain Ali, Professor, Department of Civil Engineering, BUET, for his constant guidance, critical appraisal and supervision which have made this research work possible. We also thankful to our Geotechnical lab assistants for their constant help all the time. We are grateful to the Department of Civil Engineering, BUET for giving us this opportunity for conducting this research.

REFERENCES

Al-Karni, A. A. (2010), "Evaluation of shear strength parameters of cohesionless soil due to excess pore water pressure," *Saudi Society for Geosciences 2010.*

Bardet, J. P. (1997), "Experimental Soil Mechanics*," Prentice Hall, ISBN 978-0133749359.*

Bowles, J. E. (1992), "Engineering Properties of Soils and Their Measurement," 4th Edition, McGraw-Hill, New York, 241 pp.

Bowles, J. E. (1997), "Foundation Analysis and Design," 5th Edition, pp. 29-32, 90-93, 136-137.

Chellis, R. D. (1961), "Pole Foundations," 2nd Edition, McGraw-Hill, New York, 704pp

Das, B. M. (2002), "Principles of Geotechnical Engineering," 5th Edition, pp. 18-20, 28-30, 311-320.

Lambe, T. W. (1951), "Soil Testing for Engineers," pp. 29-42, 88-97.

Miller, G. A. and Hamid, T. B. (2004), "Direct Shear Apparatus for Unsaturated Soil Interface Testing," *Geotechnical Testing Journal, Dec 2004.*

Tomlinson, M. J. (1977), "Pile Design and Construction Practice," 4th Edition, pp. 110-115.

ID : AGE 016

1st International Conference on Advances in Civil Engineering 2012 (ICACE 2012)
12 –14 December 2012
CUET, Chittagong, Bangladesh

GROUND IMPROVEMENT USING LIME

S.M. FAROOQ[1], J.C. KURI[1*], M.M. AREFIN[1] & M.A.U. SOJIB[1]

[1]*Chittagong University of Engineering and Technology, Chittagong, Bangladesh*
jhutankuri@yahoo.com

ABSTRACT

Clay soils are always harmful for civil engineering structure due to bearing capacity failure or uneven settlement. The most commonly used remedial method for this problem is addition of stabilizing agent like lime. This paper presents feasibility of using lime for improvement of engineering properties, particularly strength of clay soils. In this study different percentage of lime was mixed with clay soil collected from Rohanpur of Chapai Nababganj & improvement levels were evaluated based on unconfined compression test carried out at different curing periods. This study shows that only 8% addition of lime with Rohanpur soil increases 1.5 to 2 times the unconfined compressive strength/ undrained shear strength of untreated soil at different curing period used in this study The result showed that the maximum unconfined compressive strength was found at 8% lime content for 28 days curing period. It shows that for each percentage (0, 2, 4, 6, and 8) of lime content unconfined compressive strength increases as the curing period increases. It also showed that for each percentage (0, 2, 4, 6, and 8) of lime content 28 days curing period gives maximum unconfined compressive strength for Rohanpur soil.

Keywords: Clay soils, lime, unconfined compressive strength, curing period.

INTRODUCTION

Bangladesh is a small country with huge population. To accommodate this population in this short area, sometimes project sites are located in areas with soft or weak soils. In some region just a few feet below the ground surface crust, the low strength and highly plastic clay remains very soft and compressible. Generally thickness of clay soil varies from place to place, so there is a chance of differential settlement which is very dangerous for the structure. For this reason, a need has existed to develop engineering properties of the soil using admixtures like fly ash, lime, cement, asphalt etc. In this study soil improvement was done by using lime (Calcium hydroxide and Calcium Oxide). The use of lime for soil improvement offers many advantages like lime quickly dries the soil, reduces plasticity and improves workability. It substantially increases the stability, impermeability and load bearing capacity of the soil. This study investigates the engineering properties and improvement of unconfined compressive strength of Rohanpur soil using different percentage of lime with this soil. Additionally Un-drained shear strength or cohesion can be find using $C_u = q_u/2$ relation. Where C_u is the un-drained shear strength and q_u is the unconfined compressive strength.

MATERIALS AND METHODS

In this study the selected soil samples were collected at the depth of 3 feet from top of the ground surface which is located at Rohanpur, Chapai Nababganj district of Bangladesh. First, the collected soil sample was sieved through #40 sieve and then, physical properties of soil were determined in laboratory as shown in Table 1. After measurement of physical properties, moisture density relationship was investigated by standard proctor method (ASTM 698-07). Then the sieved soil was mixed thoroughly with 0, 2, 4, 6 and 8 percentages of lime (which is available in market at Chittagong, Bangladesh) at optimum moisture content condition. Next, four samples (10 cm in diameter and 12 cm in height) were compacted for each percentage of lime content by standard proctor method.

Table 1: Properties of Rohanpur soil

Properties	Results
Natural moisture content (%)	22.94
Specific gravity	2.78
Liquid limit (%)	41
Plastic limit (%)	20.72
Linear shrinkage (%)	9.33
Shrinkage limit (%)	20.92
Plasticity index (%)	20.28
Soil classification (Unified Soil Classification System)	CL

After compaction, the sample was trimmed carefully to 1.5 inch in diameter and 3 inch in height. Then the four trimmed soil samples were cured for 0, 7, 14 and 28 days respectively for each percentage of lime content soil. Curing was done by covering the samples with wetted jute bags for specified time period (7, 14 or 28 days). Then unconfined compression test of trimmed and cured sample was performed using a proving ring type unconfined compression testing machine at Geotechnical laboratory, CUET. The load was applied at the rate of 0.5 to 2 percent per minute and test was done up to the failure or 15% strain which one is earlier. Unconfined compressive strength was estimated by taking the stress value from peak of the stress strain diagram for all samples.

RESULTS AND DISCUSSION:

Fig.1 shows the moisture density relationship for Rohanpur soil. It is observed that maximum dry density and optimum moisture content was 101.8 lb/ft^3 and 13% respectively for the selected soil.

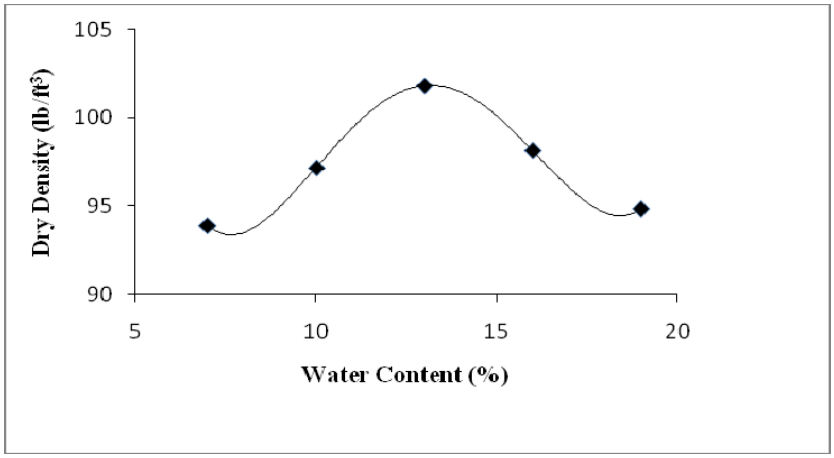

Fig.1. Compaction Test Result of Rohanpur soil

Axial stress against axial strain of unconfined compressive strength test for five different mixtures of soil and lime at optimum moisture content condition are shown in Fig.2. The 0, 7, 14 and 28 days cured sample stress strain behavior is shown in Figures 2a, 2b, 2c and 2d respectively for five lime soil mixture samples.

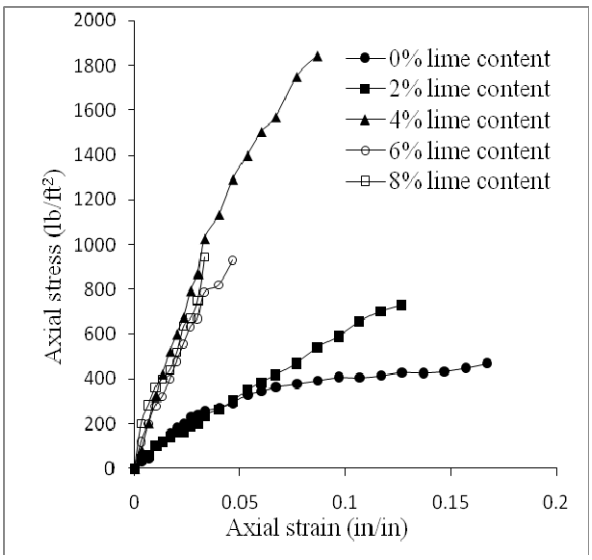

(a) 0 days curing

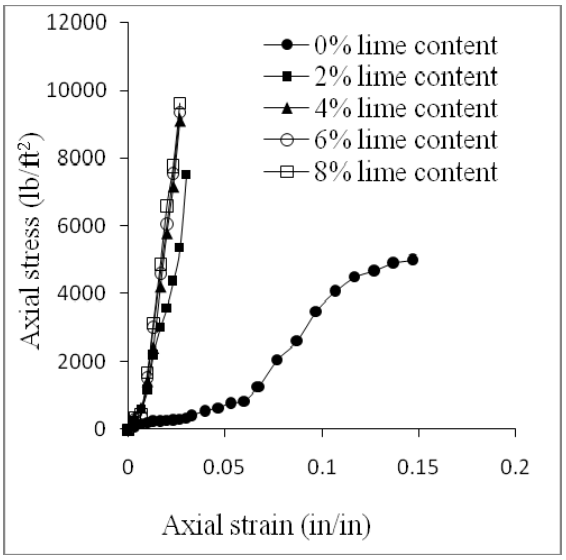

(b) 7 days curing

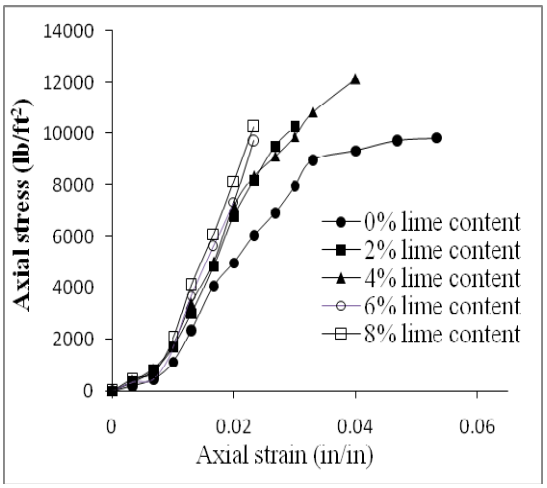

(b) 14 days curing

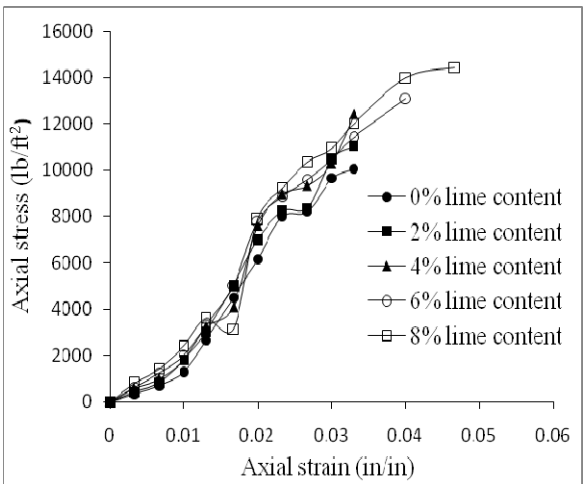

(d) 28 days curing

Fig.2. Axial stress and axial strain curve for curing period of (a) 0 days, (b) 7 days, (c) 14 days and (d) 28 days.

From fig.2, it is shown that mixing of lime with soil improved the strength of the soil in each curing period. It is showed that for without and 14 days curing period 4% lime gives maximum strength with respect to other mixture. It is also observed that 8 percent lime content in selected soil gives greatest stress for 28 days curing period (Fig. 2a-d).

The unconfined compressive strength was estimated from stress strain diagram and Fig.3 shows the plotting of unconfined compressive strength against four different curing periods for five different percentages of lime soil mixture.

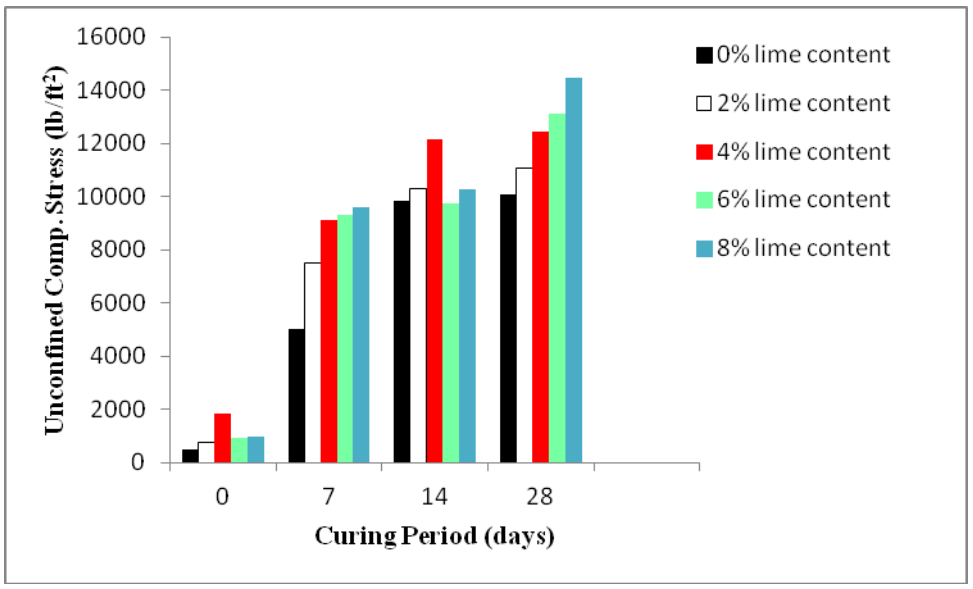

Fig.3. Unconfined Comprssive Strength against different curing periods

It shows that for each percentage (0, 2, 4, 6, and 8) of lime content, unconfined compressive strength increases as the curing period increases.
Fig.4 shows the plotting of unconfined compressive strength against five different percentages of lime content for four different curing periods. From the fig. 4, it is also found that soil without lime gives the lowest unconfined compressive strength and 8% lime content soil shows largest values of unconfined compressive strength for 28 days curing periods.

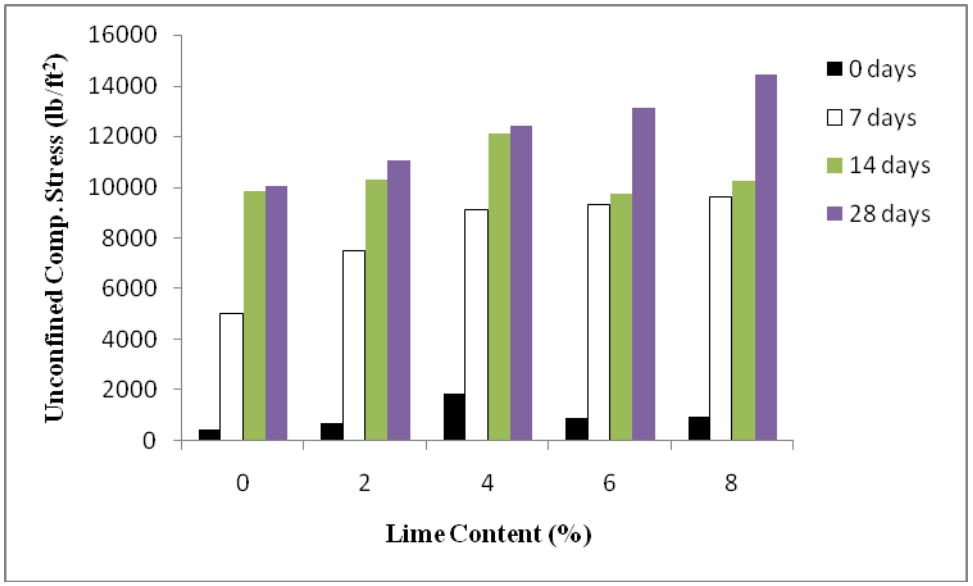

Fig.4. Unconfined Comprssive Strength against different percentage of lime

The unconfined compressive strength of 8% lime content samples is about 1.5 to 2 time higher than sample without lime content samples (for 0, 7 & 28 days curing period). Therefore, adding only 8% of lime with this soil gives considerable improvement of unconfined compressive strength.

CONCLUSION

Addition of 2% to 4% lime with the selected soil did not show significant strength variation with curing period of 14 days and 28 days but for 6% to 8% lime it gave large variation of unconfined compressive strength. This study shows that only 8% addition of lime with Rohanpur soil increases about 1.5 to 2 times the unconfined compressive strength/ undrained shear strength of the soil at curing periods of 0, 7 and 28 days. This study provides useful information about the optimum lime content to stabilize the selected soil to be used for engineering purpose.

REFERENCES

Allen, J.J., and Thompson, M.R., (1974) "Significant of Variable Confined Triaxial Testing".

Arman A. & Munfakh G.A. (1972): Lime Stabilization of Organic Soils. Transportation Research Board, Washington, DC., No.381.

Bowles J. (1992): Engineering properties of soil and their measurement. McGraw-Hill Boston, 4th edition.

Dempsey, B.J., and Thompson, M.R., (1968), "Durability Properties of Lime-Soil Mixtures", Highway Research Record 235, National Research Council, Washington, D.C., pp.61-75.

Eades, J.L., and Grim, R.E., (1960), "Reactions of Hydrated Lime with Pure Clay Minerals in Soil Stabilization", Highway Research Bulletin 262.

Spangler, M.G. & Handy, R.L. 1973. *Soil Engineering.* New York: Harper and Row Publishers.

ID : AGE 018

1st International Conference on Advances in Civil Engineering 2012 (ICACE 2012)
12 –14 December 2012
CUET, Chittagong, Bangladesh

EFFECT OF CLAY ON CBR CHARACTERISTICS OF SUB-GRADE SOIL

A. A. MASUM[1*], M. A. SOBHAN[2] & A. B. M. G. RABBANY[3]

[1] *Lecturer, Department of Civil Engineering, Rajshahi University of Engineering & Technology, Rajshahi-6204, Bangladesh, <e-mail: masum24706@gmail.com>*
[2] *Professor, Department of Civil Engineering, Rajshahi University of Engineering & Technology, Rajshahi-6204, Bangladesh, <e-mail: msobhan@yahoo.com>*
[3] *Department of Civil Engineering, Rajshahi University of Engineering & Technology, Rajshahi-6204, Bangladesh, <e-mail: palashruet@gmail.com>*
**Corresponding Author*

ABSTRACT
The sub-grade soil and its properties are important in the design of pavement structure as it gives support to the pavement. The sub-grade should possess sufficient stability under adverse climate and loading conditions. Sometimes sub-grade soil contains some clay which affects the strength properties of the soil. The use of local soil contain some clay in sub-grade should be economical. Therefore this investigation is carried out to check the possibility of using clay mix soil in sub-grade.
Fresh fine sand (FM = 0.5) was collected from river Padma and clay were mixed for the preparation of clay mix soil. Attempts were made to study and compare the California Bearing Ratio (CBR) characteristics of clay mix soil with those of fresh sand. Procedures specified by AASHTO were followed for the determination of properties of clay mix soil and fresh sand. Standard CBR test procedure specified by AASHTO T180 was followed in the preparation and testing of this sub-grade soil. The testing includes the determination of unsoaked CBR value and soaked CBR value. The results shows that fine sand containing 20% clay can be used for the construction of sub-grade considering the compaction and CBR values.

Keywords: Sub-grade, Clay, CBR, Dry density, Expansion ratio.

INTRODUCTION

General
A road pavement (Gupta, 2003) may be defined as relatively stable layer or crust constructed over the natural soil. Different types of pavement are constructed on roads for safe and comfortable movements of various types of vehicles at the desired speeds. The main function of pavement is to support and distribute the heavy wheel loads of vehicles over a wide area of the underlaying sub-grade soil and permitting the deformations within elastic or allowable range and to provide an adequate surface. All these entire pavements are laid over a prepared soil surface called sub-grade. The loads on the pavement are ultimately supported by the soil sub-grade and dispersed to the mass below (Khanna, 1985). Therefore it is necessary first to test the properties of the sub-grade soil and to evaluate its supporting capacity under the adverse loading and climatic conditions, before taking up the design and construction of the pavements. The basic tests needed on the sub-grade soil for this purpose are for the identification and classification of soil, its density and compaction characteristics. It is also necessary to determine the strength characteristics of the sub-grade for the design of pavements. To achieve all

this, it is very important to have a pre-knowledge about sub grade soil properties and to suggest suitable methods to improve then if called for.

Sub-grade failure

To understand the cause of failure of sub-grade, knowledge of soil deformation is essential. When a certain load is applied on the sub-grade it undergoes deformation (Sing, 1996). Deformation in soil mass is mainly due to slippage or shearing between soil particles. The major cause of failure of flexible pavements is excessive deformation in the sub-grade layer, which can be noticed in shape of waves or corrugations in the road surface. Lateral shoring of the pavement near the edges along the wheel paths take place also due to shear failure of the sub-grade. Insufficient stability of the soil which may be the result of excessive moisture, improper compaction or weakness of soil itself, may be the other causes of road failures.

Need of study

To be successful road engineer, it is very essential to have a sound knowledge of design and construction aspects of the road and also various defects that are likely to occur and methods of their rectification. Likely causes of failures should be investigated and designs should be done as per local conditions of the construction site (Sing, 1996).

For the design and construction of highway, it is imperative to carry out tests over construction materials for their scientific designing and economic utilization. The inherent economy of construction depends upon the maximum use of local materials. The quality and durability of a sub-grade soil is influence by many factors including gradation of particles, types of soil and degree of compaction. Fine grained soils with some clay are used for a long time in the construction of sub-grade course of road pavement in Bangladesh. Researches have been carried out to investigate their suitability. Limited information is available about their performances. However, experience has shown that their use in sub-grade is generally satisfactory. Clay free soil (sand) is not available everywhere in Bangladesh. The cost of clay free soil at the site of construction is often too high. With the above requirement in view the present investigation has been taken in order to investigate the behaviors of sub-grade soil with the various percentage of clay.

The objectives of this study are to investigate the behavior of sand-clay mixes with respect to compaction and CBR value.

LITERATURE RIVIEW

Sub-grade

The sub-grade is the foundation layer, the structure which must eventually support all the loads which come onto the pavement. Sub-grade soil is an integral part of the road pavement structure as it provides the support to the pavement from beneath. The sub-grade soil and its properties are important in the design of pavement structure. The main function of the sub-grade is to give adequate support to the pavement and for this the sub-grade should possess sufficiently stability under adverse climate and loading conditions. When soil is used in embankment construction, in addition to stability incompressibility is also important as differential settlement may cause failures. Compacted soil and stabilized soil are often used in sub-base or base course of highway pavements. The soil is therefore considered as one of the principal highway materials. Soil is a highly variable material and as much sub-grade will vary considerably. It is therefore, necessary to make a thorough study of sub-grade soils to determine the design of pavements. This investigation can be accomplished by a proper exploration program. Desirable properties which the sub-grade should possess are strength, drainage, ease of compaction, permanency of compaction and strength.

Soil strength and its determination

Soil stability or strength is the resistance to deformation of the soil under load application. The types of soil, moisture content, dry density, internal structure of soil, method of stressing are the principle factors which affect strength properties of the soil (Sing, 1996). Shearing resistance of soil represents the strength or stability of soil. Shearing resistance on any plane for soils is given by Coulomb's law

$S_r = C + \sigma \tan \Phi$ (1)

Where, S_r = Shearing resistance

C = Cohesion per unit area

Φ = Angle of internal friction and

σ = Normal stress

The value of Φ depends on dry density, grain size distribution, texture and shape of soil particles, and moisture content and the value of C depends on the type of clay, its size, surface charge and amount of water content present in the soil.

The California Bearing Ratio (CBR) test is essentially a penetration test for measuring soil strength, which is carried out either in the laboratory or in the field. The test is suitable for the evaluation of strength of soil and aggregates. This method has an important place among highway materials testing program, as it has been extensively correlated with flexible pavement design and performance.

MATERIALS AND METHODS

Sub-grade soil is normally composed of sand, silt and clay. The sands are generally divided into coarse, moderately coarse and fine fraction according to the size of individual particles. The following sections include the description of sand, clay and sand-clay mixes used in this study.

Fine sand

The fraction of soil lies between 1.60mm and 0.075mm size is called fine sand. Padma river sand from Talaimary in Rajshahi was used as the source of fine sand. The physical appearance of that sand is shown in [Fig. 1].

Clay

Clay is one of the principal types of soil, which remains mixed with other types like silt and sand. Clay is a fine-grained soil consisting of hydrated silicate of aluminium. The fraction of soil which is smaller than 0.002mm size is under the group of clay. The clayey type soil was collected from the clayey layer of the Padma river bank. The collected clayey soil was thoroughly mixed with water in a drum. After mixing the clayey soil the water was kept in rest condition for about 15 minutes. The fine sand and silt settled beyond the zone of upper half portion. Then the mix of upper half portion was collected in trays. After oven dry of collected mixer the clay sample was found. The physical appearance of that clay is shown in [Fig. 2].

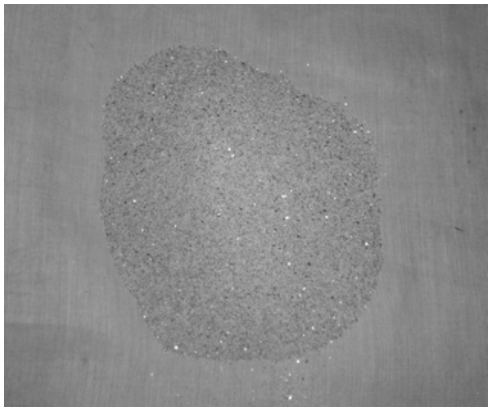

Fig. 1 Physical appearance of sand

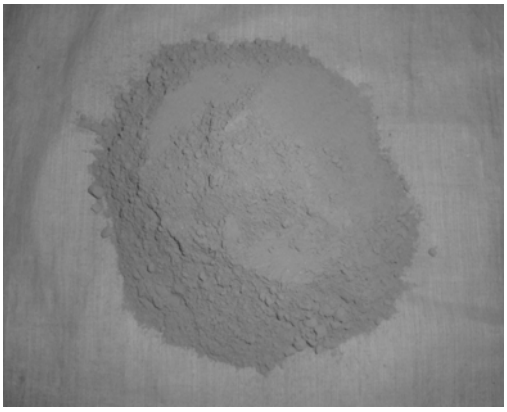

Fig. 2 Physical appearance of clay

Sand-clay mix

The main objective of this study was to make a comparative study of the different sand-clay mixes. Six mixes were studied and these were designated as A, B, C, D, E and F.

Mix A: Fine sand without clay,
Mix B: Fine sand with 10% clay,
Mix C: Fine sand with 20% clay,
Mix D: Fine sand with 30% clay,
Mix E: Fine sand with 40% clay,
Mix F: Fine sand with 50% clay.

Table 1 Properties of clay and sand-clay mixes

Mix	Compacted unit weight(Kg/m^3)	Specific gravity
Clay	1725	2.719
A	990	2.633
B	1195	2.640
C	1300	2.647
D	1370	2.661
E	1400	2.671
F	1485	2.683

CALIFORNIA BEARING RATIO (CBR) TEST

The California Bearing Ratio (CBR) test was developed by the California Division of Highway (Sharma, 1985) as a method of classifying and evaluating soil sub-grade and base course materials for flexible pavements. The test consists of causing a cylindrical plunger of 50 mm to penetrate a pavement component material at 1.25 mm/minute. The loads, for 2.5 mm and 5 mm are recorded. This load is expressed as a percentage of standard load value at a respective deformation level to obtain CBR value. Before preparation of specimens for CBR test, the optimum moisture content and dry density of the mix A, B, C, D, E and F were determined by adopting Modified Proctor test according to the procedure specified by AASHTO standard. 5 kg sand-clay mix for each batch was mixed with optimum moisture content for preparation of specimens for CBR test. The soil was compacted in five equal layers, each of compacted thickness about 26.5 mm by applying 56 evenly distributed blows of the 4.89 kg rammer. Test specimens were grouped into two groups. The first and second group were consisted of three specimens from each mixes. The specimens of group 1 were used to determine the CBR value in unsoaked condition and group 2 were placed in water tank to allow soaking of the soil specimen for 96 hours for determination of CBR value in soaked condition.

The CBR value can be calculated from the following formula:

$$\text{CBR (\%)} = \frac{\text{Unit load carried by soil sample at defined penetration level}}{\text{Unit load carried by standard crushed stone at that penetration level}} \times 100 \qquad (2)$$

RESULTS AND DISCUSSIONS

The maximum dry density and % CBR value for different mixes are presented in Table 2 and [Fig. 3] to [Fig. 4].

Table 2 Maximum dry density and % CBR value for different mixes

Mix type	A	B	C	D	E	F
Maximum dry density (gm/cm^3)	1.56	1.59	1.62	1.60	1.55	1.51
Unsoaked CBR (%)	12.2	13.6	14.7	13.1	11.2	8.4
Soaked CBR (%)	8.3	8.8	9.5	8.0	6.8	4.4

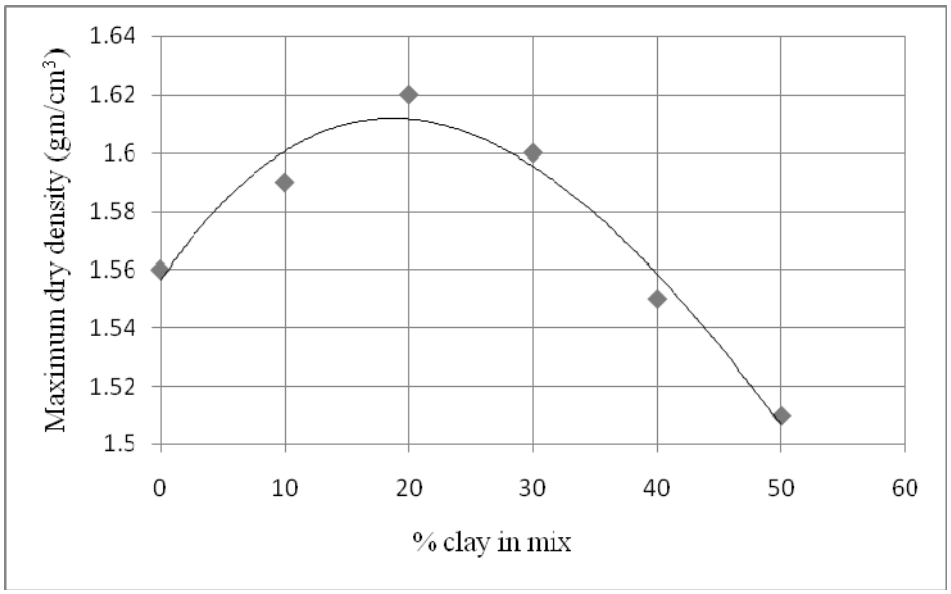

Fig. 3 Maximum dry density for various clay contents

The [Fig. 3] indicates that maximum dry density increases up to 20% clay content in the mix and then decreases. With the addition of even a small quantity of fines to a coarse grained soil, the soil attains a much higher dry density for the same compaction effort. However, if the quantity of the fines in increased to a value more than that required to fill the voids of the coarse-grained soils, the maximum dry density decreases.

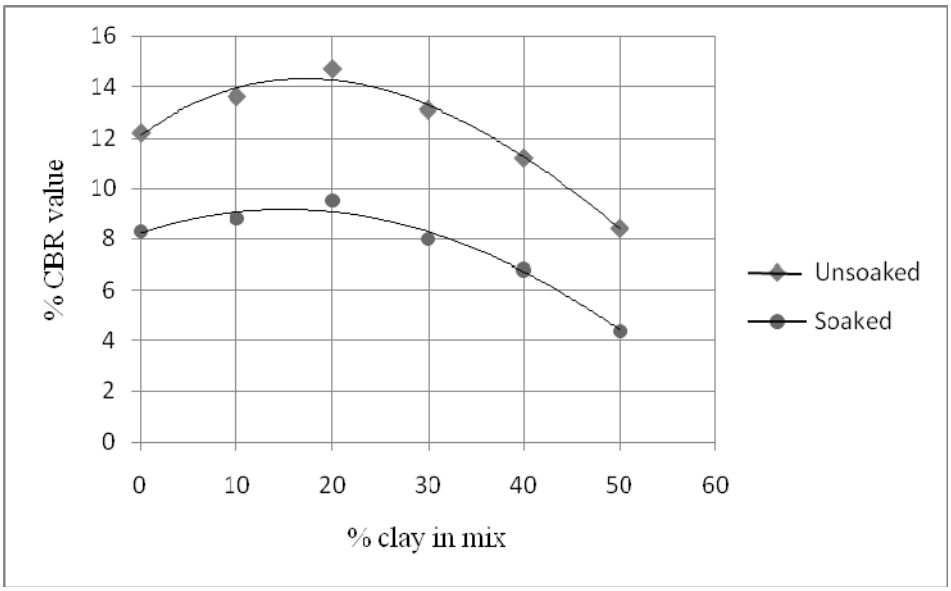

Fig. 4 CBR values for various clay contents

The [Fig. 4] indicates that CBR value increases up to 20% clay content in the mix and then decreases. With the increase of clay content voids among sand particles decreased. This causes better and compact arrangement of sand particles with higher density, which results the increase of CBR value also. After a certain limit of increasing of clay content the interlock friction among sand particles decreased and the clay act as a lubricating agent. For this reason the lowering of CBR value.

CONCLUSION

On the basis of test results in this study, it is found that both maximum dry density and CBR value increases up to 20% clay content in the mix and then decreases. So it can be concluded that fine sand containing 20% clay is good as selected fresh sand from the considerations of compaction and CBR values.

LIST OF REFERENCES

Aziz, MA. 2003. *A Textbook of Engineering Materials*. Dhaka, Bangladesh.

Gupta, BL and Gupta, A. 2003. *Roads, Railway, Bridges and Tunnel Engineering*. New Delhi, India.

Jaleel, ZT. 2011. Effect of Soaking on the CBR-Value of Subbase Soil. 29, No.6, 2011 . *Eng. & Tech. Journal, Vol.29, No.6.*

Khanna, SK and Justo, CEG. 1985. *Highway Material Testing (Laboratory manual)*. Roorkee, India.

Khanna, SK and Justo, CEG. 2001. *Highway Engineering*. Roorkee, India.

Naeini, SA and Moayed, RZ. 2009. Effect of Plasticity Index and Reinforcement on the CBR Value of Soft Clay. *International Journal of Civil Engineerng. V ol. 7, No. 2.*

Punmia, BC. 2001. *Soil mechanics and foundation*. New Delhi, India.

Sing, GC. 1996. *Highway Engineering*. New Delhi, India.

Sharma, SK. 1985. *Principles, Practice and Design of Highway Engineering*. New Delhi, India.

ID : AGE 020

1st International Conference on Advances in Civil Engineering 2012 (ICACE 2012)
12 –14 December 2012
CUET, Chittagong, Bangladesh

USE OF BROMS' CHARTS FOR EVALUATING LATERAL LOAD CAPACITY OF VERTICAL PILES IN A TWO LAYER SOIL SYSTEM

S. JAHAN[1*] & M. Z. ABEDIN[2]

[1]*Final year undergraduate student, Dept. of Civil Engineering, BUET, Dhaka-1000, Bangladesh*
[2]*Professor, Department of Civil Engineering, BUET, Dhaka-1000, Bangladesh*
**Corresponding Author*

ABSTRACT

Several analytical methods are in use to estimate the lateral load capacity of vertically installed pile foundation in order to avoid costly pile load test. One of the most common and simplified method is proposed by Broms (1965) that determines the lateral load capacity and pile deflection at ground surface. Broms uses several graphical charts to obtain ultimate bearing capacity and lateral deflection. The present paper reports a study concerning the digitization of these charts so that they can be used as inbuilt program. Once soil and pile data are given as input, the lateral capacity for both fixed and free headed piles in either purely cohesive or cohesionless soil can be evaluated by this procedure in a spread sheet without consulting the charts.

Keywords: Broms' method, Lateral capacity of pile, Pile foundation, Excel spread sheet

INTRODUCTION

As a result of wind earthquake, waves, impact and lateral earth pressure most structures are subjected to lateral loads and moments in addition to the axial downward loads due to gravity. If these structures are supported on deep foundations, the foundations have to be designed for lateral loads so that they are safe against geotechnical failure, structural failure, and excessive deflections. The allowable lateral load on piles is determined from the following two criteria:

(i) Allowable lateral load is obtained by dividing the ultimate (failure) load by an adequate factor of safety.
(ii) Allowable lateral load is corresponding to an acceptable lateral deflection.

The smaller of the two above values is the one actually adopted as the design lateral load. Methods of calculating lateral resistance of vertical piles can be broadly divided into two categories:

(i) Methods of calculating ultimate lateral resistance.
(ii) Methods of calculating acceptable deflection at working lateral load.

In engineering practice to withstand lateral load, laterally loaded piles are most commonly in use and in order to analyze them a number of theoretical methods are available such as the subgrade reaction approach by Barber (1953) and Matlock and Reese (1960), the ultimate lateral load approach by Broms (1964a), the *p-y* curve method by Reese (1977), and the elastic continuum approach by Poulos and Davis (1980), Zhang and Small (2000), and Shen and Teh (2002). Among these aforementioned methods, Broms' method is the simplest method to determine the lateral load and pile deflection at the ground surface using a convenient set of curves, ignoring axial load in the pile. In this article the solution for laterally loaded pile based on a simple spreadsheet calculation procedure using *Microsoft Excel* following Broms' method is reported along with digitalizing the curves with their trend line equations. The purpose of the paper is to provide simple, efficient and reasonable solution suitable for small projects or non-critical projects, eliminating manual effort.

SCRUTINY OF BROMS' METHOD

Broms' method was presented in three papers (Broms; 1964a, 1964b, 1965) for calculating lateral resistance of vertical piles. A pile can be designed to sustain a lateral load based on Broms' theory of earth pressure by referring to charts and graphs.

According to the theory, piles can be divided into two groups; short rigid and long flexible. "Short" pile is one that is rigid enough to move in the direction the load is tending by rotation or translation whereas "long" pier is one that the top will rotate or translate without moving the bottom of the foundation, i.e. a plastic hinge will form. In other word, a pile is considered long when the relative stiffness of the pile with respect to the soil stiffness exceeds certain limits. Broms' developed lateral capacity methods for both short and long piles in cohesive and non-cohesive soil. Broms' theorized that a short free-headed pier rotates about a center, above the lower end of the foundation, without substantial deformation along its axis. The resistance is the sum of the net of the earth pressures above and the passive earth pressure below the center of rotation. The end bearing influence or effect is neglected. Likewise, the passive earth pressure on the uppermost 1.5 diameters of shaft and the active earth pressure on the back of the pile are neglected. The advantages of this theory are:

(i) Applicable for short and long piles.
(ii) Considers both purely cohesive and cohesion less soils.
(iii) Considers both free-head and fixed-head piles that can be analyzed separately.

Spreadsheet calculation procedure

A spreadsheet calculation procedure is developed using *Microsoft Excel* to analyze a pile subjected to lateral load. The method is demonstrated in the following through an example of free headed pile.

Basic parameters

The basic parameters for a two layer soil system, i.e. depth of each layer, type of soil, fineness of cohesionless soil, Field SPT value (N_{field}), location of GWT from GL, head condition of pile, pile material, unit weight of soil (γ), embedded pile length (D), design parameter (deflection/load), working load or allowable deflection, eccentricity (e_c) etc. and basic parameters for pile i.e. diameter of pile (b), bar dia, bar no., clear cover, yield stress of steel (f_y), compressive strength of concrete (f'_c) etc. are typed in cells of *Microsoft Excel* in a manner as shown in Fig. 1. In case of a single layer of soil, the parameters of soil for both layer 1 and layer 2 in the input sheet should be similar.

INPUT				
Parameters for Soil			**Parameter for Pile**	
	Layer 1 (Top)	**Layer 2**	**Diameter of pile (m)**	0.4
Depth of layer (m)	23	28	**Bar dia-1 (mm)**	20
Type of soil	Cohesionless	Cohesionless	**No of bar-1**	8
If cohesionless (Fine / Coarse?)	Fine	Fine	**Bar dia-2 (mm)**	
Field SPT value, N_{field}	8	20	**No of bar-2**	
Location of GWT from GL (m)	0	0	**Clear cover (mm)**	40
Pile head (free /fixed?)	free	free	**Yeild stress of steel, f_y (psi)**	40000
Pile material	Concrete	Concrete	**Ultimate compression strength of concrete, f'_c (psi)**	2500
Unit weight of soil, γ (kN/m^3)	15	16		
Embedded pile length, D (m)	51	51		
Design parameter (deflection/load?)	Deflection	Deflection		
Working load, Q_a (kN)	N.A.	N.A.		
Allowable deflection, y (mm)	25	25		
Eccentricity,e_c (m)	0	0		

Fig 1: Input of basic parameters

Calculation for soil resistance and moment capacity

With the given parameters, calculation is proceeded following brooms' steps using different built-in functions of *Excel*; such as "IF", "MIN", "AND", "OR", "TAN" etc. At first horizontal subgrade reaction, K_h is determined for the predefined soil type, i.e. "Cohesive" or "Cohesionless" with the following formula:

*"=IF(B7="cohesive",(B35*B36*80*B17/B23),IF(AND(B7="cohesionless",B12="loose",B13>B24),1900,IF(AND(B7="cohesionless",B12="loose",B13=0),1086,IF(AND(B7="cohesionless",B12="loose",B13<B24,B13>0),(((B13*1900)+((B24-B13)*1086))/B24),IF(AND(B7="cohesionless",B12="medium",B13>B24),8143,IF(AND(B7="cohesionless",B12="medium",B13=0),5429,IF(AND(B7="cohesionless",B12="medium",B13<B24,B13>0),(((B13*8143)+((B24-B13)*5429))/B24),IF(AND(B7="cohesionless",B12="dense",B13>B24),17644,IF(AND(B7="cohesionless",B12="dense",B13=0),10857,IF(AND(B7="cohesionless",B12="dense",B13<B24,B13>0),(((B13*17644)+((B24-B13)*10857))/B24)))))))))".*

The value obtained is adjusted later according to loading condition. In the next step other parameters like corrected SPT value ($N_{corrected}$), unconfined compressive strength (q_u), undrained cohesion (c_u), angle of internal friction (φ), Rankine passive earth pressure coefficient (K_p), average effective unit weight (γ′), modulus of elasticity (E), moment of inertia (I), section modulus (S), shape factor (C_s), resisting moment of pile(M_y) are calculated. The flexural moment capacity of concrete pile for circular section is calculated using the formula proposed by Cosenza et. al. (2011) as in equation (1a).

$$M_y = kA_s f_{yd} r \qquad (1a)$$

Where,

$$k = 0.76\omega^{-0.11} \qquad (1b)$$

and,

$$\omega = \frac{A_s}{\pi R^2}\frac{f_{yd}}{0.9 f_{cd}} \qquad (1c)$$

In which, A_s = area of reinforcement

f_{yd} = yield strength of reinforcement
f_{cd} = concrete cylinder strength
R = half of pile diameter
r = half of diameter of reinforcement cage in pile

Calculation for design load

After the moment capacity of both soil and pile is obtained, the smaller value is considered for further calculation. For determination of design load, whether the pile is "long" or "short" need to be identified by evaluating the value of dimensionless length factor $\beta_h D$ (for cohesive soil) or ηD (for cohesionless soil).

With the help of numerical set of values of Broms' charts, ultimate lateral load (Q_u) is obtained using *"Treandline equation"* of the desired curve (Table-1) which is divided by a factor of safety of 2.5 to obtain the maximum allowable load for a single pile (Q_m). Similarly, working load (Q_a) or deflection (y) is calculated using *"Treandline equation"* of desired Broms' digitalized charts (table-2). A comparison is made between Q_a and Q_m and the smallest value is selected as design load (Q). If Qa and y were not given earlier as input Q_m is used as Q. In the same manner caculation for the second type of soil is made and by taking the weighted average of two type of soil according to their individual layer's depth estimation for a two layer system is done. The entire calculation for analyzing a lateral loaded pile in *Microsoft Excel* is shown in Fig. 2.

	Layer 1	Layer 2
Depth of layer (m)	23	28
Type of soil	Cohesionless	Cohesionless
Texture	Fine	Fine
N_{field}	8	20
$N_{corrected}$	5.410281564	10.80383957
Over-burden pressure,σ_0(kN/m^2)	264.69	315.69
More specification of soil	loose	medium
Location of groundwater from GL	0	0
Location of groundwater from pile	above	above
Type of pile	free	free
Pile material	Concrete	Concrete
Unconfined compressive strength,q_u (kPa)	2	8
Angle of internal friction, φ	25.4	29.7
Unit weight of soil,γ (kN/m^3)	15	16
Average effective unit weight of soil,γ' (kN/m^3)	5.19	6.19
Passive earth pressure coefficient,K_p	2.502	2.964
Undrained cohession,c_u (kPa)	1	4
Diameter of pile,b (m)	0.4	0.4
Embedded pile length,D (m)	51	51
Design deflection,y (m)	0.025	0.025
Yield stress,f_y or f'$_c$ (MPa)	17.25	17.25
Modulus of elasticity, E (MPa)	19665	19665
Moment of inertia,I (m^4)	0.00125664	0.00125664
Section modulus,S (m^3)	0.0062832	0.0062832
Eccentricity,e_t (m)	0	0
Shape factor,C_1	N/A	N/A

	Layer 1	Layer 2
Resisting moment of soil,$M_{r,soil}$ (kN-m)	108	108
Resisting moment of structure,$M_{r,pile}$ (kN-m)	89	89
Governing resisting moment,M_r (kN-m)	89	89
Empirical coefficient,n_1	0.32	0.32
Empirical coefficient,n_2	1.15	1.15
Coefficient of horizontal subgrade reaction,K_h (kN/m^3)	1086	5429
Adjusted K_h (kN/m^3)	271.5	2714.5
βh or η	0.40567	0.64292
βhD or ηD	20.689	32.789
Long or short pile	long	long
For short cohessive-D/b	127.5	127.5
For long cohessive-M_y/c_ub^3	1384.302	346.076
e_t/b	0.00	0.00
e_t/D	0	0
For short cohessionless-D/b	127.5	127.5
For long cohessionless-$M_y/\gamma' b^4 k_P$	266.46188	188.62771
Ultimate lateral load,Q_u (kN)	54.90707461	55
Maximum allowable working load, Q_m (kN)	21.963	22
Working load,Qa (kN)	30.43	156
Individual layer's design load,Ql (kN)	21.963	22
Individual layer's deflection at working load, y_m(m)	0.03	0.03
Individual layer's deflection at design load, y_d (m)	0.018044922	0.00352
Design load, Q (kN)	21.96282984	
Design defleciont,y (m)	0.018044922	

Diameter,D (m)	0.4
Bar dia-1 (mm)	20
No of bar-1	8
Bar dia-2 (mm)	0
No of bar-2	0
Total area of steel (mm^2)	2513.28
Yeild stress of steel,fy (psi)	40000
Ultimate compression strength of concrete,f'c (psi)	2500
Clear cover (mm)	40
ω	0.355413
k	0.851595
r (mm)	150
Moment capacity,M (kip-ft)	65.30443
Moment capacity,M (kN-m)	88.59533

Fig. 2: Typical Calculation Sheet of *Microsoft Excel*

Digitalization of charts

The set of charts Broms' presented for determination of ultimate lateral load and lateral deflection load is digitalized by taking values from the original graphs and plotting the points and drawing the best fit curve in *Excel* using "Trendline" function. Also the equation of the curves and regression values are determined (Figs. 3, 4, 5, 6, 7, 8).

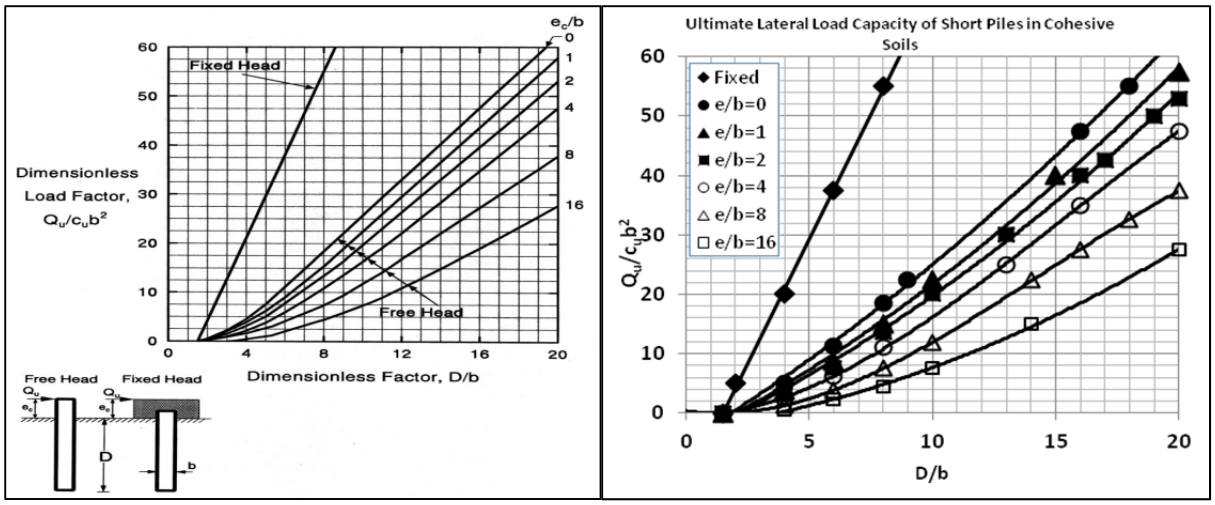

Fig. 3: Ultimate Lateral Load Capacity of Short Piles in Cohesive Soils

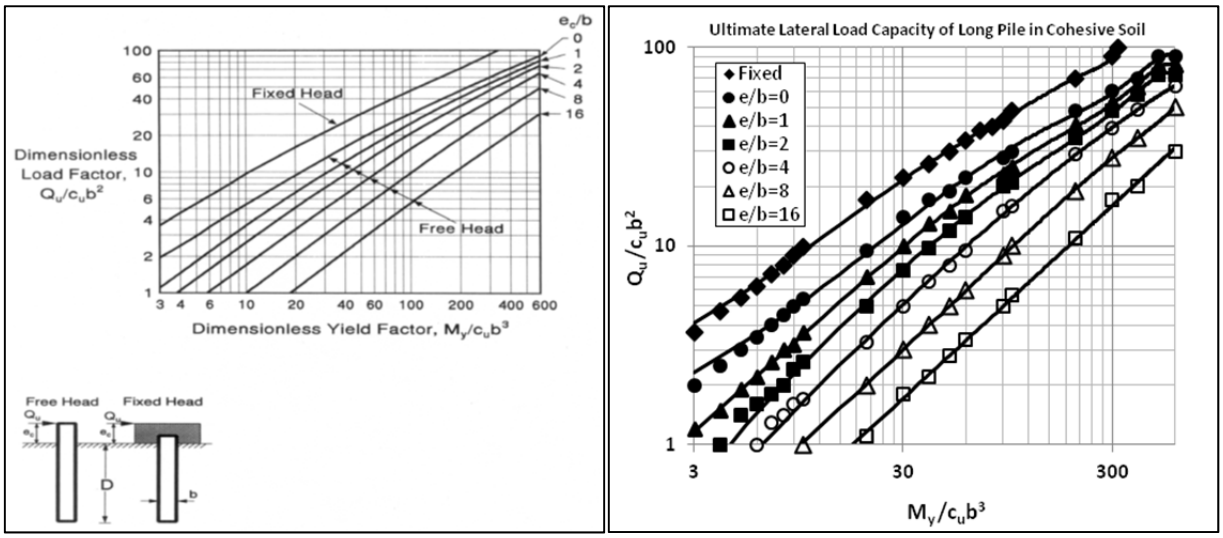

Fig. 4: Ultimate Lateral Load Capacity of Long Piles in Cohesive Soils

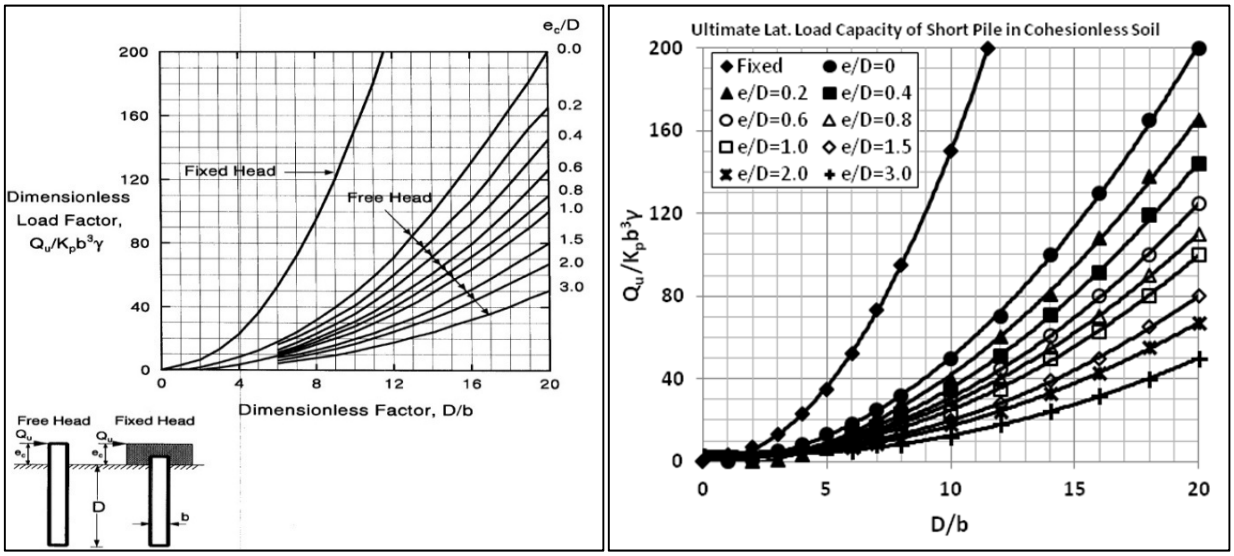

Fig 5: Ultimate Lateral Load Capacity of Short Piles in Cohsionless Soils

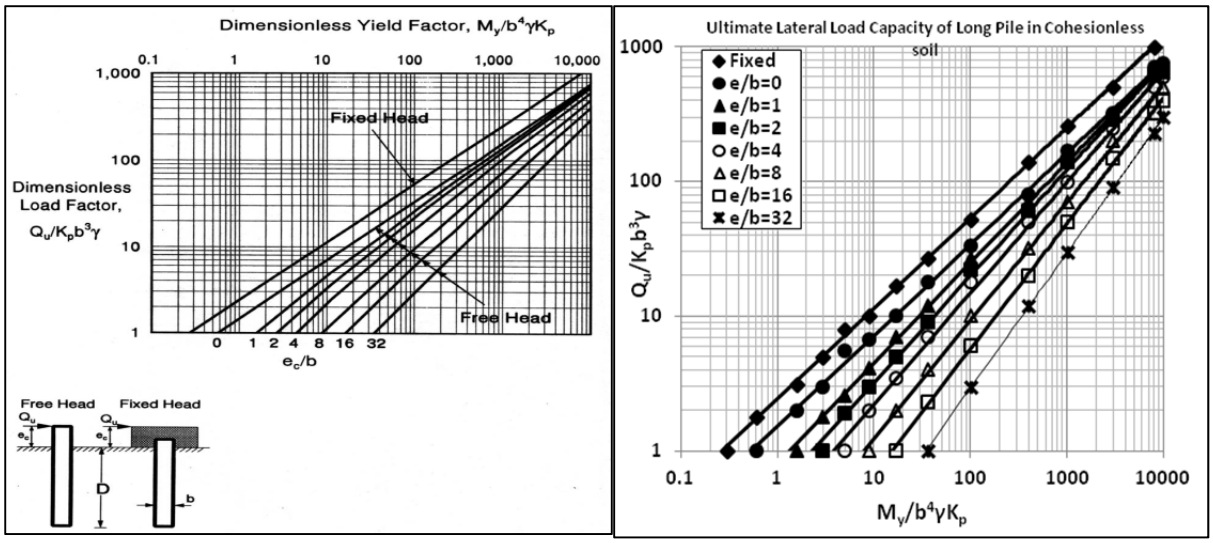

Fig. 6: Ultimate Lateral Load Capacity of Long Piles in Cohesionless Soils

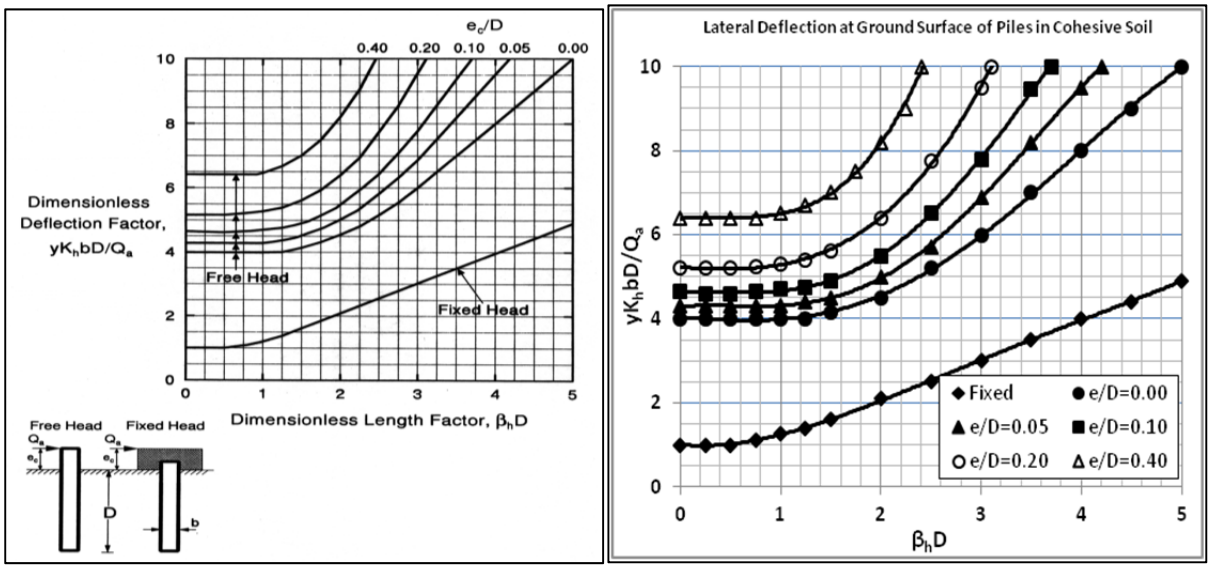

Fig. 7: Lateral Deflection at Ground Surface of Piles in Cohesive Soils

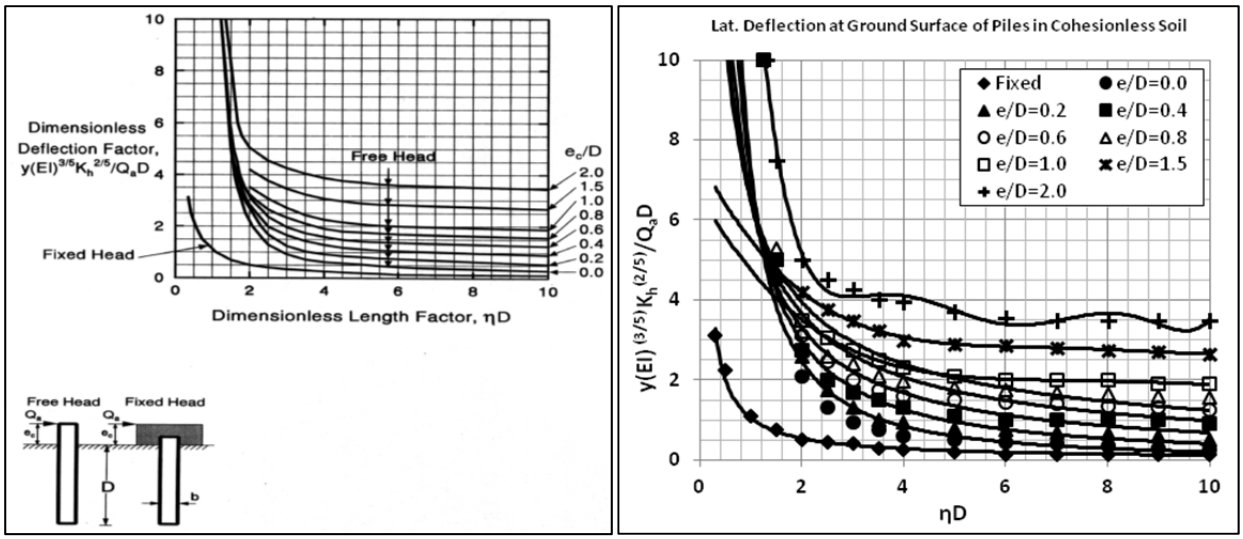

Fig. 8: Lateral Deflection at Ground Surface of Piles in Cohesionless Soils

RESULTS AND DISCUSSIONS

The trendline equations for ultimate lateral loads along with their regression values are provided in Table 1. The trendline equations for lateral deflection along with their regression values are provided in Table 2.

Soil Type	Pile Type	Load Eccentricity	Regression Equation	Coeff. of Correlation (R^2)
Cohesive	Short	Fixed Head	$y = 8.3809x - 12.538$	0.9991
		e/b=0	$y = 0.0456x^2 + 2.5171x - 4.7259$	0.9987
		e/b=1	$y = 0.0509x^2 + 2.1202x - 4.572$	0.9973
		e/b=2	$y = 0.0496x^2 + 1.9207x - 4.4186$	0.9977
		e/b =4	$y = -0.0043x^3 + 0.2032x^2 + 0.0832x - 0.6457$	0.9999
		e/b =8	$y = -0.0053x^3 + 0.2286x^2 - 0.598x + 0.3813$	0.9999
		e/b =16	$y = 0.0475x^2 + 0.5719x - 2.7819$	0.9991
	Long	Fixed Head	$y = 2\times10^{-10}x^5 - 2\times10^{-7}x^4 + 5\times10^{-5}x^3 - 0.0078x^2 + 0.858x + 1.5975$	0.9996
		e/b =0	$y = -3\times10^{-9}x^4 + 4\times10^{-6}x^3 - 0.0018x^2 + 0.4444x + 1.0073$	0.9983
		e/b =1	$y = -3\times10^{-9}x^4 + 3\times10^{-6}x^3 - 0.0014x^2 + 0.3664x + 0.0732$	0.9987
		e/b =2	$y = -2\times10^{-9}x^4 + 2\times10^{-6}x^3 - 0.001x^2 + 0.2937x - 0.2795$	0.9992
		e/b =4	$y = -2\times10^{-10}x^4 + 3\times10^{-7}x^3 - 0.0002x^2 + 0.181x - 0.13$	0.9998
		e/b =8	$y = 2\times10^{-10}x^4 - 2\times10^{-7}x^3 + 3\times10^{-5}x^2 + 0.0973x + 0.0636$	0.9999
		e/b=16	$y = 0.064x^{0.9676}$	0.9986
Cohesion -less	Short	Fixed Head	$y = 1.583x^2 - 0.9527x + 1.3798$	0.9998
		e/D=0	$y = 0.5013x^2 + 0.0754x - 0.4717$	0.9997
		e/D =0.2	$y = 0.393x^2 + 0.685x - 4.2724$	0.9988
		e/D =0.4	$y = 0.3749x^2 - 0.3014x + 1.0335$	0.9996
		e/D =0.6	$y = 0.3237x^2 - 0.3261x + 1.8051$	0.9998
		e/D =0.8	$y = 0.276x^2 - 0.0834x + 1.472$	0.9998
		e/D =1	$y = 0.2658x^2 - 0.4985x + 3.3612$	0.9991
		e/D =1.5	$y = 0.2289x^2 - 0.8219x + 5.1296$	0.9997
		e/D =2	$y = 0.1727x^2 - 0.1808x + 1.7916$	0.9996
		e/D =3	$y = 0.1419x^2 - 0.5122x + 3.4596$	0.9988
	Long	Fixed Head	$y = 2.4169x^{0.6723}$	0.9994
		e/b=0	$y = 1.5142x^{0.676}$	0.9988
		e/b =1	$y = 0.7988x^{0.7458}$	0.9992
		e/b =2	$y = 0.5175x^{0.7909}$	0.9984
		e/b =4	$y = 0.3329x^{0.8239}$	0.9975
		e/b =8	$y = 0.1651x^{0.8756}$	0.9991
		e/b =16	$y = 0.0776x^{0.9327}$	0.9992
		e/b =32	$y = 0.0284x^{1.0054}$	0.9998

Table 1: Correlation Obtained from Regression Analysis

Soil Type	Load Eccentricity	Regression Equation	Coeff. of Correlation (R^2)
Cohesive	Fixed Head	$y = 0.0087x^4 - 0.1189x^3 + 0.5797x^2 - 0.2305x + 1.0031$	0.9997
	e/D=0	$y = -0.019x^4 + 0.1509x^3 - 0.0068x^2 - 0.1762x + 4.0347$	0.9997
	e/D=0.05	$y = -0.0486x^4 + 0.3977x^3 - 0.5412x^2 + 0.2207x + 4.2866$	0.9998
	e/D=0.1	$y = -0.0536x^4 + 0.4312x^3 - 0.513x^2 + 0.1746x + 4.6212$	0.9997
	e/D=0.2	$y = 0.1541x^3 + 0.0728x^2 - 0.1677x + 5.2266$	0.9995
	e/D=0.4	$y = 0.4366x^3 - 0.5234x^2 + 0.202x + 6.3847$	0.9973
Cohesion-less	Fixed Head	$y = 1.0435x^{-0.949}$	0.9849
	e/D=0	$y = 7.2174x^{-1.552}$	0.9255
	e/D=0.2	$y = 6.974x^{-1.235}$	0.8914
	e/D=0.4	$y = 6.4996x^{-0.979}$	0.8460
	e/D=0.6	$y = 6.4296x^{-0.817}$	0.8194
	e_c/D=0.8	$y = 6.4814x^{-0.717}$	0.8000
	e/D=1	$y = 0.001x^4 - 0.0341x^3 + 0.4202x^2 - 2.2819x + 6.6382$	0.9988
	e/D=1.5	$y = 0.0014x^4 - 0.0435x^3 + 0.4946x^2 - 2.4856x + 7.5206$	0.9968
	e/D=2	$y = 0.0017x^6 - 0.0611x^5 + 0.8923x^4 - 6.6278x^3 + 26.273x^2 - 52.735x + 46.121$	0.9909

Table 2: Equations of Broms' Charts for Lateral Deflection of Pile at Ground Surface

The typical output or the results obtained from *Microsoft Excel*, is presented in a tabular form shown in Fig. 9.

OUTPUT		
Final Design		
	Layer 1	**Layer 2**
Corrected SPT value, N	5.410281564	10.80383957
Average effective unit weight of soil,γ' (kN/m³)	5.19	6.19
Resisting moment of soil,$M_{y,soil}$ (kN-m)	108.3852	108.3852
Resisting moment of structure,$M_{y,pile}$ (kN-m)	88.5953285	88.5953285
Governing resisting moment,M_y (KN-m)	88.5953285	88.5953285
Ultimate lateral load,Q_u (kN)	54.90707461	54.90707461
Maximum allowable working load, Q_m (kN)	21.96282984	21.96282984
Working load,Qa (kN)	30.42799243	156.1767842
Allowable deflection,y (mm)	25	25
Design load,Q (kN)	21.96282984	21.96282984
Design deflection,y_d (mm)	18.04492187	3.515700166
Eccentricity,e_c (m)	0	0
Design load, Q (kN)	21.96282984	
Design defleciont,y (mm)	18.04492187	
Remark	Design OK	

Fig. 9: Typical Output of *Microsoft Excel*

Numerical Example

A short free headed pile in cohesive soil has diameter (b) = 305mm, moment of inertia (I_p) = $1.75x10^{-4}$ m^4, load eccentricity (e) = 0.61m, embedded depth of pile (D) =2.44m. The

undrained shear strength of soil (c_u) =47.8 kPa. Calculated value for ultimate load, Q_u=60 kN. And using the proposed equations the value obtained is 62.9 kN with only a 4.87% variation.

CONCLUSION

The proposed equations of Broms' curves for ultimate lateral capacity and deflection has the potential to be used in engineering practice for the analysis or design of laterally loaded piles in both single and two layered soil just through spreadsheet calculation using *Microsoft Excel*. Trials were made with various examples to check the accuracy of the method. The variations were found to be within 10 percent for both lateral capacity and deflections. As such, the input of the proposed regression equations for lateral load capacity and deflection may be suggested to be used in excel sheet in order to calculate lateral load capacity and pile head deflection, thus avoiding cumbersome method of curve manipulation.

REFERENCES

Broms, B. B. (1964a), Lateral Resistance of Piles in Cohesive Soils, Journal of SMFED, Proc. ASCE, No. SM2, pp. 27-63.

Broms, B. B. (1964b), Lateral Resistance of Piles in Cohesionless Soils, Journal of SMFED, Proc. ASCE, No. SM3, pp. 123-156.

Broms, B. B. (1965), Design of Laterally Loaded Piles, Journal of SMFED, ASCE, No. SM3, pp. 79-99.

Cosenza, E., Galasso, C. & Maddalonib, G. (2011), A Simplified Method for Flexural Capacity Assessment of Circular RC Cross-sections, Engineering Structures Vol. 33, Issue 3, 2011, pp. 942–946, Elsevier publishers.

Matlock, H. and Reese, L.C. (1960), Generalised Solution for Laterally Loaded Piles, Journal of SMFED, ASCE, No. SM5, Part I, pp. 63-91.

ID: AGE 021

1st International Conference on Advances in Civil Engineering 2012 (ICACE 2012)
12 –14 December 2012
CUET, Chittagong, Bangladesh

NUMERICAL ANALYSIS OF EMBANKMENT FOUNDATION SOIL SUPPORTED BY DCM (DEEP CEMENT MIXING) COLUMNS BY FINITE ELEMENT METHOD

MD. M. RAHMAN[1*] & LEE YOUNG DAI[2]

[1*]*Doctoral Candidate, Dept. of Civil Engineering, Pukyong National University, Busan, 608-739, Korea*
(amizankuet2008@yahoo.com)
[2] *Professor, Dept. of Civil Engineering, Pukyong National University, Busan, 608-739, Korea*
(ydlee@pknu.ac.kr)

ABSTRACT

This study was carried out to investigate the effect of DCM (Deep Cement Mixing) columns in two dimension by a newly proposed method '*Replacement Weighted Area'* using finite element analyses with PLAXIS computer software. In proposed method, an equivalent modulus of elasticity of DCM columns and soil surrounding columns has been used to convert three dimension DCM columns to dimension DCM columns model whereas the established '*Same Area Replacement Ratio*' method was considered as beam elements to convert from three dimension to two dimension DCM columns models. This method has provided reasonable values comparing with the existing method as well as field observations. It can easily be applied to calculate the effects of DCM column.

Keywords: Finite element method, Settlement, Lateral displacement, DCM column, PLAXIS

INTRODUCTION

Background : Numerical simulations by means of the Finite Element Method (FEM) have been a valuable tool to predict and understand the behavior of complex structures and extensive research has been recently carried out in geotechnical engineering, Duncan et al. (1988), Bransby et al. (1996), Woodward et al. (2001), Salgado et al. (2004), and Comment et al. (2004). FEM analysis has been employed some researchers for only the purpose of simulating the centrifuge tests to illustrate that the DCM column is likely to be failed by bending (Inagaki et al. (2002); Kitazume et al.(2000) and Miyake et al. (1991). Tam et al. (2005) has measured and plotted results from centrifuge test of Inagaki et al. (2002) to calibrate the FEM analysis. A research conducted by Navin et al. (2005) has shown that the 'Same Area Replacement Ratio (Same, a_s)' matches very much with the three dimensional analysis than using the 'Same Moment of Inertia (Same I_c)' in plane strain analysis.

A new method named as 'Replacement Weighted Area (RWA)' has been investigated in this study.

This method has been employed in plane strain element to evaluate the effect of DCM column using two dimensions PLAXIS computer programs. This study compared the proposed 'Replacement Weighted Area' method with the established 'Same Area Replacement Ratio' using a numerical model based FEM in plane strain element and field observations.

Methods of study

FEM analyses were performed on assuming two-dimensional model in which the DCM columns were modeled as mixed up with soil surrounding columns. In 'Replacement Weighted Area' method an equivalent modulus of elasticity of soil and DCM columns has been used to evaluate from three–dimensional model converted into two-dimensional model according to area replacement ratio. However, in case of 'Same Area Replacement Ratio' method DCM columns from three-dimensional model converted into two-dimensional model has been considered as beam elements to convert three-dimension to two dimension DCM columns model. An equivalent width of beam element depends on area replacement ratio and spacing of DCM column- as described hereunder.

An equivalent modulus of elasticity, E_{eqv} of DCM and soil surrounding of DCM columns by the method is expressed in Eqs. (1)

$$E_{eqv} = a_s \times E_{DCM} + (1 - a_s) E_{soil} \qquad (1)$$

Where, E_{DCM} and E_{soil} are the modulus of elasticity of DCM column and soil surrounding columns, respectively and a_s is the area replacement ratio, defined by the Eqs. (2) And other parameters also find according to area replacement ratio.

$$a_s = \frac{A_{col}}{A_{col} + A_{soil}} \qquad (2)$$

A_{col} and A_{soil} are the area of DCM column and soils surrounding columns respectively as shown in 1

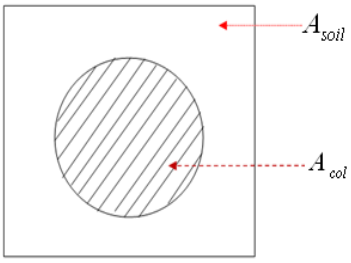

Fig. 1 Area of DCM column and surrounding soils

According to 'Same Area Replacement Ratio' method an equivalent width of DCM column trip from three–dimensional model converted into two -dimensional model by the 'Same, a_s' in Fig. 2

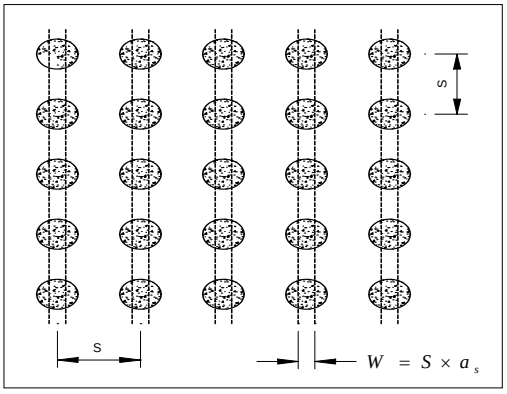

Fig. 2 DCM column strip idealization by 'Same Area Replacement Ratio'

From the equilibrium principle of 'Same Area Replacement Ratio' in simplifying a 3-D dimensional problem to a two dimensional problem, the spacing of the column is related to the width of column in the two dimensional model. An equivalent width of DCM column in 2-D model is presented by the Eqs.(3)

$$W = s \times a_s \qquad (3)$$

Where s is spacing of column in three-dimensional problem.

MATERIAL AND NUMERICAL MODELING

The geometry of the embankment with subsoil's profile is shown in Fig. 3 and the physical and engineering characteristics of materials used in the numerical analyses have been listed in Table 1 and Table 2.

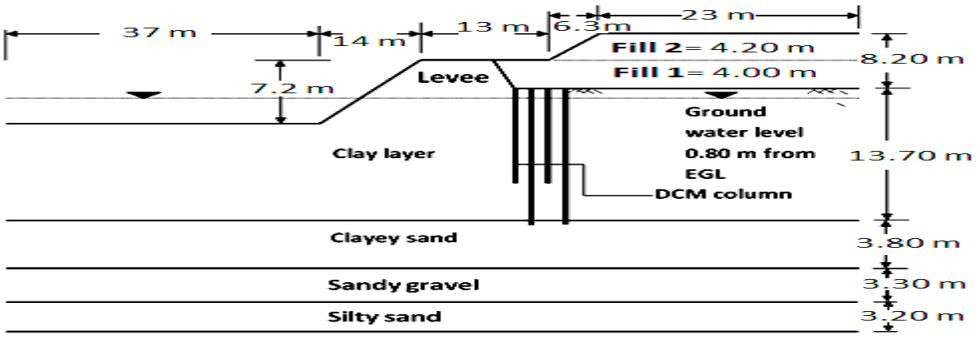

Fig. 3 Geometry of embankment with soil profile

The area replacement ratio, a_s, according to the configuration of DCM column pattern arrangement as shown in Fig. 4 has been calculated to be 44%. The diameter of DCM column is 1.9 meter and center to center spacing of the DCM column is 1.8 meter. The length of the DCM column is 15 m and 10 m alternatively with 10 meter length of H-pile (having cross-section 300 x 300 x 10 x 15 mm) are used in this research.

Table 1 Materials parameters used in FEM analysis

Material	Model	Parameter values
Levee	Mohr-Coulomb	γ = 17 kN/m^3, γ_{sat} = 18 kN/m^3, c_u=18 kPa, ϕ_u=20^o, ν=0.30, E = 30000 kPa, k=1.0E-4m/day
Under levee-1	Mohr-Coulomb	γ = 17 kN/m^3, γ_{sat} = 18 kN/m^3, c_u=11 kPa, ϕ_u=20^o, ν=0.30, E = 2000kPa, k=1.0E-4m/day
Under levee-2	Mohr-Coulomb	γ = 16 kN/m^3, γ_{sat} = 17 kN/m^3, c_u=9 kPa, ϕ_u=25^o, ν=0.28, E = 3500kPa, k=0.10 m/day

Table 2 Materials parameters used in FEM analysis

Material	Model	Parameter values
Clay layer	Mohr-Coulomb	γ = 15.5 kN/m^3, γ_{sat} = 16 kN/m^3, c_u=11 kPa, ϕ_u=15^o, ν=0.33, E = 560 kPa, k=2.6E-4m/day
Sandy clay	Elastic	γ = 16kN/m^3, γ_{sat} = 17 kN/m^3, E=3000 kPa, ν=0.28, K_o=0.577, k= 0.10 m/day
Fill-1	Elastic	γ = 17 kN/m^3, γ_{sat} = 19 kN/m^3, E=30000 kPa, ν=0.3, K_o=0.577, k= 0.25 m/day
Fill-2	Elastic	γ = 17 kN/m^3, γ_{sat} = 19 kN/m3, E=25000kPa, ν=0.3, K_o=0.577, k=0.25 m/day
DCM column	Elastic	γ = 16 kN/m^3, γ_{sat} = 17 kN/m3, E=58,000 kPa, ν=0.30; K_o= 1.0, k=1.0E -5 m/day
DCM with soil	Elastic	γ = 15.72kN/m^3, γ_{sat} = 16.44kN/m3, E=25833 kPa, ν=0.32, K_o= 1.0, k= 1.5E-4 m/day

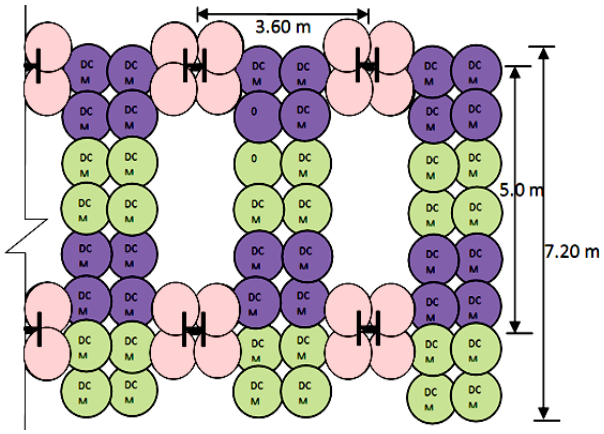

Fig. 4 Arrangement of four rows DCM column with H-pile

The deformations of the deep sandy gravel and silty sand layers shown in Fig. 3 are assumed to be zero. Hence these two layers were not included in the model and fixed base has been used in the model instead of two layers of gravel and sand. The finite element mesh by ‘Replacement Weighted Area’ and ‘Same Area Replacement Ratio’ in plane strain element is shown in Fig. 5.

RESULTS OF NUMERICAL ANALYSES

The numerical analyses by two method (i) ‘Replacement Weighted Area’ and (ii) ‘Same Area Replacement Ratio’ in plane strain elements with PLAXIS 8.2 computer software, has been predicted the maximum settlement, horizontal displacement and safety factor of the embankment as shown in Table: 3 The results in Table 3 shown that the vertical settlement and lateral displacement calculated by (RWA) and (Same a_s) methods in plane strain elements are reasonably closer values. Both of methods of ‘Replacement Weighted Area’ and ‘Same Area Replacement Ratio’ in plane strain element have shown almost same safety factor result. After 556 days, the field observation of maximum settlements and horizontal displacements were measured 2.59 meter and 32.20 centimeter respectively from the gauges.

The vertical settlement and horizontal displacement found to be increased with time is shown in Fig. 6 and Fig. 7 and subsequently it matched nearly with the predicted limit. The effect of the two method have indicated almost same settlement at the center of the embankment but it little varied at the toe of the embankment as shown in Fig. 6. The lateral displacement predicted by (RWA**)**, (Same a_s) in plane strain and field observed horizontal displacements under the toe of the embankment at 470 and 556 days are presented in Fig. 7. The lateral displacements predicted by (RWA) and (Same a_s) methods in plane strain element showed very little differences. The lateral displacement predicted by ‘Replacement Weighted Area’ was very close in lower depth (within -5 to -20 m) but it varied in little amount (within -5 to +5 m) from field observation and (Same a_s) method in plane strain elements as shown in Fig. 7. The difference was observed as, area replacement ratio a_s was used in both the proposed ‘Replacement Weighted Area’ and ‘Same Area Replacement Ratio’ methods to calculate the effects of DCM columns. Only converting method was different of DCM column from three-dimension to two-dimension model. In case of ‘Same Area Replacement Ratio’ DCM columns from three-dimensional converted into two-dimensional model considered as beam elements. The width of beam element depends on area replacement ratio and spacing of DCM columns.

Whereas in proposed ‘Replacement Weighted Area’ DCM columns converted from three-dimensional to two dimensional models by theoretically mixing up soils surrounding DCM columns according to area replacement ratio. An equivalent modulus of elasticity of DCM columns and soils surrounding DCM column has been used to evaluate the effects DCM columns by the ‘Replacement Weighted Area’ in plane strain elements.

The observed lateral displacement was greater at 556 than 470 days i.e. the horizontal displacement increased with time and would nearly matches with the predicted one. The horizontal displacements were predicted by ‘Replacement Weighted Area’ varied very little from (-5m to +5m) compared with

'Same Area Replacement Ratio' in plane strain elements. Because for 'Replacement Weighted Area' an equivalent modulus of elasticity others soil parameters were calculated from DCM column and soils surrounding DCM column according to area replacement ratio. But in case of 'Same Area Replacement Ratio' DCM circular column converted into beam element according to area replacement ratio and spacing of DCM columns. There was no need to evaluate the equivalent parameters from DCM and soils parameters surrounding DCM column. The results between two methods in plane strain element varied little bit due to above mentioned fact. A very little difference of horizontal displacement only in the upper part of graph shown in Fig. 7 is very reasonable difference in geotechnical engineering problem.

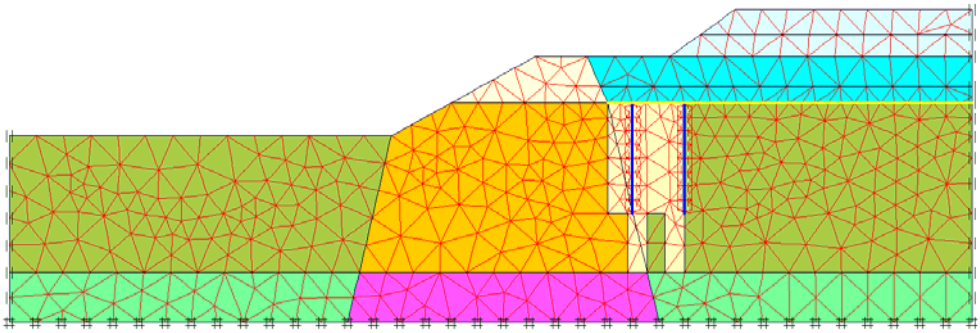

Fig. 5 Finite element mesh by 'Replacement Weighted Area' and 'Same Area Replacement ratio' methods

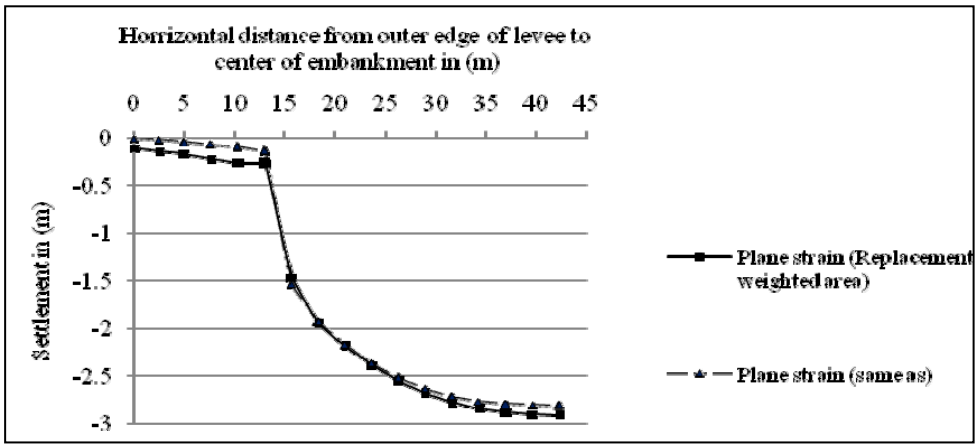

Fig. 6 Vertical settlement of ground surface of embankment by Plane strain (RWA and same a_s) methods

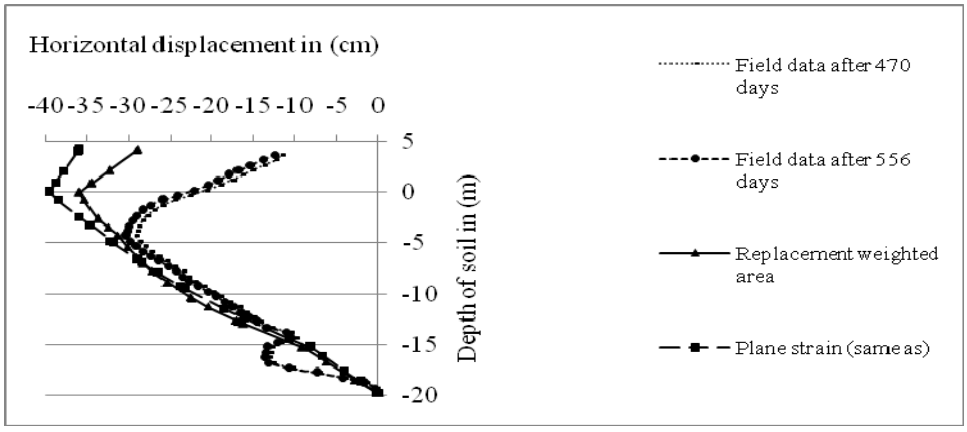

Fig. 7 Predicted lateral displacement by Plane strain (RWA and same a_s) methods and field observation

Table: 3 The predicted values by plane strain (Replacement Weighted Area and Same Area Replacement Ratio)

Particulars	Vertical settlement (m)	Horizontal displacement.(cm)	FS
Plane strain (RWA)	2.90	35.95	1.894
Plane strain (same a_s)	2.83	39.53	1.842

CONCLUSIONS

The summary of findings and recommendations based on present research are follows:

1. The ‘Replacement Weighted Area’ and ‘Same Area Replacement Ratio’ in plane strain element have indicated almost identical value of surface settlement.
2. The maximum lateral displacements predicted by ‘Replacement Weighted Area’ in plane strain are reasonably closer values to results obtained from ‘Same Area replacement Ratio’ and field observations.
3. From safety analysis point of view, ‘Replacement Weighted Area’ method indicated almost equal of factor of safety as compared with ‘Same Area Replacement Ratio’ in Plane strain elements.

The results from the effects of DCM column with soils surrounding DCM columns would be easily calculated by ‘Replacement Weighted Area’ and satisfactory results have been found in comparison with field observation and ‘Same Area Replacement Ratio’ in plane strain elements. So these results have verified that the ‘Replacement Weighted Area’ method in plane strain element can be applied to calculate the effects of DCM column with soils surrounding DCM columns as well.

ACKNOWLEDGMENTS

The authors are grateful to the authority of Daewoo Engineering & Construction Co. LTD and DongAa Geotechnical Engineering Co. LTD for providing field observation data complete the research work smoothly.

REFERENCES

Bransby MF. And Springman SM. (1996) 3-D finite element modelling of pile groups adjacent to surcharge loads. Comput Geotech 19(4), pp. 301–24.

Commend S, Geisera F, and Crisinel J. (2004) Numerical simulation of earthworks and retaining system for a large excavation. Adv Eng Softw 35, pp 669–678.

Duncan JM and Schaefer VR. (1988) Finite element consolidation analysis of embankments. Comput Geotech 6(2), pp 77–93.

Inagaki, M., Abe, T., Yamamoto, M., Nozu, M., Yanagawa, Y., and Li, L. (2002) Behavior of Cement Deep Mixing Columns under Road Embankment. *Physical Modelling in Geotechnics*, pp. 967 – 972.

Kitazume, M., Okano, K., and Miyajima, S. (2000) Centrifuge model tests on failure envelope of

column type deep mixing method improved ground. *Soils and Foundations*, 40(4), pp. 43-55.

Miyake, M., Wanda, M., and Satoh, T. (1991) Deformation and Strength of Ground Improved by Cement Treated Soil Column. *Geo-Coast 91,* Yokohama, pp. 369 -372.

Navin, M. P. Kim, M. and Filz, G. M. (2005) Stability of embankments founded on deep-mixing method columns: three-dimensional considerations. *Proc. of the 16th Int. Conf. on Soil mech. and Geo. Engg. (16ICSMGE),* Osaka, Japan, pp. 1227-1230.

Salgado R., Lyamin AV., Sloan SW. and Yu HS. (2004) Two- and three-dimensional bearing capacity of foundations in clay. Geotechnique 54(5), pp. 297–306.

Tam N.M., Jung D.H., and Phan V. (2005) The distribution of bending moment and bending moment capacity of DCM column under embankment, The 2005 international symposium on advanced engineering, Pukyong National University, Pusan, South Korea, pp. 46-53.

Woodward PK. and Berenji AP. (2001) Advanced numerical investigation of Terzaghi's superposition theory. Adv Eng Softw 32(10–11), pp. 797–804.

ID: AGE 022

1st International Conference on Advances in Civil Engineering 2012 (ICACE 2012)
12 –14 December 2012
CUET, Chittagong, Bangladesh

A PARAMETRIC STUDY OF STABILITY OF GEOTEXTILE REINFORCED SOIL UNDER THE HIGHWAY EMBANKMENT

MD. M. RAHMAN[1*] & LEE YOUNG DAI[2]

[1]*Doctoral Candidate, Dept. of Civil Engineering, Pukyong National University, Busan, 608-739, Korea*
(amizankuet2008@yahoo.com)
[2] *Professor, Dept. of Civil Engineering, Pukyong National University, Busan, 608-739, Korea*
(ydlee@pknu.ac.kr)

ABSTRACT

This study was carried out to investigate the behavior of geotextile-reinforced soil in different layers of the embankment using two-dimensional finite element analyses considering the plane stain condition by PLAXIS software. The effects of tensile stiffness, number and length of reinforcement layers have been investigated. It has been found that vertical settlements and lateral displacements have been reduced with increasing in tensile stiffness, number and length of reinforcement. In this study, maximum settlements reduced with increase in the length of reinforcement. However, over certain thresholds, the vertical settlements and lateral displacements had not been reduced significantly with increasing tensile stiffness, number and length of geotextile.

Keywords: Finite element method, Settlement, Lateral displacement, Geotextile, PLAXIS

INTRODUCTION

In this study, the finite element method by PLAXIS software has also been used to investigate the effects of geosynthetic (geotextile) in the different layers of embankment. This element needs only an axial stiffness, AE, where A is the cross-sectional area per unit width and E is the modulus of elasticity of the material. The axial stiffness was obtained from air tensile test, which was performed by Prempramote (2005). Geosynthetic materials are used widely in the embankment to increase stability of structure (Giroud (1982); Bergado and Teerawattanasuk, (2008); Briançon and Villard, (2008); Chen et al., (2008); Li and Rowe, (2008); Rowe and Taechakumthorn, 2008; Sarsby, (2007). Bonaparte and Berg (1987)) have utilized the tensioned membrane theory with a consideration of the soil arching effect. This approach was further extended by Giroud et al. (1990) for analysis and design of soil geosynthetic systems overlying voids. Poorooshasb (2002) has studied on subsidence

evaluation of geotextile reinforced gravel mats bridging a sinkhole by integro differential numerical technique. Yoo and Shin (2000) and Tahmasebipoor et al. (2010) have conducted a parametric study on the effect of reinforcing layouts on the deformation behavior of the tunnel face and on the effect of geotextile reinforcing laid outs on stability of soil over a circular underground cavity respectively. In this study, a series of parametric finite element analyses were performed in order to investigate the effect of influencing parameters on the stability of the geotextile-reinforced soil in the different layers of embankment.

MATERIAL AND NUMERICAL MODELING

The geometry of the embankment with subsoil's profile is shown in Fig. 1 and the physical and engineering characteristics of materials used in the numerical analyses have been listed in Table 1.

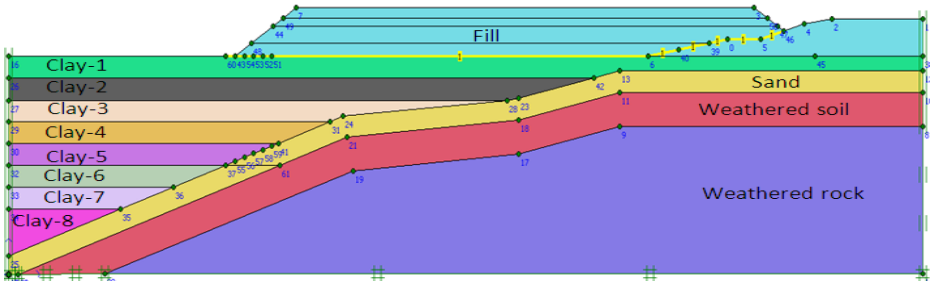

Fig. 1 Geometry of embankment with soil profile considered for numerical analysis

Table 1 Materials parameters used in FEM analysis

Material	Model	Parameter values
Fill	Elastic	γ = 19 kN/m^3, γ_{sat} = 20 kN/m^3, E=50000 kPa, ν=0.3, K_o=1.00, k= 1.00 m/day
Clay	Mohr-Coulomb	γ = 15.5 kN/m^3, γ_{sat} = 17kN/m^3, c_u= 8~11 kPa, ϕ_u=11~15^o, ν=0.33, E = 450~560 kPa, k=1.0E-4m/day
Sandy	Elastic	γ = 17 kN/m^3, γ_{sat} = 19 kN/m^3, E=40000 kPa, ν=0.30, K_o=0.577, k= 1.00 m/day
Weathered soil	Elastic	γ = 18 kN/m^3, γ_{sat} = 19 kN/m^3, E=50000 kPa, ν=0.3, K_o=1.00, k= 0.25 m/day
Weathered rock	Elastic	γ = 20 kN/m^3, γ_{sat} = 21 kN/m^3, E=100000 kPa, ν=0.25, K_o=1.00, k= 0.010 m/day
DCM column	Elastic	γ = 15 kN/m^3, γ_{sat} = 16 kN/m3, E=58,000 kPa, ν=0.30; K_o= 1.0, k=1.0E -6 m/day
DCM column with soil	Elastic	γ = 15.72kN/m^3, γ_{sat} = 16.44kN/m3, E=25833 kPa, ν=0.32, K_o= 1.0, k= 1.5E-4 m/day

The increasing performance of computers may eventually lead to the situation that geotechnical engineers can apply non-linear two and three-dimensional finite analysis on daily basis for ordinary design and consulting purposes. The finite element method is a widely accepted numerical method for analysis and design in all most all branches of engineering. PLAXIS is a finite element code for soil and rock analyses, originally developed for analyzing deformation and stability in geotechnical engineering projects. The PLAXIS code calculates the strains, stresses and failure states of soil, and permits full automatic mesh generation based on the triangulation principle. PLAXIS is a powerful tool for studying the geotextile-reinforced soil above the foundation soil in the different layers of embankment. In this study, parametric studies have been evaluated based on the effect of geotextile inclusion and variation of its tensile stiffness, length and number of layers of geotextile by the vertical and horizontal displacement as well as safety of factor analysis. The finite element mesh of geometry is presented in Fig. 2. The material property of reinforcement in the elastic axial stiffness (EA) has been used in this numerical analysis model based FEM in plane strain element. In this study, finite element method analysis are performed with using a wide range of geotextile tensile stiffness, EA_{geo}= 100, 500, 1000, 2000, and 5000 KN/m; the length of geotextile at 20 m, 35 m and 50 m; and number of geotextile layers n = 1 layer, 2 layers, 3 layers and 4 layers etc.

RESULTS OF NUMERICAL ANALYSES

Effect of tensile stiffness of geotextile

The effect of tensile stiffness of the single layer geotextile have been studied for different stiffness equal to 100kN/m, 500kN/m, 1000kN/m 2000 kN/m and 5000 kN/m. In this analysis, the length of the geotextile layer has been considered as 50 m. It was observed that the vertical settlement decreased with increasing the stiffness of the reinforcing layer, because the load carried by the reinforcement is in proportion to its stiffness. For example, when tensile stiffness of geotextile increases from 100 to 5000 kN/m, the surface settlement decreased from 3.49 to 3.24m, it was about 25 cm. The vertical settlement of the ground surface varied with the tensile stiffness of the geotextile is shown in Fig. 3. It was also observed that the lateral displacement reduced with increasing in stiffness of the reinforcing layer, because the effective characteristics of geosynthetics (geotextile) having high tensile capacity but soil does not have that property. The tensile load carried by the geotextile reinforcement is directly proportional to its stiffness. For example, when tensile stiffness of geotextile increases from 100 to 5,000 KN/m, the lateral soil displacement has reduced from 44.07 to 41.64 cm, it was about 25 mm. The lateral soil movement varied with the tensile stiffness of the geotextile as shown in Fig. 2. The safety factors, FS, summarized in Table 4 were determined from FEM analyses. It was observed that the stability of embankment has been increased with increasing the stiffness of geosynthetics but it has increased rapidly in early stage and then slowed down when the stiffness of geosynthetics was greater than about 1000 kN/m shown in Figure 5.

Effect of length of geotextile

The effect of length of geotextile layer on settlement of ground surface has been studied for different length at 50 m, 35 m and 20 m and tensile stiffness equal to 1000 kN/m. Fig. 6 has shown that the effect of length of reinforcement layer on vertical settlements for different length of the geotextile. It is observed that the settlement has been decreased with increasing the length of geotextile reinforced soil. It was decreased from 3.57 to 3.24m. It was about 33 centimeters. The effect of length of reinforcement layer on lateral movement for different length of the geotextile is shown in Fig. 7. In this observation, it has seen that horizontal displacement decreased with increasing the length of reinforcement and then become approximately constant even though there was further increasing the length of geotextile layer. In this case, the lateral displacement was decreased about 40 mm and the length of geotextile 50 and 35m has given almost same lateral displacement in Fig. 7. So in this analysis, the critical length of reinforcement layer was 35 m.

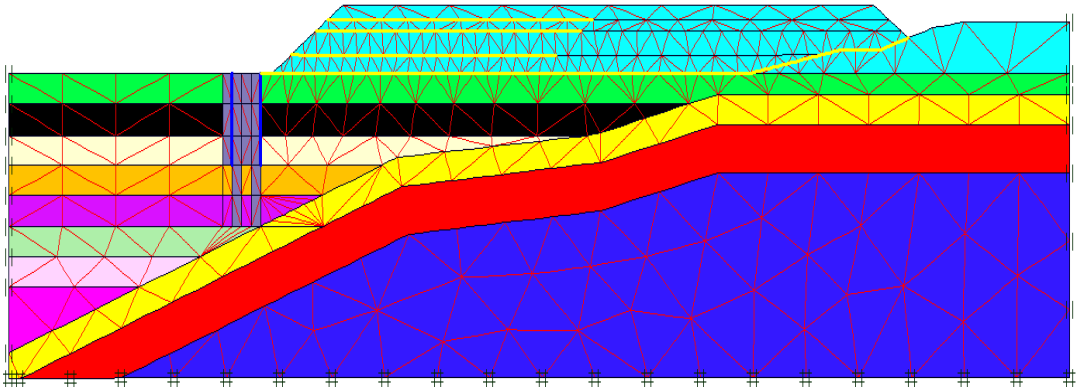

Fig. 2 Finite element mesh of the geometry for a parametric study of geo-synthetics (geotextile)

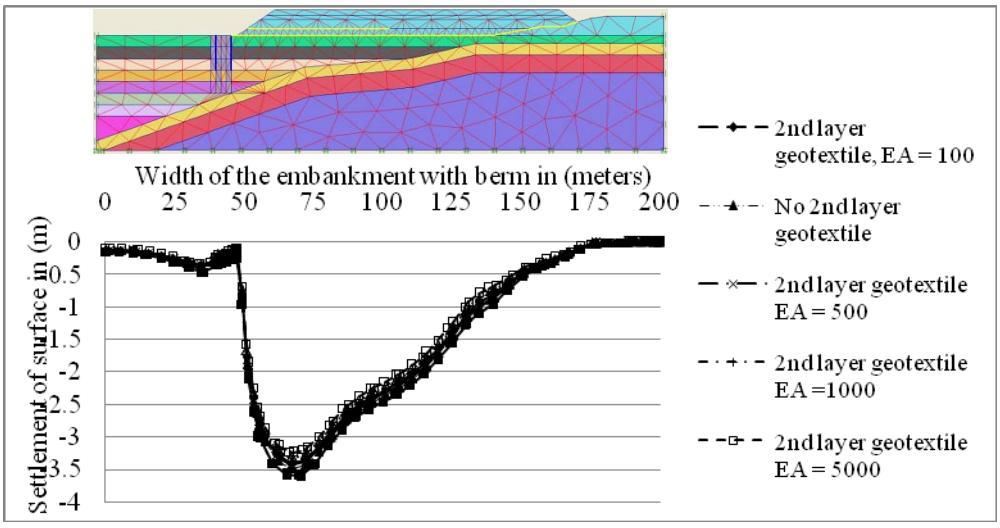

Fig. 3 Effect of geotextile tensile stiffness on settlement of ground surface under embankment

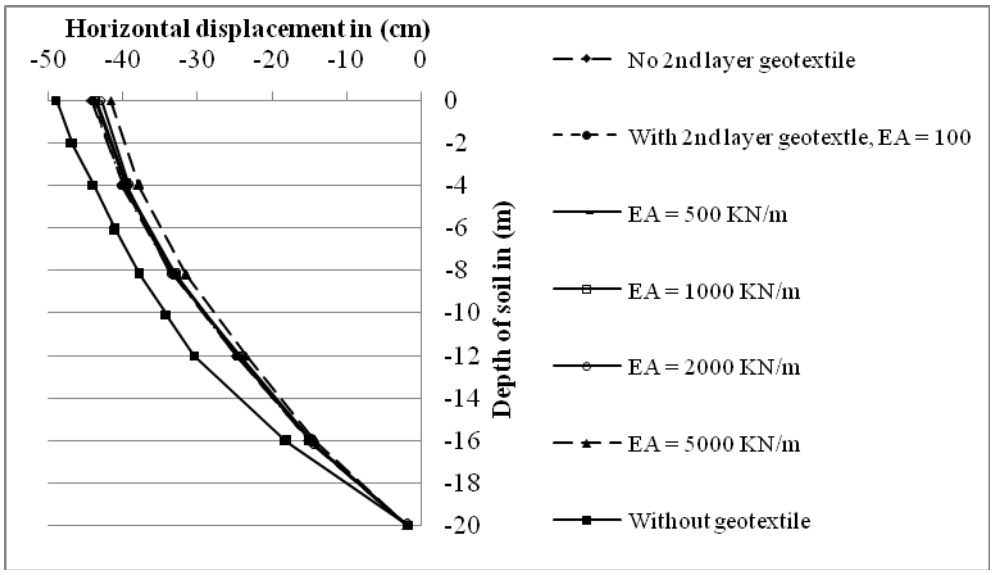

Fig. 4 Effect of geotextile tensile stiffness on lateral displacement at toe of the embankment

Table 2 Factor of safety, FS, calculated from FEM analysis

Case	Geosynthetic (geotextile)				
	E=100 kN/m	E=500 kN/m	E=1000 kN/m	E=2000 kN/m	E=5000 kN/m
FS	1.814	1.920	2.021	2.074	2.099

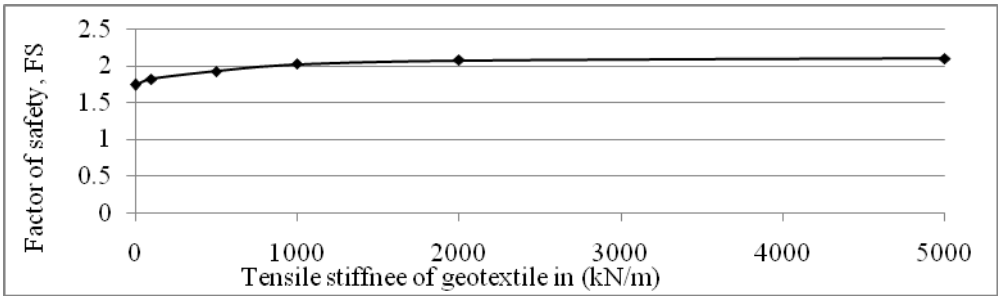

Fig. 5 Factor of safety variation with stiffness of geosynthetic

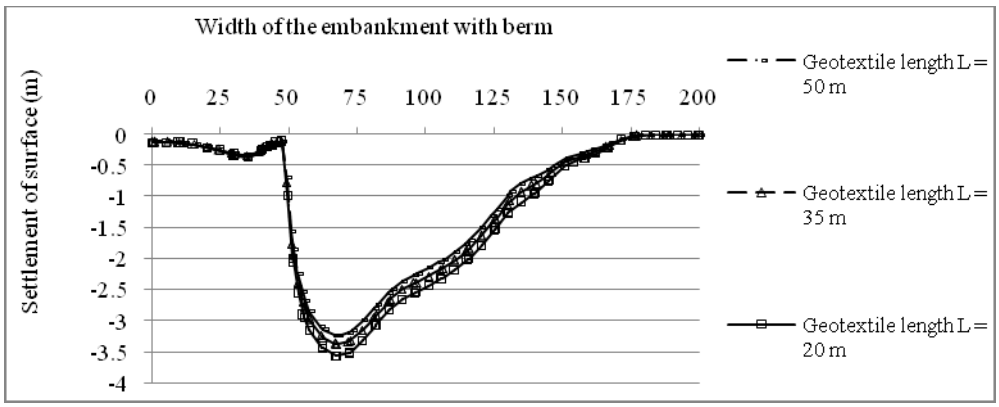

Fig. 6 Effect of geotextile length on settlement of ground surface under embankment

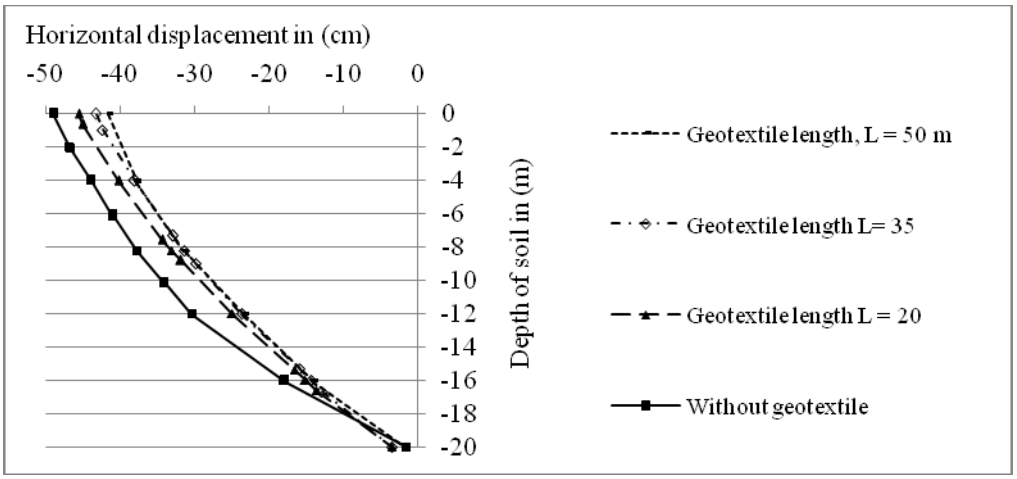

Fig. 7 Effect of geotextile length on lateral displacement

Effect of number of geotextile layers

To investigate the effect of reinforcement layer numbers on settlement and lateral displacement, a series of analysis have been carried out on model with different number of geotextile layers for tensile stiffness equal to 1000 KN/m. In all analyses, the length of reinforcement layer was constant and equal to 35 m. Fig. 8 and Fig. 9 has shown the effect of number of geotextile layer on maximum settlement of ground surface and the lateral displacement at same tensile stiffness. From this analysis, it has been observed that the settlement and lateral displacement decreased with increasing the number of reinforcement layers and then becomes approximately constant even though there was further increasing the number of geotextile layers. It has clearly indicated that there was a reduction of settlement up to maximum extent at that particular stiffness. The critical number of geotextile is equal to 3.

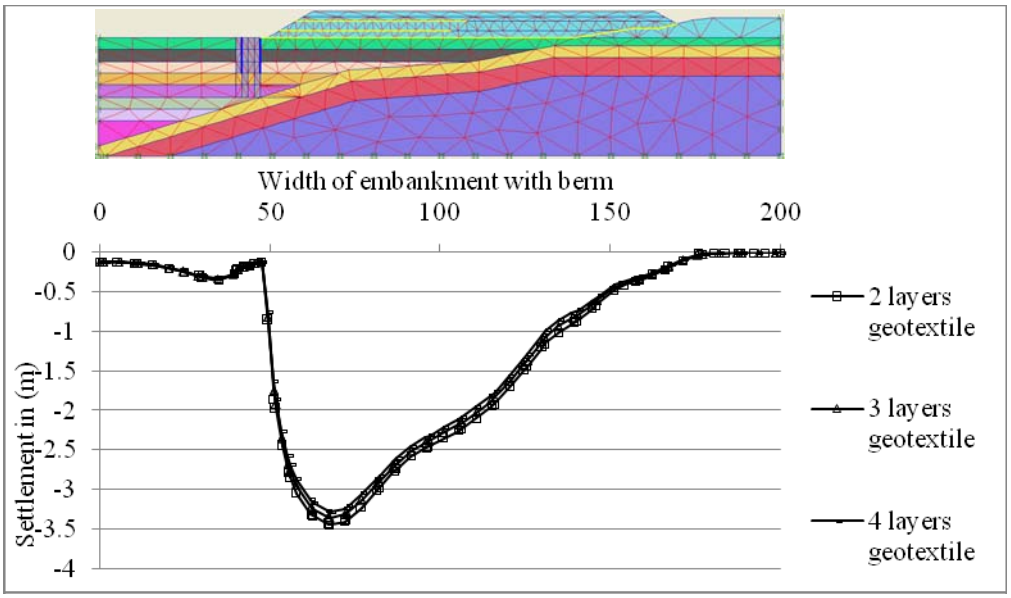

Fig. 8 Effect of geotextile number of layers on ground surface settlement

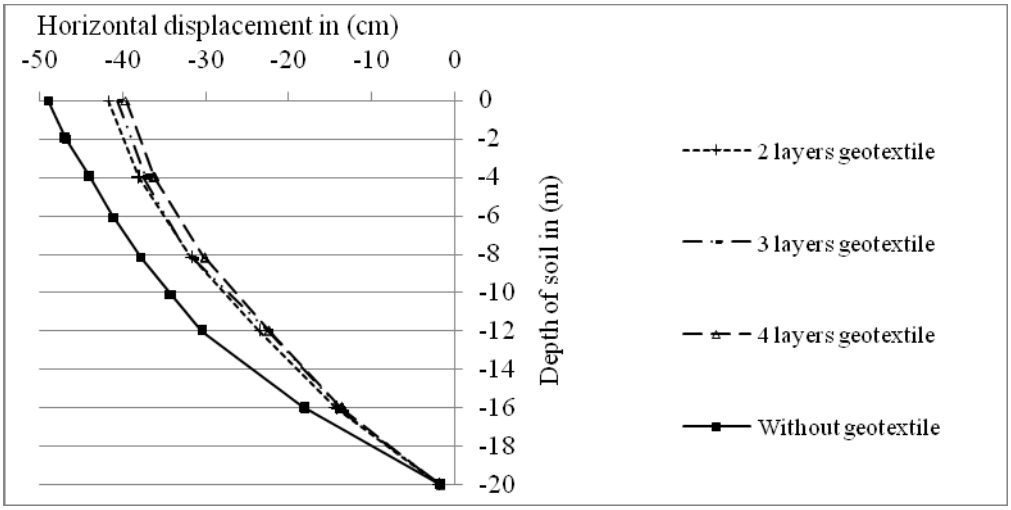

Fig. 9 Effect of geotextile no. layers on lateral displacement at toe of the embankment

Tahmasebipoor et al. (2010) investigated the behavior of geotextile-reinforced soil above an underground cavity. The effects of geotextile tensile stiffness (20KN/m to 1000 KN/m), length (8 m to 13 m) and number of reinforcement (1 to 7) layers have been investigated. These results have indicated that maximum ground surface settlements reduced with increasing the stiffness of reinforcement as well as settlements reduced with increasing the length and number of reinforcement. Tahmasebipoor et al. (2010) also found that ground surface settlement reduced with increasing the stiffness, length and number of geotextile layer is about 10~35 mm from a parametric study of stability of geotextile-reinforced soil above an underground cavity.

CONCLUSIONS

The main conclusions from this study are:

(i) The maximum vertical settlement of ground surface and horizontal displacement has been reduced with increasing the stiffness of the reinforcement soils.

(ii) The maximum settlements of ground surface and horizontal displacements were decreased with increasing the length of reinforcement. However, a critical length has been observed in this study, beyond which no significant effect on reduction of settlements and horizontal displacement has been found. In this study the critical length of geotextile has been recorded as 35 m.

(iii) The maximum settlements of ground surface and maximum horizontal displacements have been found in reducing trend with increasing the number of geotextile layers. However a critical number of geotextile layers found, beyond which no effects in settlements and horizontal displacements reduction was observed. In this study the critical number of geotextile layer is found to be 3 for EA equal to 1000 KN/m and L= 35m.

(iv) The FS has been found to be increasd rapidly in early stages and subsequently slow down when the tensile modulus of geosynthetics is greater than 1000 kN/m.

ACKNOWLEDGMENT

The authors are grateful to the authority of Korea Expressway Corporation for providing necessary data to complete the research work smoothly.

REFERENCES

Bergado, D.T. and Teerawattanasuk, C. (2008) 2D and 3D numerical simulations of reinforced embankments on soft ground. Geotextiles and Geomembranes 26 (1), pp. 39–55.

Bonaparte R. and Berg RR. (1987) The use of geosynthetics to support roadways over sinkhole prone areas. In: Proceedings of the 2nd Multidisciplinary Conference on Sinkholes and the Environmental Impacts of Karst, Orlando, FL. pp. 437–445

Briançon, L. and Villard, P. (2008) Design of geosynthetic-reinforced platforms spanning localized sinkholes. Geotextiles and Geomembranes 26 (5), pp. 416–428.

Chen, Y.-M., Cao, W.-P. and Chen, R.-P. (2008) An experimental investigation of soil arching within basal reinforced and unreinforced piled embankments. Geotextiles and Geomembranes 26 (2), pp. 164–174.

Giroud JP. (1982) Design of geotextile associated with geomembranes. In: Proceedings of the 2nd International Conference on Geotextiles, Las Vegas, NV, pp. 37–42

Li, A.L. and Rowe, R.K. (2008) Effects of viscous behavior of geosynthetic reinforcement and foundation soils on embankment performance. Geotextiles and Geomembranes 26 (4), pp. 317–334.

Poorooshasb HB. (2002) Subsidence evaluation of geotextile reinforced gravel mats bridging a sinkhole. J Geosynthetics Int 9(3), pp. 259–282

Prempramote, S. (2005) Interaction between geogrid reinforcement and tire chip-sand mixture. M.Eng. Thesis No. GE-04-12 Asian Institute of Technology, Thailand

Rowe, R.K. and Taechakumthorn, C. (2008) Combined effect of PVDs and reinforcement on embankments over rate-sensitive soils. Geotextiles and Geomembranes 26 (3), pp. 239–249.

Sarsby, R.S. (2007) Use of 'Limited Life Geotextiles' (LLGs) for basal reinforcement of embankments built on soft clay. Geotextiles and Geomembranes 25 (4–5), pp. 302–310.

Tahmasebipoor A., Noorzad R., Shooshpasha E, and Barari A. (2010) A parametric study of stability of geotextile-reinforced soil above an underground cavity. Arab J Geosci, DOI 10.1007/s 12517-010-0188-0.

Yoo CS, Shin HK. (2000) Behavior of tunnel face pre-reinforced with sub-horizontal pipes. In: Proceeding Of Geotechnical Aspect of Underground Construction in Soft Ground, Balkema. pp 441–446

ID : AGE O26

1st International Conference on Advances in Civil Engineering 2012 (ICACE 2012)

12 –14 December 2012

CUET, Chittagong, Bangladesh

WAVE IMPACT ON VERTICAL SEA-WALL: NUMERICAL SIMULATIONS WITH THE NEWLY IMPROVED MPS METHOD

M. M. RAHMAN[1*], T. IRIBE[2], E. NAKAZA[3] & M. A. ROUF[4]

[1]MS, Dept. of Civil Eng. and Architecture, University of The Ryukyus

Senbaru 1, Nisihara, Nakagami, Okinawa 903-0213, Japan, e-mail: rahman_ku@yahoo.com

[2] Assist. Professor, Dept. of Civil Eng. and Architecture, University of The Ryukyus

Senbaru 1, Nisihara, Nakagami, Okinawa 903-0213, Japan, email: iribe@tec.u-ryukyu.ac.jp

[3] Professor, Dept. of Civil Eng. and Architecture, University of The Ryukyus

Senbaru 1, Nisihara, Nakagami, Okinawa 903-0213, Japan, email: enakaza@tec.u-ryukyu.ac.jp

[4] Professor, FMRT Discipline, Khulna UniversityKhulna-9208, Bangladesh, email: roufku@yahoo.com

**Corresponding Author*

ABSTRACT

Large wave causes terrifying impact on the protective coastal structures. The coastal structures should be stable enough against devastating wave impact. Verified numerical simulation method is urgent to develop with the experimental results. This study shows the verification of a newly improved moving particle semi-implicit (MPS) method with the experimental results of wave impact on vertical sea-wall. The relationship between wave impact pressure and wave height in front of vertical sea-wall exhibits in this study. The numerical simulation results show good agreement with the experimental results. The relationship between wave height and wave impact pressure on sea-wall has been figured out with different numerical simulation results. It shows the potentiality of this newly improved MPS method to simulate wave impact problems on sea-wall.

Keywords: Coastal structures, wave impact, numerical simulation, MPS method

INTRODUCTION

Vertical sea-walls have been constructed around the coast to secure coastal community against sea waves. However, large wave may cause terrifying impact on the protective coastal structures. Therefore,

the structures should be stable enough against devastating wave impact. Experimental and numerical research on wave impact on vertical sea-wall has been carried out in different studies (Hanbin et al., 2003; Mingham et al., 2003; Iribe et al., 2012). Recently, in coastal engineering field, a particle method, called moving particle semi implicit (MPS) method, has been expected to assess complex wave-structure interaction. However, the original MPS method (Koshizuka and Oka, 1996) shows low accuracy than the newly improved MPS method (Iribe and Nakaza, 2011). The newly improved MPS method shows good agreement with the experimental results related to the wave impact on sea-wall (Arikawa et al., 2005). The wave impact on the vertical sea-wall has been measured and the relation between the impact pressure and wave height are detected in this study. In addition, bore impact pressure and clapotis wave pressures are calculated successfully by the newly improved numerical simulation. The numerical results show good consistency with the experimental results.

EXPERIMENT

An extensive large experiment of wave impact on sea-wall was conducted by Arikawa et al. (2005). Fig. 1 shows the complete scheme for the simulation. Wave generator was used to promote the wave. Wave height (H_a and H_b) in different positions on the tank and wave impact on a vertical sea-wall were estimated. More detail illustration of this experimental plan can be found in Arikawa et al. (2005).

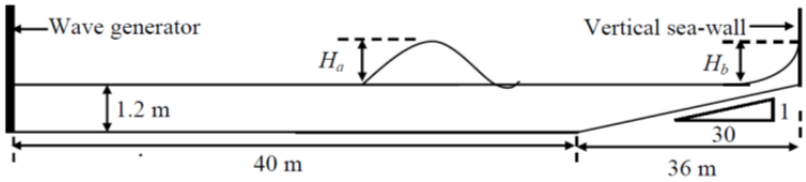

Fig. 1: Wave tank model for wave impact on sea-wall simulation.

NUMERICAL SIMULATION

The wave impact on vertical sea-wall was simulated by using newly improved moving particle semi-implicit (MPS) method (Iribe and Nakaza, 2011). This method has frequently been used in coastal engineering field (Nakaza et al., 2010; Nakaza et al., 2012; Iribe et al., 2012). The newly improved MPS method can be briefly described as follows:

Weight Function

Equation [1] shows the calculation of interaction between particle i and its neighboring particles j, a weight function w.

$$w(r)=\begin{cases}\dfrac{r_e}{r}-1 & r\le r_e\\ 0 & r_e<r\end{cases} \tag{1}$$

Where, r is the distance between particles i and j, the radius of the interaction area is represented by parameter r_e. The particle number density with respect to particle i is given by the summation of the weight function of neighboring particles j in Eq. (2). Initial particle positions can be identified by calculating the initial particle number density n^0.

$$\langle n\rangle_i=\sum_{j\neq i}w\left(\left|\vec{r}_j-\vec{r}_i\right|\right) \tag{2}$$

Gradient Model

The pressure gradient for the particle i was defined based on the arrangement of neighboring particles j in originally developed MPS method. Particles must be arranged at regular lattice points in this original method. However, in actual numerical process, the arrangement of neighboring particles j is generally irregular so that the accuracy based on original gradient method is not well enough. The newly improved MPS method uses the following formula which does not depend on the particle arrangement and it shows higher accuracy than the original MPS method.

$$\nabla\phi|_{ij}=\left[\frac{1}{n^0}\sum_{j\neq i}w\left(\left|\vec{r}_j-\vec{r}_i\right|\right)\frac{\left(\vec{r}_j-\vec{r}_i\right)}{\left|\vec{r}_j-\vec{r}_i\right|}\otimes\frac{\left(\vec{r}_j-\vec{r}_i\right)}{\left|\vec{r}_j-\vec{r}_i\right|}\right]^{-1}\left(\frac{1}{n^0}\sum_{j\neq i}w\left(\left|\vec{r}_j-\vec{r}_i\right|\right)\frac{\phi_j-\phi_i}{\left|\vec{r}_j-\vec{r}_j\right|}\frac{\left(\vec{r}_j-\vec{r}_i\right)}{\left|\vec{r}_j-\vec{r}_i\right|}\right) \tag{3}$$

Where, ϕ is a physical quantity, w is the weight function.

Poisson Equation of Pressure

Tanaka and Masunaga (2008) proposed the following improved Poisson equation of pressure to get the better accuracy than the original MPS method.

$$\nabla^2 p_i=\frac{\rho}{\Delta t}\nabla\cdot\vec{u}_i^{\,*}+\gamma\frac{\rho}{\Delta t^2}\frac{n^0-n_i^{\,k}}{n^0} \tag{4}$$

Where, ∇^2 is the Laplacian, p is the pressure, ρ is the density, Δt is the time increment, u^* as speed between time steps, n^k is the particle number density of the previous time step. In this equation, second term in the right hand side must be zero as to keep the incompressibility of flow.

Simulation Algorithm

A semi-implicit algorithm is applied to the Navier-Stokes equation of an incompressible fluid.

$$\frac{\partial\vec{u}}{\partial t}=-\frac{1}{\rho}\nabla p+\nu\nabla^2\vec{u}+\vec{F} \tag{5}$$

Where, ρ is the fluid density and ν is the kinematic viscosity coefficient. In a time step, external force terms, viscosity terms and pressure gradient terms are calculated explicitly. The Poisson equation of

pressure is calculated implicitly using an iteration solver. First, external terms and viscosity terms of the Navier-Stokes equation are calculated explicitly, and the temporary velocity $\vec{u}_i^{\,*}$ is obtained.

$$\vec{u}_i^{\,*} = \vec{u}_i^{\,k} + \nu\nabla^2\vec{u}_i^{\,k}\Delta t + \vec{F}\Delta t \tag{6}$$

Where, Δt is the time increment.

The temporary particle position $\vec{r}_i^{\,*}$ is calculated as

$$\vec{r}_i^{\,*} = \vec{r}_i^{\,k} + \vec{u}_i^{\,*}\Delta t \tag{7}$$

The temporary particle number density n^*, which is evaluated from the temporary position, generally deviates from the initial particle number density n^0. In this case, the fluid density is not constant. Therefore, pressures at the particles are calculated by using Eq.(4).The pressure at the time $t+\Delta t$, p_i^{k+1} is obtained by solving the Poisson Eq.(4). Substituting p_i^{k+1} into Eq.(8), we obtain the correction velocity $\vec{u}_i^{\,'}$.

$$\vec{u}_i^{\,'} = -\frac{1}{\rho}\nabla p_i^{\,k+1}\Delta t \tag{8}$$

Adding the correction velocity to the temporary velocity, we have the new velocity of particle *i*

$$\vec{u}_i^{\,k+1} = \vec{u}_i^{\,*} + \vec{u}_i^{\,'} \tag{9}$$

After adding the correction displacement to the temporal position, the new position of particle *i* is

$$\vec{r}_i^{\,k+1} = \vec{r}_i^{\,*} + \vec{u}_i^{\,'}\Delta t \tag{10}$$

Numerical Model

The amplitudes for the wave generator were 1.5 m, 2.0 m, 2.5 m and 3.0 m with 14.0 s wave period. Distance between particles was 0.005 m with the 0.002 s time increment. Total number of particles was 33,198.

RESULTS AND DISCUSSIONS

Fig. 2 shows the relationship between wave heights (H_a and H_b) and wave pressure on the sea-wall. Wave pressure gradually increases with the wave height. Wave pressure exhibits the dependency on wave height at different positions in tank. However, the relationship between wave pressure and wave height H_b shows similar pattern with the approximate experimental line. The numerical simulation results lead to the good agreement with experimental results.

Fig. 3 shows the numerical simulation results of water depth and water height relationship. Water depth was calculated in front of the sea-wall, whereas water height was estimated from the obtained pressure on sea-wall. It shows the significant relationship between water depth and water height from pressure. It specifies the dependency of wave impact pressure on sea-wall on height of the water which is also found in Fig. 2.

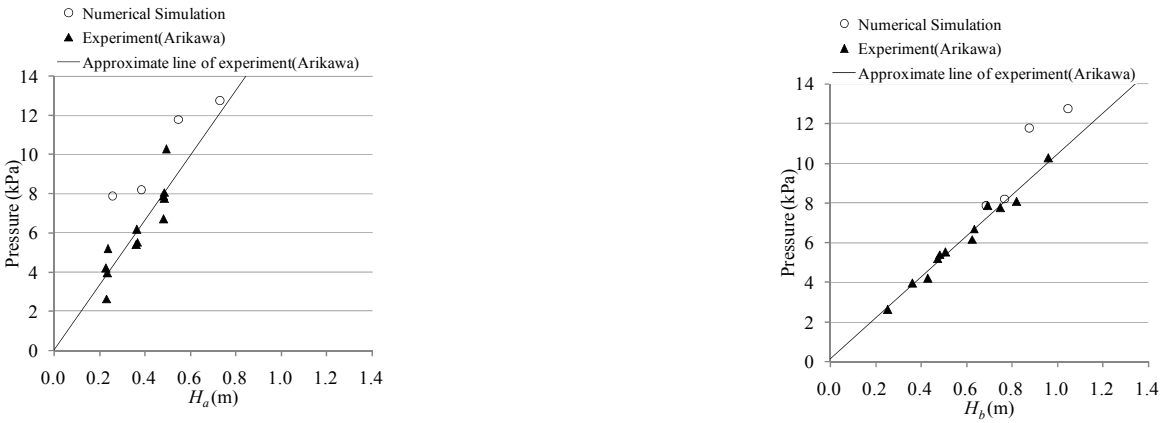

Fig. 2: Relationship between wave pressure and wave height.

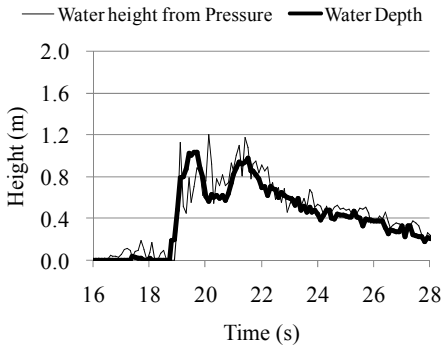

Fig. 3: Comparison of water depth and wave height.

Fig. 4 exhibits the numerically obtained wave shoaling phenomena with wave breaking. The wave height changes with the distance from the origin and it experiences the shallow water as to have slope from the sea-wall. Wave height depends on the distance from the origin and the mode of the flume bed.

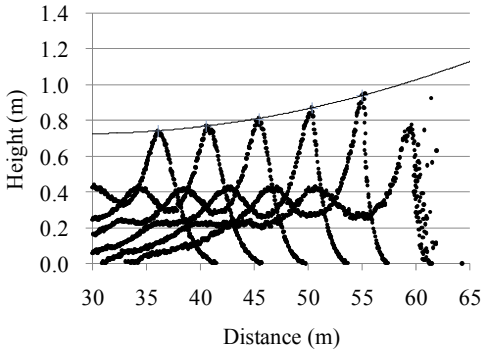

Fig. 4: Wave shoaling with wave breaking.

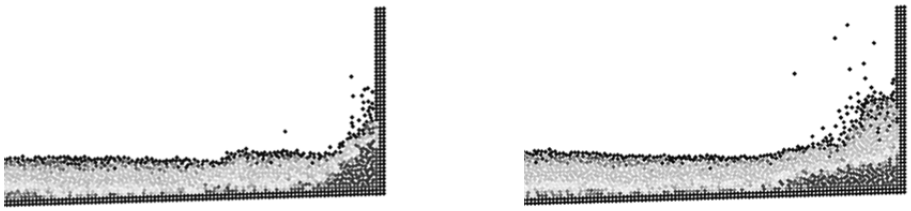

Fig. 5: Wave impact on sea-wall at 19.00 s (left) and 19.50 s (right).

Wave impact phenomena on sea-wall are shown in Fig. 5. Wave impacts on the sea-wall with splash. It also exhibits the water height in front of sea-wall on which the strength of wave impact pressure depends. Pressure increases with the wave height. The wave height increases at 19.50 s which can be found in Fig. 3.

CONCLUSION

A newly improved MPS method was used to assess the wave impact phenomena on vertical sea-wall. The relationship between wave height and wave impact pressure on sea-wall was compared between experimental results and numerical simulation results. Numerical simulation results show good agreement with experimental results. Furthermore, this relationship was figured out with different numerical simulation results. This newly improved MPS method can be used to simulate wave impact problems on sea-wall.

LIST OF REFERENCES

Arikawa, T; Ikebe, M; Yamada, H; Shimosako, K and Imamura, H. 2005. Experiment of Tsunami force acting on the sea-wall and onshore structures. *Proceedings of Coastal Engineering,* JSCE, 52: 746-750 (*in Japanese*).

Hanbin, GU; Pengzhi, LIN; Yanbao, LI; Taiwen, HSU and Jianlue HSU. 2003. Wave characteristics in front of vertical sea-walls. *International Conference on Estuaries and Coasts,* Hangzhou, China.

Iribe, T and Nakaza, E. 2011. A study to improve accuracy of MPS method by a new gradient computation method. *Proceedings of Coastal Engineering,* JSCE, 6 (1): 36-48 (*in Japanese*).

Iribe, T; Nakaza, E; Rusila, S; Rahman MM and Seiya I. 2012. Estimations of Impact wave force of tsunami acting on a vertical sea wall with MPS method. *33rd International Conference on Coast. Eng.,* Santander, Spain.

Koshizuka, S and Oka, Y. 1996. Moving particle semi-implicit method for fragmentation of incompressible fluid. *Nucl. Sci. and Eng.,* 123: 421-434.

Mingham, CG; Causon, DM; Ingram, DM and Richardson SR. 2003. Numerical simulation of wave-seawall interaction. *Coast. Eng.,* 2002: 2264-2272.

Nakaza, E; Iribe, T and Rouf, MA. 2010. Numerical simulation of tsunami currents around moving structures. *Proceedings of 32nd Conference on Coast. Eng.*, Shanghai, China, ICCE, 32.

Nakaza, E; Iribe, T; Rusila, S; Rahman MM and Watanabe T. 2012. Numerical simulation of the runup of solitary waves with the improved MPS method. *33rd International Conference on Coastal Engineering,* Santander, Spain, ICCE, 33.

Tanaka, M and Masunaga, T. 2008. Stabilization and smoothing of pressure on MPS method by quasi-compressibility. *Transactions of JSCES,*20080025 (*in Japanese*).

ID: AGE 027

1st International Conference on Advances in Civil Engineering 2012 (ICACE 2012)
12 –14 December 2012
CUET, Chittagong, Bangladesh

CONDITIONAL SIMULATION OF GEOLOGICAL TEXTURES BY IMAGE QUILTING

K. MAHMUD[1*], G. MARIETHOZ[2] & A. BAKER[3]

[1]National Centre for Groundwater Research & Training and Connected Waters Initiative Research Centre, University of New South Wales, Sydney, NSW, <kashif.mahmud@unsw.edu.au>
[2]National Centre for Groundwater Research & Training and Connected Waters InitiativeResearch Centre, University of New South Wales, Sydney, NSW, <gregoire.mariethoz@unsw.edu.au>
[3]National Centre for Groundwater Research & Training and Connected Waters InitiativeResearch Centre, University of New South Wales, Sydney, NSW, <a.baker@unsw.edu.au>
**Corresponding Author*

ABSTRACT

Stochastic simulation is an invaluable tool for modelling three-dimensional geological characteristics. Stochastic simulation allows creating multiple realistic realizations of an unknown three-dimensional geological domain, with conditioning to any existing observations and reproducing a given spatial continuity. Some of the most successful methods in this field are multiple-point geostatistics, which define spatial continuity based on the concept of a training image. It was found that similar methods have been proposed in computer graphics. One such method, Image Quilting, is introduced in this paper.The main difficulty with it is that it was not originally designed to produce conditional simulations. In this paper, the existing MATLAB code developed for computer graphics has been modified for conditional 2D image quilting by using the rejection method and applied to geoscience. We have established the deviation due to the error tolerance to the conditioning data in the 2D conditional image quilting process by executing elapsed time for various number of conditioning points. The rejection method can be applied to image quilting for very few conditioning points with reasonable accuracy. The time required with this method increases enormously when moreconditioning points are considered. In such casesthe computational cost can be very high to obtaingeological texturesthat havethe correct data values at the conditioning locations. Herewe investigate another improved procedure (Selection Method)that allows accurate conditioning while performing with reasonable computing times.

Keywords: Geological texture synthesis,Multiple-point geostatistics, Conditioning, Image quilting, Sub-surface heterogeneity.

INTRODUCTION

Modelling subsurface heterogeneity is extremely important for predicting the behaviour of hydrogeological systems. Geological texture synthesis is a great challenge of subsurface modelling. For more than 50 years it has been extensively used for the management and the estimation of uncertain water resources. A broad variety of methods have been developed in geostatistics, aimed at characterizing the spatial structure, or texture, of the variable considered (e.g. hydraulic conductivity in hydrogeology).

In most cases, spatial covariance or variogram analysis is used to quantify the spatial geological continuity. Variograms only illustrate correlation among any two points in space and aredefined as a two-point statistic which cannot reproduce connected geological patterns. Boolean models are the

most commonly used algorithms for object-based models which work with deterministic shapes illustrated by stochastic constraints (Renard et al., 2006). The main critique towardstraditional geostatistical approaches is related to their failure to represent realistically some connected geological structures.

A solution to this criticism was suggested by Strebelle (2002), with an approach consisting ofthe assessment of the conditional probability distribution for a simulated value based on a training image (TI). Multiple-point (MP) geostatistics is able to produce images similar to those found with object-based models, with the benefit that it can be easily conditioned with field data, therefore exceeding the major difficulty of object-based model (Renard et al., 2006). The TI is a theoretical but explicit concept which can represent 2D or 3D spatial geological continuity. TI may originate from real data representative of the geology under consideration, or a large unconditional realization of a stochastic simulation technique. Strebelle recommends using TIs which can be developed from expert information, outcrops, or even a geologist's sketching. Therefore it is not necessary for a TI to be locally constrained to any data and be the equivalent size as the area under consideration, but can reproduce the spatial continuity inferred as same as the real geological character (Arpat and Caers, 2007). Guardiano and Srivastava (1993) initially used multiple-point statistics based on TIs in the field of geostatistical simulation. This was inspired by building upon the sequential indicator model that uses only two point statistics for generating facies geological models (Journel, 2005).

The concept of simulating models using Multiple-Point statistics from a TI seems easy, straightforward and smart for geologists (Hu and Chugunova, 2008). However, some limitations originate from the difficulty to find TIs, their reliability to characterize particular reservoir irregularities, the precision of the simulated forecast, the consistency among a particular TI and a particular data set, and computational issues. Therefore, more research is needed in this area.Our aim is to develop a method that better reproduces the TI patterns while reducing computational cost, inspired by the state-of-the-art in texture synthesis. To this end, we adaptthe method of image quilting that proceeds by stitching together geological texture patches based on training images to form the output realization.

In the field of texture synthesis, an early method was proposed by Efros and Leung (1999), which uses non-parametric sampling to "grow" texture by enforcing statistics locally, pixel by pixel. All the neighbours are synthesized by the conditional distribution of each pixel and this is done by searching the training image and searching all likely neighbourhoods. The algorithm gives decent outputs for an extensive variety of textures, but is computationally disadvantaged because every pixel has to be synthesized by thorough searching of the input image. This means that a lot of searching effort is wasted on pixels. Hence rather than taking a particular pixel as the unit of synthesis, a block or patch has to be considered (Efros and Freeman, 2001). Then the texture synthesis method will be nothing but matching a jigsaw puzzle, quilting together the blocks until they all match together.

Conditioning means that the resulting textures precisely replicates data values at the measured locations, and is an imperative requirement to integrate geological data. The image quilting method originates from the field of computer graphics and texture synthesis (Efros and Freeman, 2001), where most applications do not require conditioning. Therefore the method has never been adapted for conditioning. We are studying ways of implementing a conditional version of the method. Firstly, the simulated realization needs to be conditional to a range of data sets such as hard and soft data. The image quilting algorithm is mostly built from empirical arguments having neither a formal theory nor a certain explicit modelling. There may be possible conflict between the training image patterns and the patterns of the existing hard data, which is not resolved by the image quilting method as implemented in computer graphics. Such conflict will exist in most practical cases and therefore our final aim is to minimize it by accommodating both texture and data conditioning constraints.

In this paper, we first present an outline of the image quilting method, we then test the sensitivity of its parameters for the reproduction of structures observed in natural geological systems, and finally we propose ways of modifying the method to accommodate conditioning data. Two avenues are investigated to this end: conditioning by rejection, which is correct but very inefficient, and conditioning by selection that gives much better results.

IMAGE QUILTING FOR GEOLOGICAL TEXTURE SYNTHESIS

In computer graphicsthere is a need to generate realistic textures in applications such as animation movies or computer games. Texture synthesis methods should be capable of taking a sample of texture image and produce an unlimited amount of data which are not exactly similar to the original, but will be observed to be the similar texture by humans. Efros and Freeman (2001) presented a straightforward algorithm to synthesize larger similar texture (Figure 1,right side) by using a given geological texture example (Figure 1, left side). Their key idea was to generate similar texture by considering small pieces of existing texture and then sewing those pieces together in a coherent manner. This image quilting algorithm has reasonably good performance on semi-structured textures as well as stochastic textures. Extreme repetition and mismatched or distorted boundaries are the two most usual complications. Both these problems occur generally when the input texture does not cover adequate variability. The MATLAB code used by Efros and Freeman (2001) to generate single output image typically runs within few minutes. The simulation time is greatly governed bytwo parameters: the sizes of the input and output and the user defined block size.

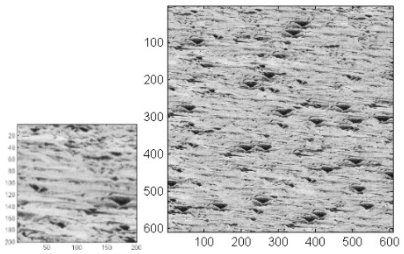

Figure 1: Texture synthesis by Image quilting process

Efros and Freeman (2001) developed this patch-based texture synthesis procedure having the following steps:

1) From the input texture image having the set of all overlapping patches, select the unit of synthesis as a square of user-specified size.
2) To synthesize a new realization, search the input image for such blocks that by some measure agrees with their neighbours along the section of overlaps.
3) Then for better representation of the features in the texture, let the blocks have ragged edges, and look at the error in the overlap area between it and the other block(s) before putting a selected block into the texture. Let, B_1 and $B_2$are two overlapping blocks along their vertical edges shown in Figure 2 with the overlapping regions of B_1^{ov} and B_2^{ov}, respectively. Then, the error surface is described as $e = (B_1^{ov} - B_2^{ov})^2$. To get the minimal vertical cut through the error surface, track *e(i = 2..N)* and calculate the cumulative minimum error E for all paths (Dijkstra, 1959) as shown in Eq.(1). Here *i* and *j* represent the corresponding row and column numbers respectively.

$$E_{i,j} = e_{i,j} + \min(E_{i-1,j-1}, E_{i-1,j}, E_{i-1,j+1}) \qquad (1)$$

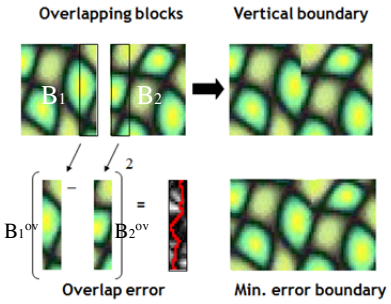

Figure 2: Minimum error boundary cut phenomena to find out the least error path between two overlapping blocks

4) Finally, one can find the end of the minimal vertical path through the surface by searching the minimum value of E in the last row. From there one can follow backward and get the path of the finest cut and state that to be the border of the new patch. For horizontal overlaps, asimilar

procedure can be followed and when there is both horizontal and vertical overlap, the best paths meet in the central and the global minimum is taken for choosing the appropriate cut. In this image quilting process, the only user-defined parameter is the size of the patch which depends on the characteristics of a particular training image. The patch must be big enough to capture the related properties from the image as well as small enough so that the interface between these structures is left up to the algorithm.

CONDITIONAL IMAGE QUILTING PROCESS

Rejection Method

The development of existing MATLAB code for Conditional 2D Image Quilting was performed by the Rejection Method. The elapsed time for various number of conditioning points was recorded. We have also established the time deviation due to the error tolerance in conditioning 2D image quilting process. For this conditioning:

1) Primarily we have assigned conditioning error tolerance in the mathematical model and then calculated absolute error as well as error percentage for each conditioning point.
2) After the first simulation of image quilting function we have checked whether conditioning is satisfied or not by rejection method.
3) If satisfied then go with that output image as the final realization, otherwise reject this image by changing it to a new one, and finally measuring the elapsed time and loop count i.e. the required number of simulation for conditioning through this procedure.

In this process, we have made the output realization conditioning by rejecting the simulated image until it satisfies with the particular data set at specific locations.

Selection Method

We are now in the process of developing another conditioning method named 'Selection process' where a compatible block has to be selected by considering the training image and forcing it to have similar related statistics as in the training image, as well as the relevant field data at certain specific locations of the final realization. In this process, we will search the input training image for blocks that by some measureagrees both with their neighbours along the section of overlaps and at the same time all hard data available within the realization as shown in Eq. 2. Therefore, total error (E_t) will be calculated by considering both the quilting error (E_q) and conditioning error (E_c) multiplied with weightage factorsw_1 and w_2 respectively. Then all the neighbours will be synthesized by the conditional distribution of each block and available field data.

$$E_t = w_1 E_q + w_2 E_c \qquad (2)$$

RESULTS AND DISCUSSIONS

Application of image quilting in hydrogeology

We have applied image quilting to different geological patterns and obtainednumerous variations in texture synthesis outputs. Here we have used colour values of a satellite image of the Lena Delta in Russian Federation shown in Figure 3 (a) (Landsat 7 image, USGS/EROS and NASA Landsat Project). With this particular image we performed a sensitivity analysis of the parameters of Image Quilting. The outputs are discussed here.

i) Variation in overlapping region between pixels:

Figure 3 shows different realizations found due to variation in the amount of overlap to allow between pixels while synthesizing the final texture. Sometimes we found 'verbatim copy' (Figure 3d, Figure 4d) of the training image as the final realization, where the realization is exactly the TI. This may occur when the patches are too big, and is not desirable (lack of variability between realizations). The elapsed timeshown in Table 1 rises with increasing overlapping region.

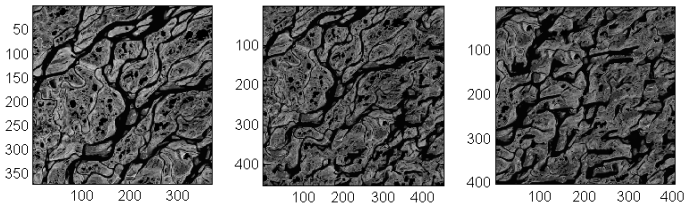

(a) Satellite image of the Lena Delta (b) 10% overlap (c) 20% overlap

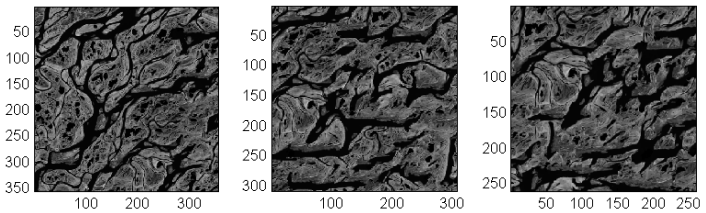

(d) 30% overlap (e) 40% overlap (f) 50% overlap

Figure 3: Different realizations due to the variation in overlapping amount to allow between pixels

Table 1:Elapsed times due to the variation in the amount of overlap to allow between pixels

Overlap (%)	10	20	30	40	50
Elapsed time (sec)	34.9	38.1	42.6	47.5	63.7

ii) Variation in error tolerance:

Figure 4 shows different realizations found due to variation in the error tolerance used when computing list of compatible blocks. The elapsed times not varying significantly due to this deviation are shown in Table 2.

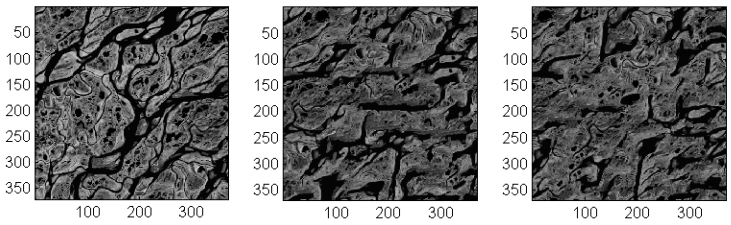

(a) Satellite image of the Lena Delta (b) 2% error tolerance(c) 4% error tolerance

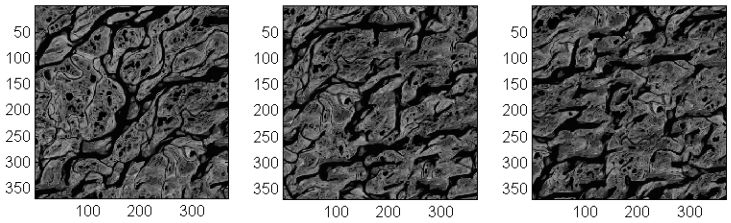

(d) 6% error tolerance (e) 8% error tolerance (f) 10% error tolerance

Figure 4: Different realizations due to the variation in error tolerance

Table 2:Elapsed times due to the variation in error tolerance

Error tolerance (%)	2	4	6	8	10
Elapsed time (sec)	67.9	68.5	68.4	68.5	68.7

Conditional image quilting by rejection method

Elapsed time and loop count number are illustrated in Figure 5 for various number of conditioning points by Rejection Method. From the diagram, it is evident that as the number of conditioning points

increases the required time rises enormously, making this method inappropriate. The deviation for various error tolerances is also shown in Figure 5. Here it is seen that the elapsed time and number of simulations needed increase with the accuracy of the conditioning to be done. There are few discrepancies present in this investigation as this process is fully a stochastic random process.

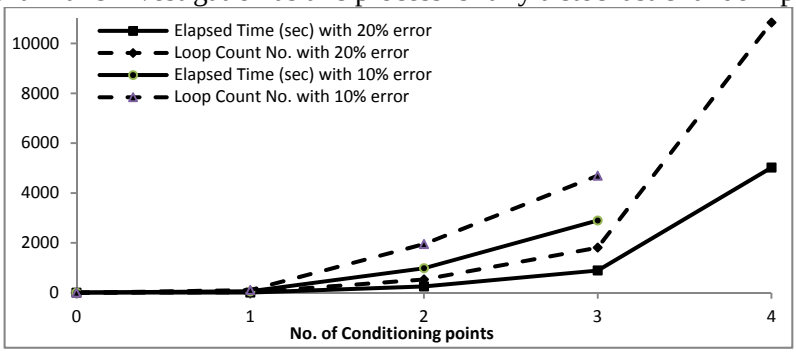

Figure 5: Elapsed Time and Loop Count No. for various number of conditioning points by Rejection Method

CONCLUSION

The image quilting process is mostly effective for semi-structured textures which were always the hardest for the geostatistician to synthesize.This image quilting method is extremely easy to apply in geostatistics and plenty of similar geological realizationscan be obtained through this algorithm very quickly.From this preliminary analysis, we found that the rejection method can be applied on image quilting for very few conditioning points with reasonable accuracy. The time required with this method increases enormously when moreconditioning points are considered. In such casesthe computational cost can be very high to obtaingeological textures having the data values at the conditioning locations.Here we investigate another improved procedure (Selection Method) that allows accurate conditioning while performing with reasonable computing times.

LIST OF REFERENCES

Arpat, G and Caers, J. 2007. Conditional Simulation with Patterns.*Mathematical Geology*, 39(2):177-203.

Dijkstra, E. 1959.A note on two problems in connexion with graphs.*NumerischeMathematik*, 1:269-271.

Efros, AA and Freeman, WT. 2001. Image quilting for texture synthesis and transfer. *Proceedings of the 28th annual conference on Computer graphics and interactive techniques*. pp. 341-346.

Efros, AA and Leung, TK. 1999. Texture synthesis by non-parametric sampling.*In International Conference on Computer Vision*, pp 1033–1038, Corfu, Greece.

Guardiano, F and Srivastava, M. 1993. *Multivariate geostatistics: Beyond bivariate moments*, in Geostatistics Troia'92, edited by SoaresA, Springer, Dordrecht, Netherlands, pp. 133–144.

Hu, LY and Chugunova, T. 2008. Multiple-point geostatistics for modeling subsurface heterogeneity: A comprehensive review. *Water Resources Research*, 44: W11413.

Journel, A. 2005.*Beyond covariance: The advent of multiple-point geostatistics*, in Geostatistics Banff 2004, edited by Leuanthong O, and Deutsch CV, pp. 225–233, Springer, Dordrecht, Netherlands.

Renard, P; Gómez-Hernández, JJ and Ezzedine, S. 2006. Characterization of Porous and Fractured Media.*Encyclopedia of Hydrological Sciences.*

Strebelle, S. 2002. Conditional simulation of complex geological structures using multiple-point statistics.*Mathematical Geology*, 34(1):1–22.